NASA CR-152482

(NASA-CR-152482) A DEPOLARIZATION AND ATTENUATION EXPERIMENT USING THE CTS SATELLITE. VOLUME 2: DATA Final Report, 1 Oct. 1975 - 30 Sep. 1976 (Virginia Polytechnic Inst. and State Univ.) 102 p HC G3/32

N77-21277

HC A06/MF A01

Unclas 24445

Virginia Polytechnic Institute and State University

Electrical Engineering

BLACKSBURG, VIRGINIA 24061

Final Report (First Year of Work)

on

A DEPOLARIZATION AND ATTENUATION EXPERIMENT USING THE CTS SATELLITE

Volume 2. Data

Text by

C. W. Bostian
S. B. Holt, Jr.
S. R. Kauffman
E. A. Manus
R. E. Marshall
W. L. Stutzman
P. H. Wiley

Artwork by

Cynthia R. Will

Electrical Engineering Department
Virginia Polytechnic Institute and State University
Blacksburg, Virginia 24061

Prepared for

NASA Goddard Space Flight Center
Greenbelt, Maryland 20771

Contract NAS5-22577

February 23, 1977

1 Report No	2 Government Accession No	3 Recipient's Catalog No
4 Title and Subtitle A Depolarization and Attenuation Experiment Using the CTS Satellite, Volume 2. Data		5 Report Date February 23, 1977 6 Performing Organization Code
7 Author(s) C.W. Bostian, S.B. Holt, Jr., S.R. Kauffman, E.A. Manus, R.E. Marshall, W.L. Stutzman, P.H. Wiley		8 Performing Organization Report No
9 Performing Organization Name and Address Electrical Engineering Department Virginia Polytechnic Institute & State Univ. Blacksburg, Virginia 24061		10 Work Unit No 11 Contract or Grant No NAS5-22577
12 Sponsoring Agency Name and Address NASA Goddard Space Flight center Greenbelt, Md. 20771 E. Hirschmann, Code 953, Technical Officer		13 Type of Report and Period Covered Final Report: First Year of Work 1 Oct. '75-30 Sept. '76 14 Sponsoring Agency Code
15 Supplementary Notes		

16. Abstract

This report describes an experiment for measuring precipitation attenuation and depolarization on the CTS 11.7 GHz downlink. It presents the first year's data.

17. Key Words (Selected by Author(s))	18 Distribution Statement		
polarization, depolarization, attenuation, millimeter wave propagation, communications satellites, antennas, receiver electronics, CTS			
19 Security Classif (of this report)	20 Security Classif (of this page)	21 No of Pages	22 Price*
U	U	99	

*For sale by the National Technical Information Service, Springfield, Virginia 22151

Table of Contents

1. Introduction

This volume presents the rain propagation data taken on the Communications Technology Satellite (CTS) 11.7 GHz downlink during the first year of work at Virginia Polytechnic Institute and State University (VPI&SU). It completes a two-volume first year final report for NASA Contract NAS5-22577. The following sections contain (a) a summary of the first year's operation and a breakdown of the data collected, (b) a discussion of the data trends and our conclusions about them, and (c) time plots of the significant propagation events which occurred during the reporting period.

2. Summary of the First Year's Operations

The CTS spacecraft was launched on January 17, 1976. The VPI&SU earth station first acquired the signal on May 27, 1976, using a 4.5 inch (11.4 cm) horn antenna. With the installation of the station's main antenna the horn was replaced and serious data collection began on June 11, 1976. This continued without interruption until a lightning stroke on August 13, 1976, severely damaged the antenna positioning system and the computer which controls the experiment. The lightning damage halted data collection until after the spacecraft had been turned off for the eclipse period (August 30 through October 16, 1976).

This report, then, presents data from 63 consecutive days of operation (June 11 - August 13, 1976). It includes data from all storms which occurred during that period. Except for one minor rain during August 13-30 and the part of the August 13 storm after the lightning strike, all rain events between satellite acquisition and satellite turnoff were covered. Table 2-1 summarizes the data collected.

Table 2-1. Summary of First Year's Data Collection

Date Julian	1976 Calendar	Rain Accumulation, mm RG 9	RG 10	RG 11	Peak Rain Rate, mm/hr RG 9	RG 10	RG 11	Max.Fade dB	Min.Isol. dB
166	6/14	2.8	3.3	4.3	29.5	32.7	63.5	4.0	27.0
167	6/15	0	0	0	0	0	0	T*	T
168	6/16	75.9	26.4	62.5	321.4	93.4	91.5	26.4	19.3
169	6/17	20.3	1.0	20.6	43.2	35.5	48.2	6.6	25.3
170	6/18	0.3	0.3	0	0	0	0	1.4	28.3
171	6/19	17.8	12.2	18.0	71.5	61.0	84.7	12.0	20.0
172	6/20	30.5	27.2	27.9	75.0	55.8	67.3	10.7	13.9
173	6/21	26.9	26.4	23.1	123.6	127.1	83.2	12.6	11.7
174	6/22	0	0	0	0	0	0	27.4	21.7
175	6/23	0	0	0	0	0	0	1.0	28.9
176	6/24	0	0	0	0	0	0	0.8	29.5
177	6/25	1.0	1.3	1.0	15.5	33.4	14.8	6.6	25.1
178	6/26	17.0	15.5	16.3	48.7	38.4	64.4	14.2	17.7
179	6/27	0.3	0.5	0.5	0.2	3.1	2.3	1.4	28.3
180	6/28	0	0	0	0	0	0	1.4	28.3
181	6/29	0	0	0	0	0	0	2.1	26.7
182	6/30	0	0	0	0	0	0	3.4	25.3
183	7/1	1.8	1.5	1.0	30.3	17.8	13.5	3.6	30.9
184	7/2	0	0	0	0	0	0	3.4	25.5

Table 2-1 (Cont'd) Summary of First Year's Data Collection

Date Julian	1976 Calendar	Rain Accumulation, mm RG 9	RG 10	RG 11	Peak Rain Rate, mm/hr RG 9	RG 10	RG 11	Max. Fade dB	Min. Isol. dB
185	7/3	7.1	7.9	7.9	17.0	25.4	31.1	2.8	30.5
186	7/4	0.3	0.3	0.3	0.1	0.2	0.2	2.4	30.9
187	7/5	0	0	0	0	0	0	1.4	30.7
188	7/6	5.3	4.8	4.3	9.9	6.8	10.0	L**	L
189	7/7	2.8	2.3	0	101.7	89.7	0	L	L
190	7/8	0	0	0	0	0	0	L	L
191	7/9	3.3	2.8	3.6	6.2	6.4	6.6	L	L
192	7/10	0	0	0	0	0	0	L	L
193	7/11	0	0	0.3	0	0	0	L	L
194	7/12	8.6	7 9	6.9	88.0	83.2	75.0	L	L
195	7/13	0	0	0	0	0	0	L	L
196	7/14	0	0	0	0	0	0	L	L
197	7/15	3.6	4.1	11.2	19.8	36.9	80.3	36	9.1
198	7/16	2.5	1.5	1.8	21.8	11.2	20.3	4.4	31.1
199	7/17	0	0	0	0	0	0	1.6	31.7
200	7/18	0	0	0	0	0	0	1.6	31.5
201	7/19	0	0	0	0	0	0	0.8	30.9
202	7/20	0	0	0	0	0	0	1.6	28.5
203	7/21	0	0	0	0	0	0	1.4	28.5
204	7/22	0	0	0	0	0	0	1.4	28.1
205	7/23	0	0	0	0	0	0	1.4	31.3
206	7/24	4.6	3.6	1.3	86.3	78.9	8.3	3.6	30.3

Table 2-1 (Cont'd) Summary of First Year's Data Collection

Date Julian	1976 Calendar	Rain Accumulation, mm RG 9	RG 10	RG 11	Peak Rain Rate, mm/hr RG 9	RG 10	RG 11	Max.Fade dB	Min.Isol. dB
207	7/25	0.3	0.3	0.5	0.1	0.8	1.4	2.2	31.5
208	7/26	0	0	0	0	0	0	1.4	31.0
209	7/27	0	0	0	0	0	0	D***	D
210	7/28	0.8	0.5	0.8	1.1	0.7	0.5	4.2	29.7
211	7/29	0.3	0.3	1 3	0	0	26.0	7.0	25.7
212	7/30	18.8	13.7	16.0	454.5	254.2	93.4	36.0	12.5
213	7/31	0	0	0	0	0	0	0	28.1
214	8/1	1.5	1.8	2 0	8.2	4.5	8.0	5.4	27.0
215	8/2	0	0	0	0	0	0	4.6	26.1
216	8/3	0	0	0	0	0	0	3.6	26.3
217	8/4	0	0	0.3	0	0	0	3.4	29.5
218	8/5	0	0	0	0	0	0	6.4	27.1
219	8/6	0	0	0	0	0	0	0	33.1
220	8/7	2.3	2.3	2.3	23.1	32.4	39.1	5.8	28 1
221	8/8	30.2	25.9	21.8	89.7	104.0	41.6	10.4	19.3
222	8/9	0	0	0	0	3.4	6.9	0	33 3
223	8/10	0	0	0	0	0	6.9	1.4	32.7
224	8/11	0	0	0	0	0	0	1.4	28 9
225	8/12	0	0	0	0	0	0	2.0	30.3
226	8/13	17.5	16.3	14.2	120.4	157.8	30.5	28.0	9.1

*T: Receiver was in test mode and no data were recorded.
**L: Data were lost due to a computer malfunction
***D: No data were recorded due to a computer failure.

3. Data Analysis and Discussion

3.1 Clear-Weather Effects

Normal signal behavior in clear weather provides a necessary baseline against which to measure rain effects on the received signal. Thus far we have noted no changes in clear weather that are not directly attributable to the combined effects of small variations in receiver gain and slight changes in the pointing accuracy of our receiving antenna/tracking system.

To illustrate the behavior of the signals in clear weather and the way in which this is changed by rain, consider the period June 25-27, 1976. As Figure 3.1-1 indicates, a small shower took place on June 25 and a larger convective storm took place on June 26.

During clear weather periods the co-polarized received signal showed net peak-to-peak variations of 1 dB (See Fig. 3.1-2). This is the long-term gain stability of the IF signal processors; repeated IF calibrations yield curves of detector output versus IF input power (in dBm) that differ from each other by a maximum spread of 1 dB (peak-to-peak).

The amplitude of the cross-polarized component of the received signal is much more sensitive to antenna pointing than is the co-polarized amplitude. For this reason the cross-polarized signal component shows a diurnal variation caused by small errors made by the tracking program in determining the exact position of the satellite. These produce the behavior shown in Figure 3.1-3. The net effect is to produce a slow variation in the clear weather polarization isolation of the satellite-earth station system between about 29 and 40 dB. See Fig. 3.1-4 for a plot of isolation versus attenuation (including rain events) for June 25-27.

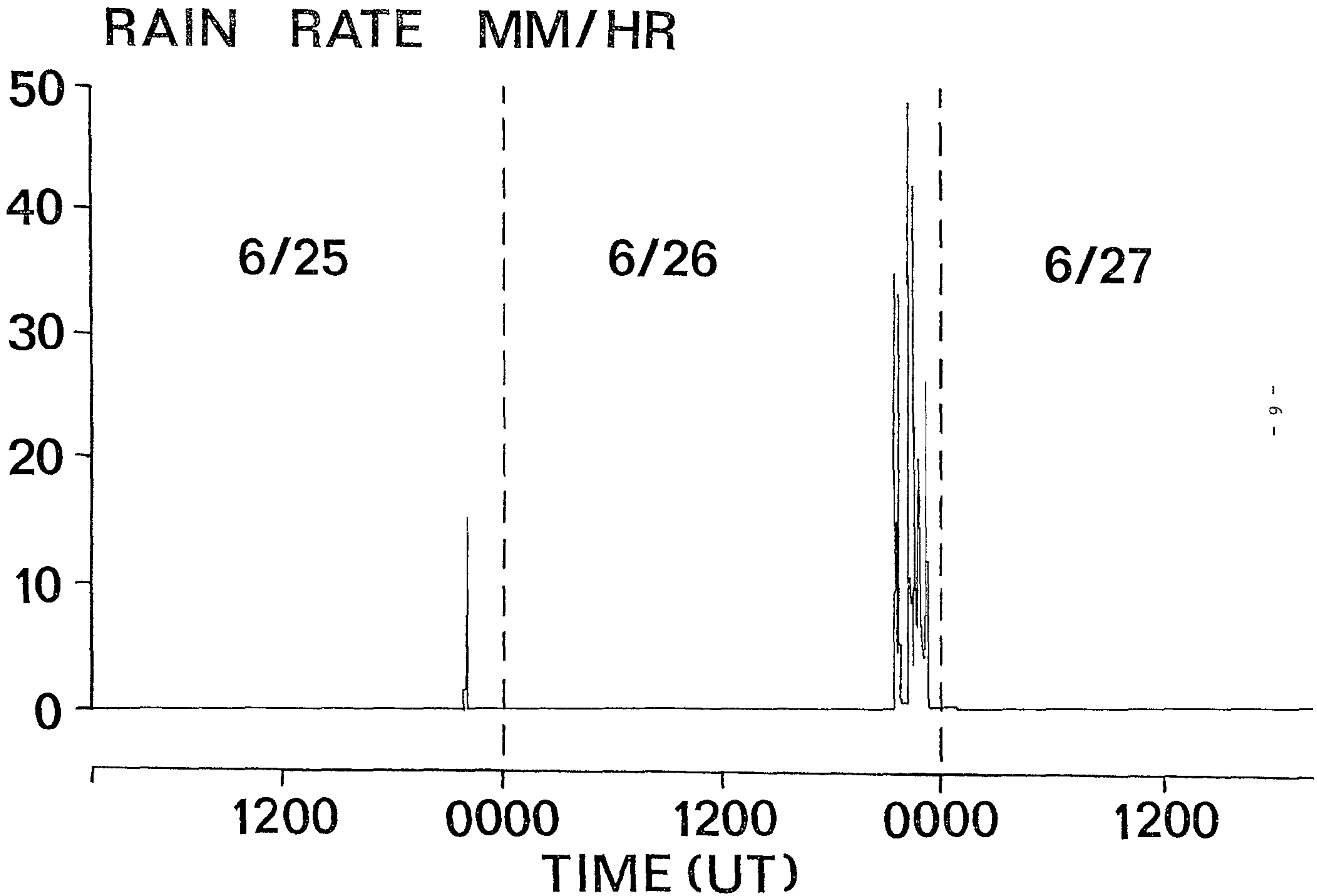

Figure 3.1-1 Rainfall for June 25-27, 1977.

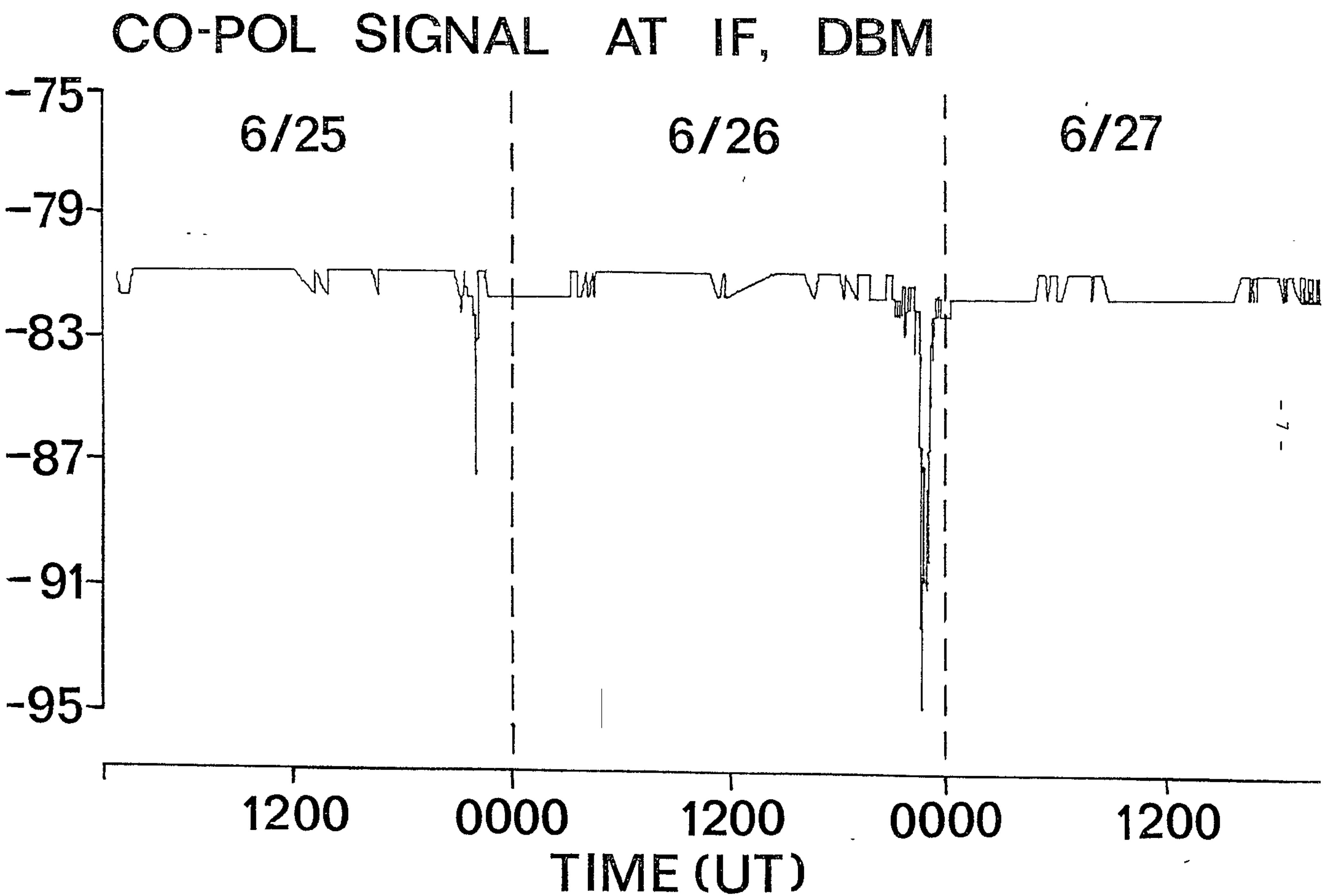

Figure 3.1-2 Co-polarized signal behavior for June 25-27, 1977.

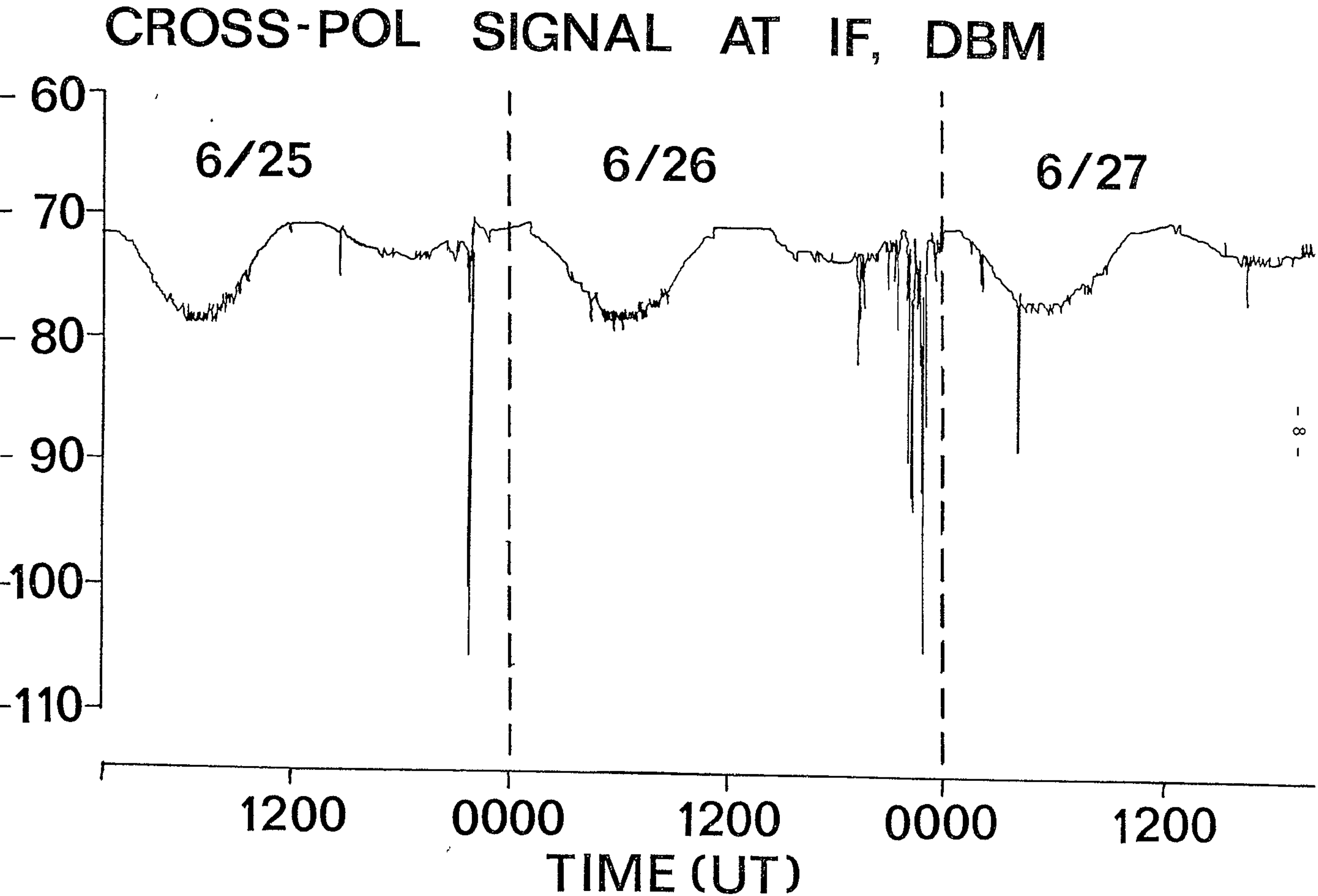

Figure 3.1-3 Cross-polarized signal behavior for June 25-27, 1977.

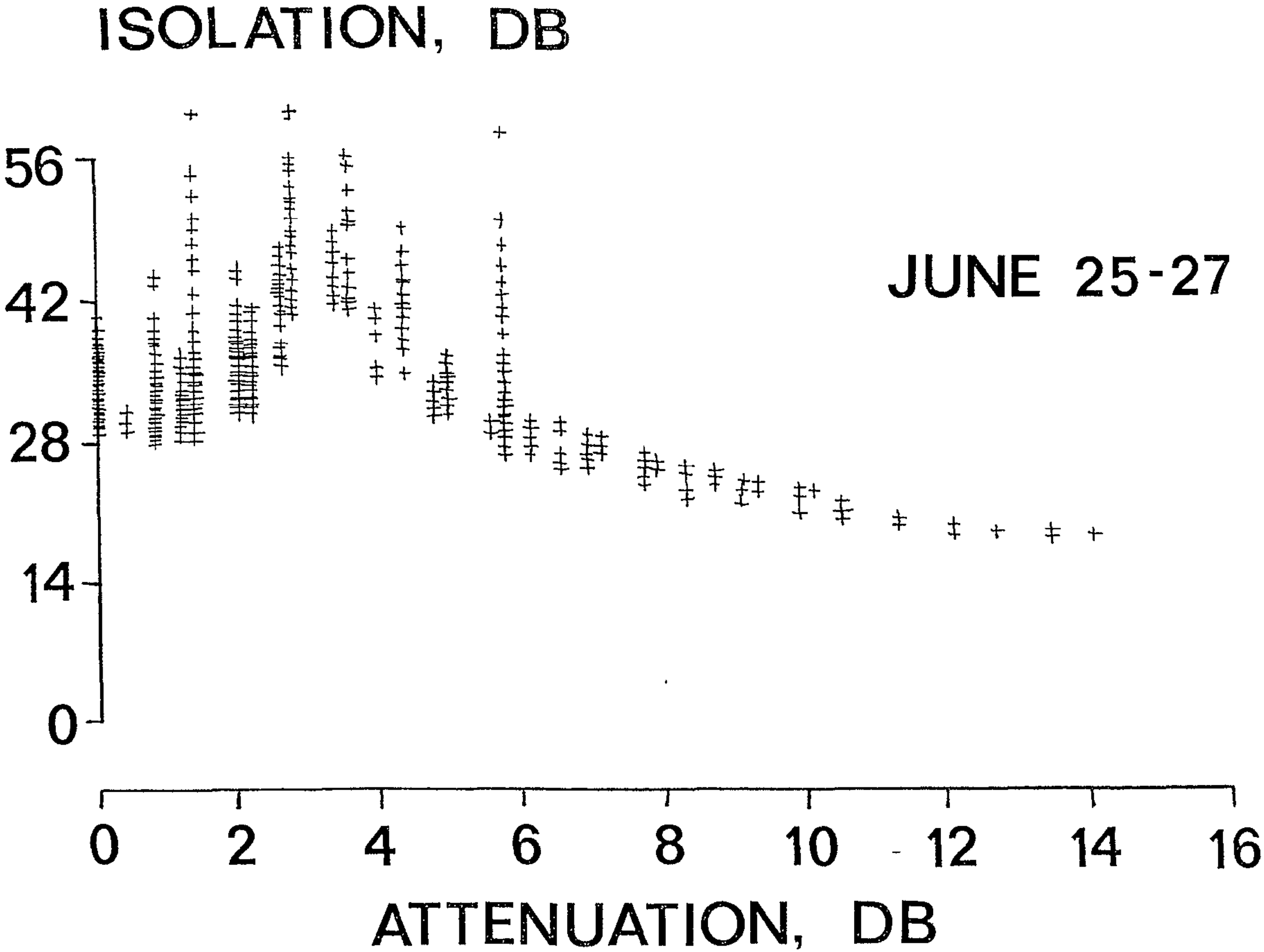

Figure 3.1-4 Isolation versus attenuation for June 25-27, 1977.

The diurnal isolation variations are less serious than they might appear for two reasons. First, system designers are concerned with events which reduce isolation below 20 or 25 dB. This would happen in any significant rain event, and rain depolarization would quickly override the clear weather background. Second, any station using orthogonal polarization frequency sharing would have to contend with diurnal variations at least as severe as those noted by our system. (Depolarization measurements require tracking accuracy at VPI&SU that is significantly tighter than that used by most commercial or experimental earth stations.)

During clear weather conditions the relative phase between the co- and cross-polarized signal components exhibits a diurnal variation with a 12-hour period. These are displayed in Fig. 3.1-5 which shows rain effects superimposed on the diurnal cycle. The large downward spikes represent a momentary loss of phaselock that occurs when the onset of rain fading brings a sharp phase change. This loss of phaselock is an artifact of the receiver and was corrected before the second-year's data collection began.

3.2 Rain Attenuation and Depolarization

This section displays the data highlights and discusses the trends that we have noted. Data from all significant rain events from the first year's operation are presented in Section 4.

Figures 3.2-1 presents the rain rate measured at a rain gauge next to the receiving antenna for a storm on July 15, 1976. While the peak rate was not particularly high, significant attenuation and depolarization occurred. This is evidenced by Figures 3.2-2 and 3.2-3 which display the rain effects on the co-polarized and cross-polarized signal components. Both curves have

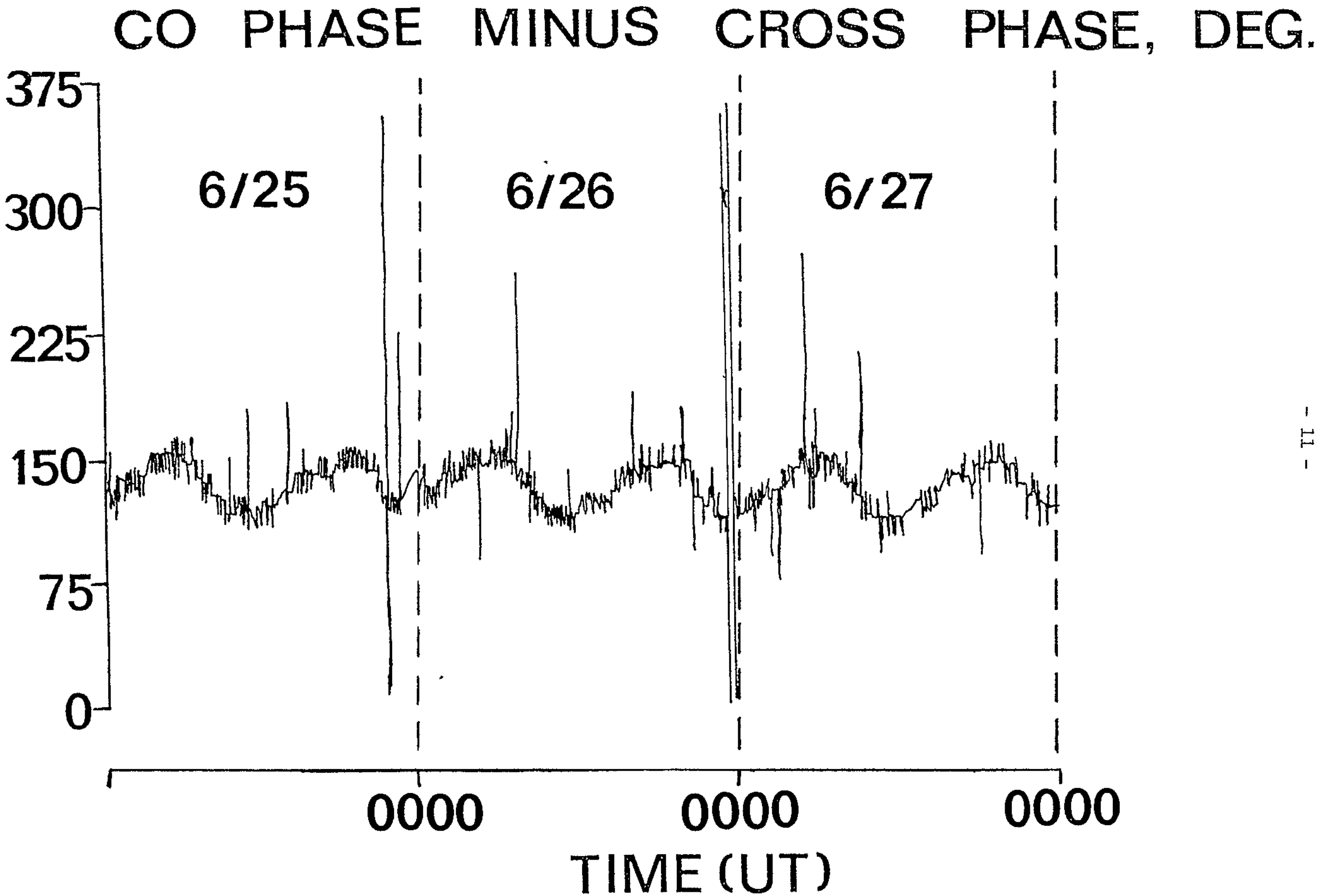

Figure 3.1-5 Phase variations for June 25-27, 1977.

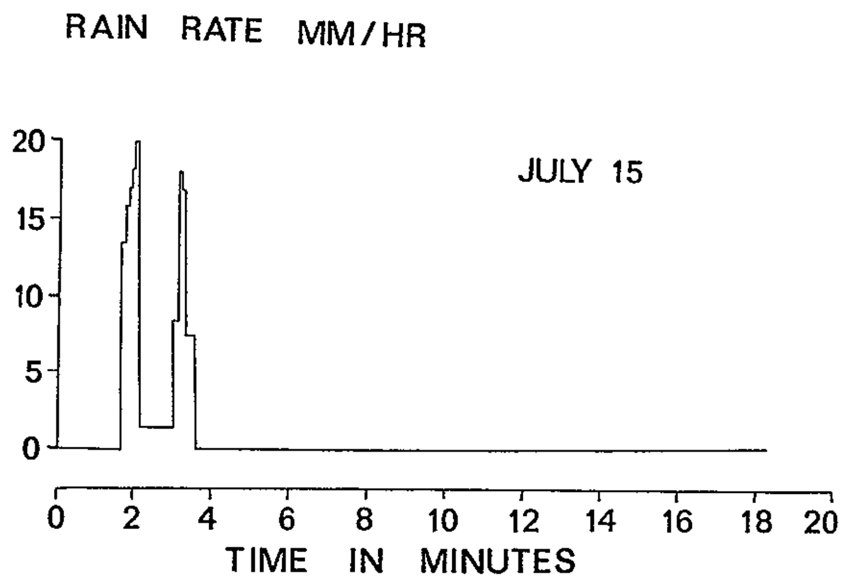

Figure 3.2-1 Rain rate for the storm of July 15.

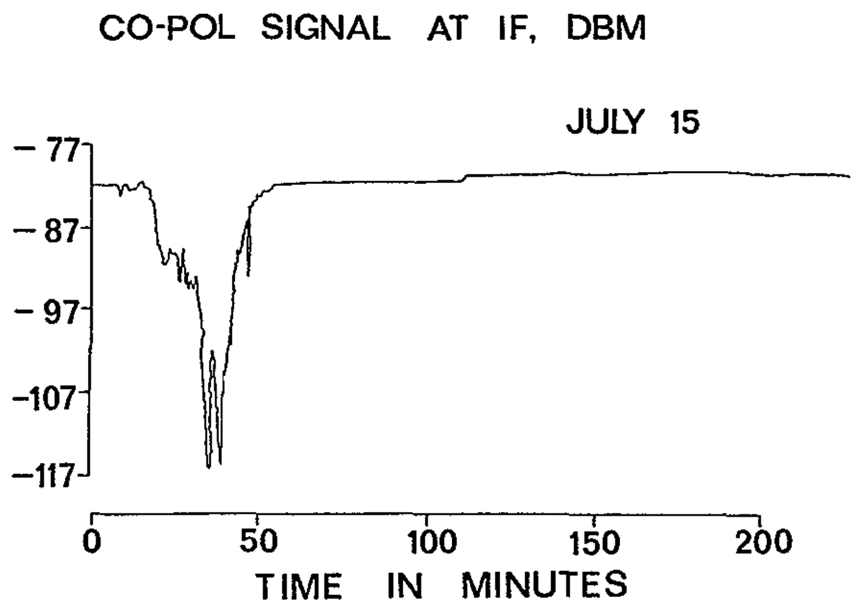

Figure 3.2-2 Co-polarized signal behavior during the storm of July 15.

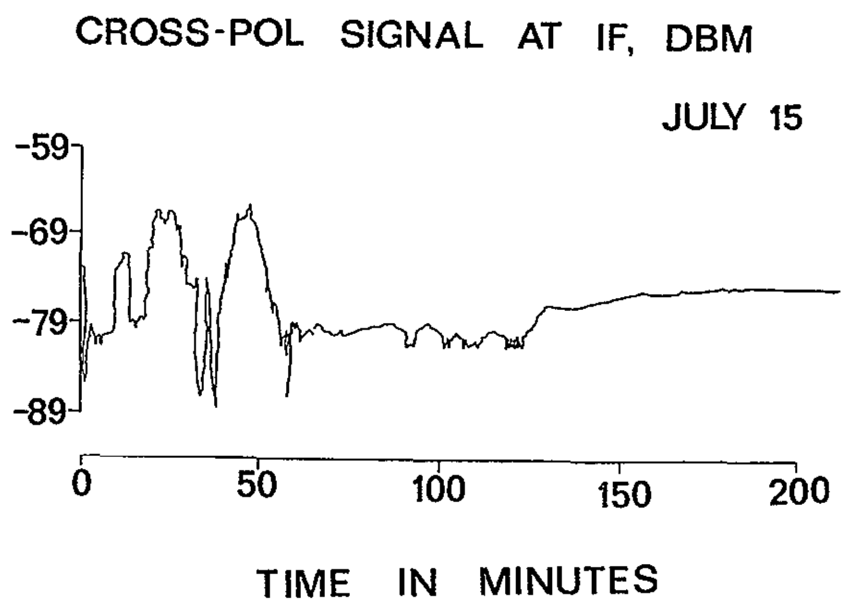

Figure 3.2-3 Cross-polarized signal behavior during the storm of July 15.

the same double-peaked structure found in the rain rate plot.

For the most part large fade events are accompanied by decreased isolation, as one would expect. This is demonstrated by the smooth curve obtained for an isolation versus attenuation plot as shown for this storm in Fig. 3.2-4. The data scatter in this plot is relatively large for attenuations less than about six dB. This is because at low attenuation antenna-wave interaction becomes important, and small fluctuations in the polarization state can cause relatively large changes in isolation. For example, when the wave and antenna polarizations are well matched high isolation values are observed.

Another interesting storm on July 30, 1976, broke all local records for rain intensity. The rain rate plotted in Figure 3.2-5 goes off scale at 325 mm/hr, but several gauges reported peak readings in excess of 800 mm/hr. While numbers in this magnitude from tipping bucket gauges are of little quantitative value, qualitatively they indicate the relative magnitude of the rain. The effects on the received signal were catastrophic; the co-polarized component (Figure 3.2-6) had faded completely out by the time the first raindrops reached the ground. The cross-polarized signal (Figure 3.2-7) initially increased and then faded. The short gap in Figure 3.2-7 represents a momentary loss of phaselock by the cross-polarized receiver. This was produced by a rapid phase change that frequently occurs at the onset of rain. Figure 3.2-8 displays the plot of isolation versus attenuation for this storm.

The plots of isolation versus attenuation for all of the severe storms that we have observed agree well with each other, as evidenced by Figure 3.2-9. At this point it is difficult to make a definitive comparison of the experimental points with theory because so many variables are involved. The theoretical calculation depends on the effective path length, the distribution

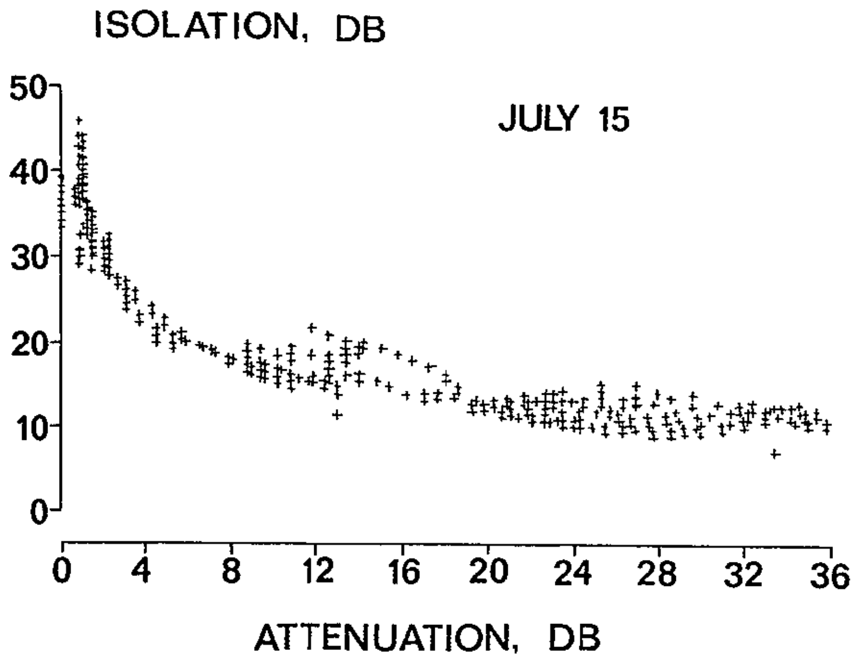

Figure 3.2-4 Isolation versus attenuation for the storm of July 15.

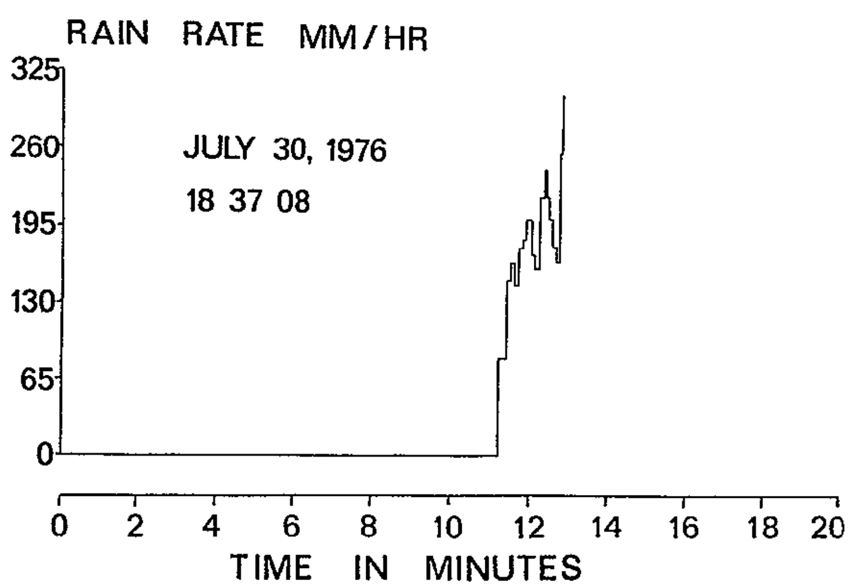

Figure 3.2-5 Rain rate for the storm of July 30.

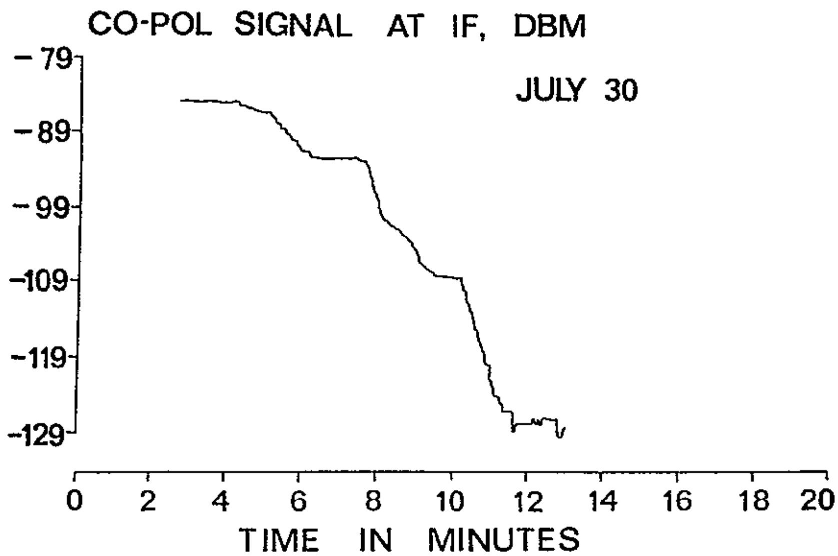

Figure 3.2-6 Co-polarized signal behavior during the storm of July 30.

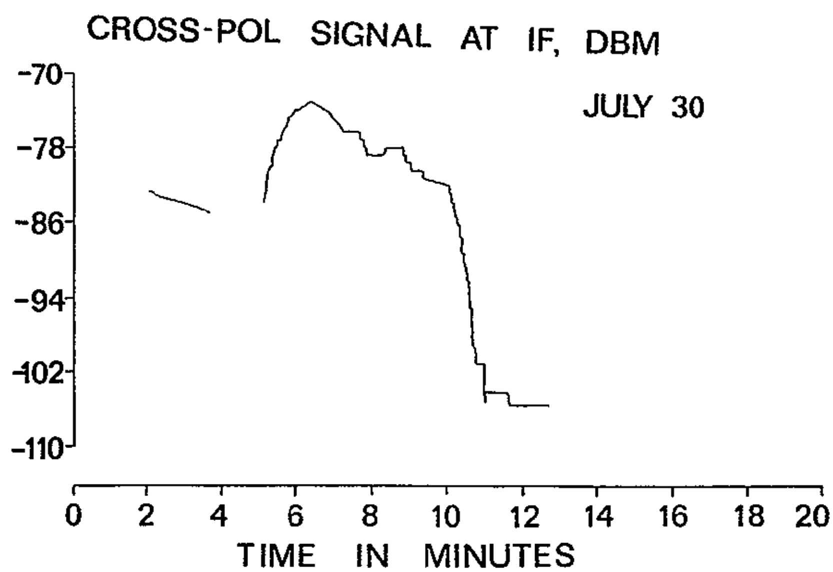

Figure 3.2-7 Cross-polarized signal behavior during the storm of July 30.

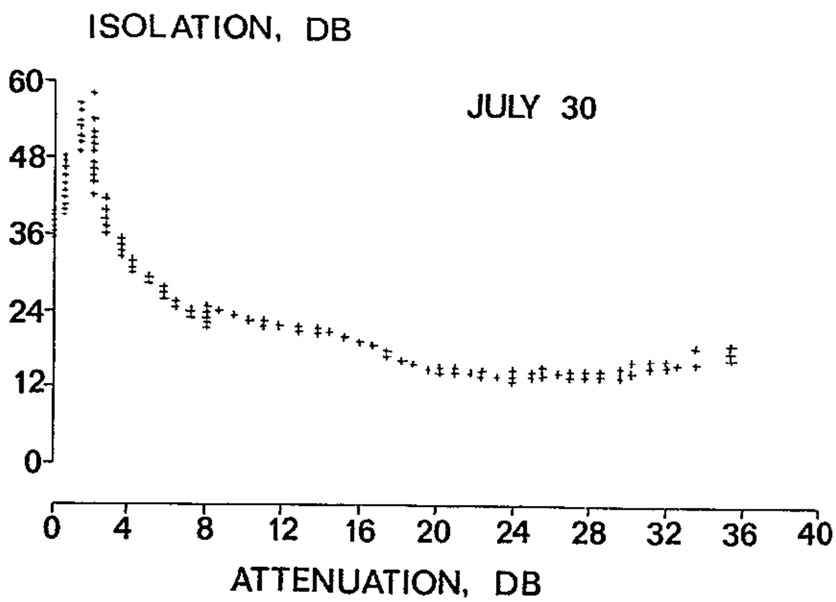

Figure 3.2-8 Isolation versus attenuation for the storm of July 30.

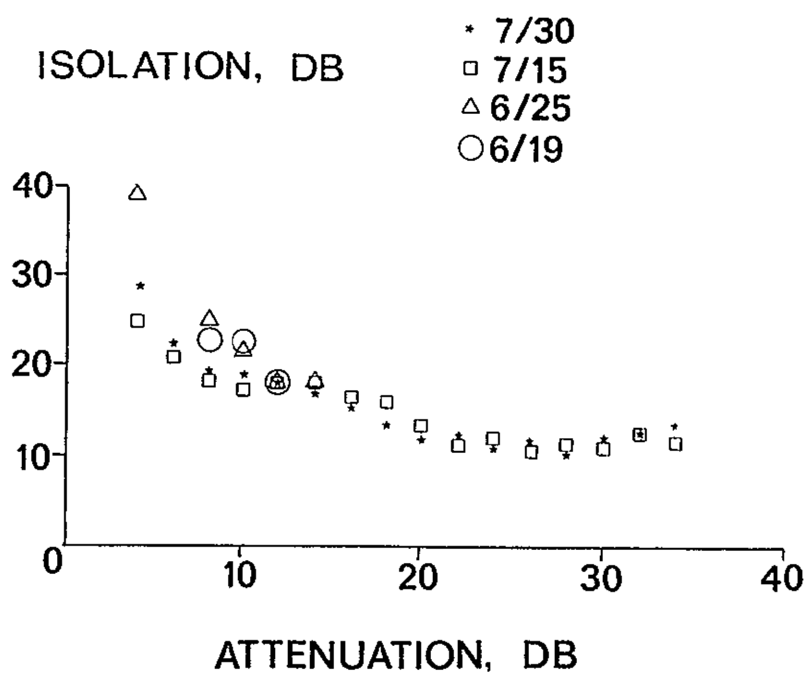

Figure 3.2-9 Composite isolation versus attenuation plot for four storms.

of rain drop shapes, and the polarization characteristics of the transmitting and receiving antennas. Figure 3.2-10 displays some theoretical curves which generally agree with the data, they are based on a rain height of 2500 meters and an elevation angle of 33 degrees. The top curve assumes that 60% of the drops are oblate spheroids and the bottom curve assumes 100% oblate spheriods. Antenna effects are important only at low rain rates, and the way in which the antennas influence the cruves is indicated. The calculations are based on Oguchi's 11 GHz scattering coefficients at 40° elevation angle for the oblate drops and Morrison and Cross' coefficients for spherical drops. [1,2]

Ground-measured rain rates occasionally show no correlation with co-polar fades or isolation decreases. The most prominent example of this occurred on June 20 at 2100 GMT. At that time the co-polar signal intensity (Figure 3.2-11) began to decrease and continued to do so (almost linearly) for about four hours, reaching a peak attenuation of about 13 dB. It then returned rapidly (in several minutes) to the clear weather value. In the same fashion the cross-polarized signal level increased smoothly (Figure 3.2-12), and the isolation dropped to 13 dB (Figure 3.2-13). After this minimum was reached, the signals returned to their clear-weather values in a period of about 10 minutes. During the entire interval no rain was measured by the rain gauge network. However, rain began an hour after the end of this anomalous propagation event and continued intermittently for over five hours.

3.3 Phase Effects

Along with isolation and attenuation our receiver measures the phase difference between the co-polarized and cross-polarized signal components. These data are taken by a phase detector with a 10-second time constant. Hence fast phase fluctuations are suppressed.

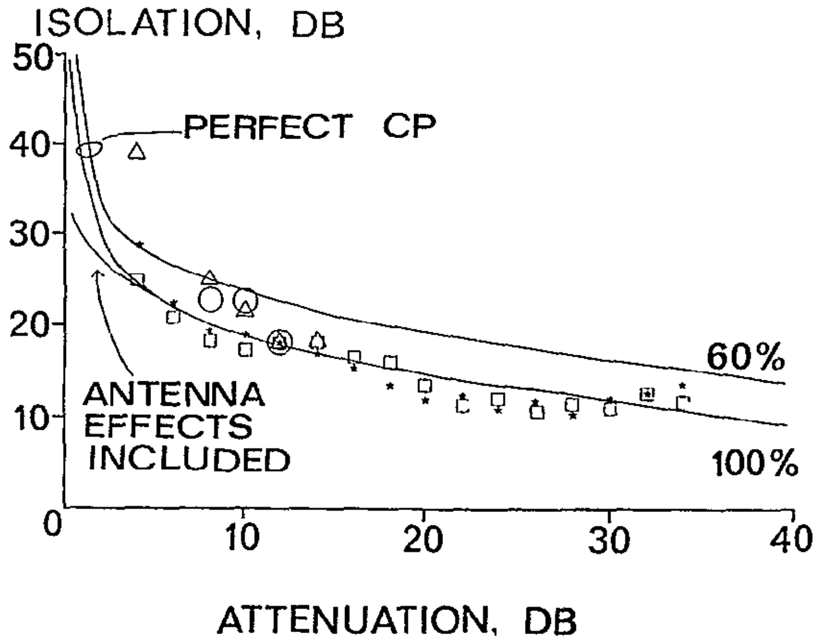

Figure 3.2-10 Comparison of theoretical values and experimental data.

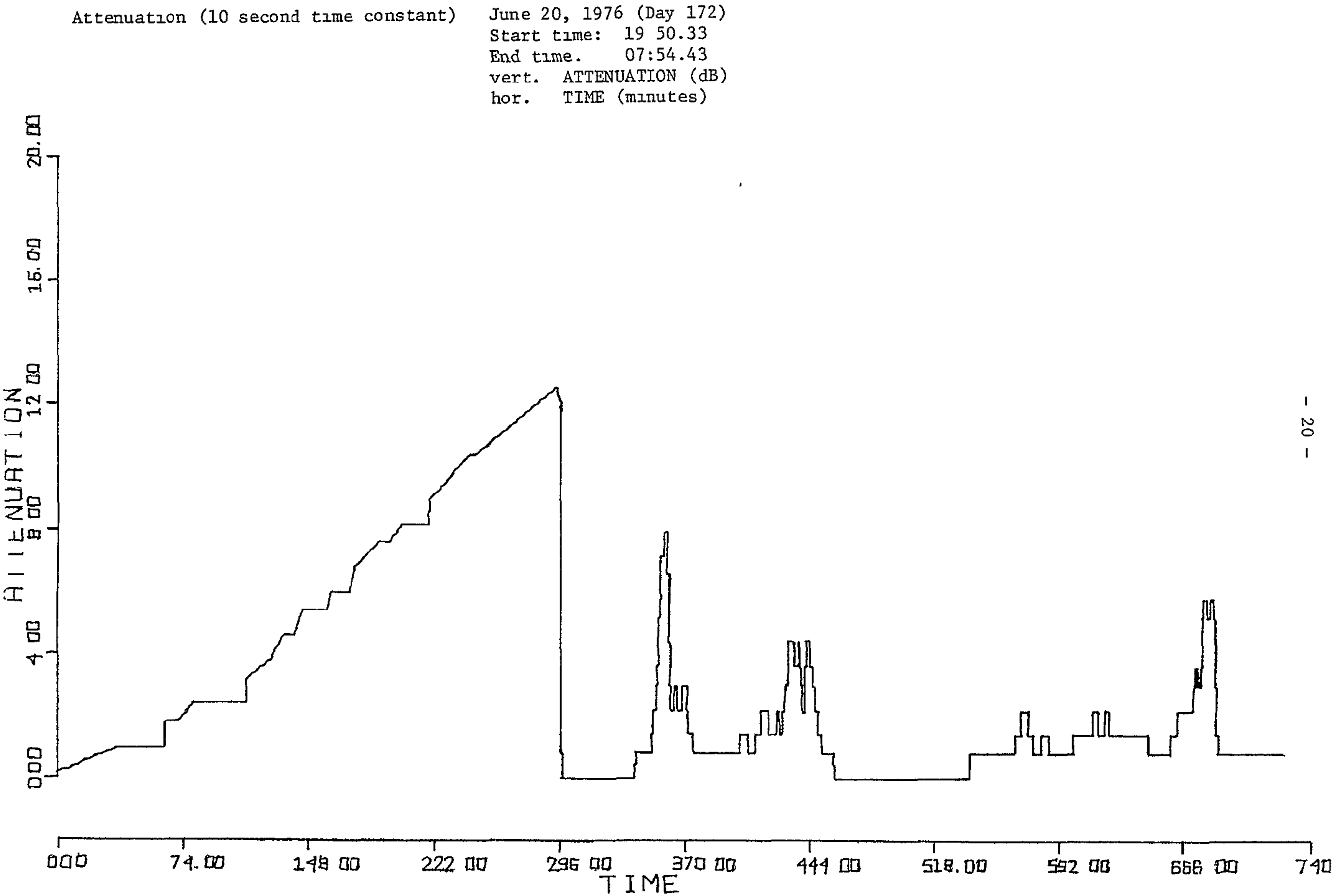

Figure 3.2-11 Attenuation for the event of June 20, 1976.

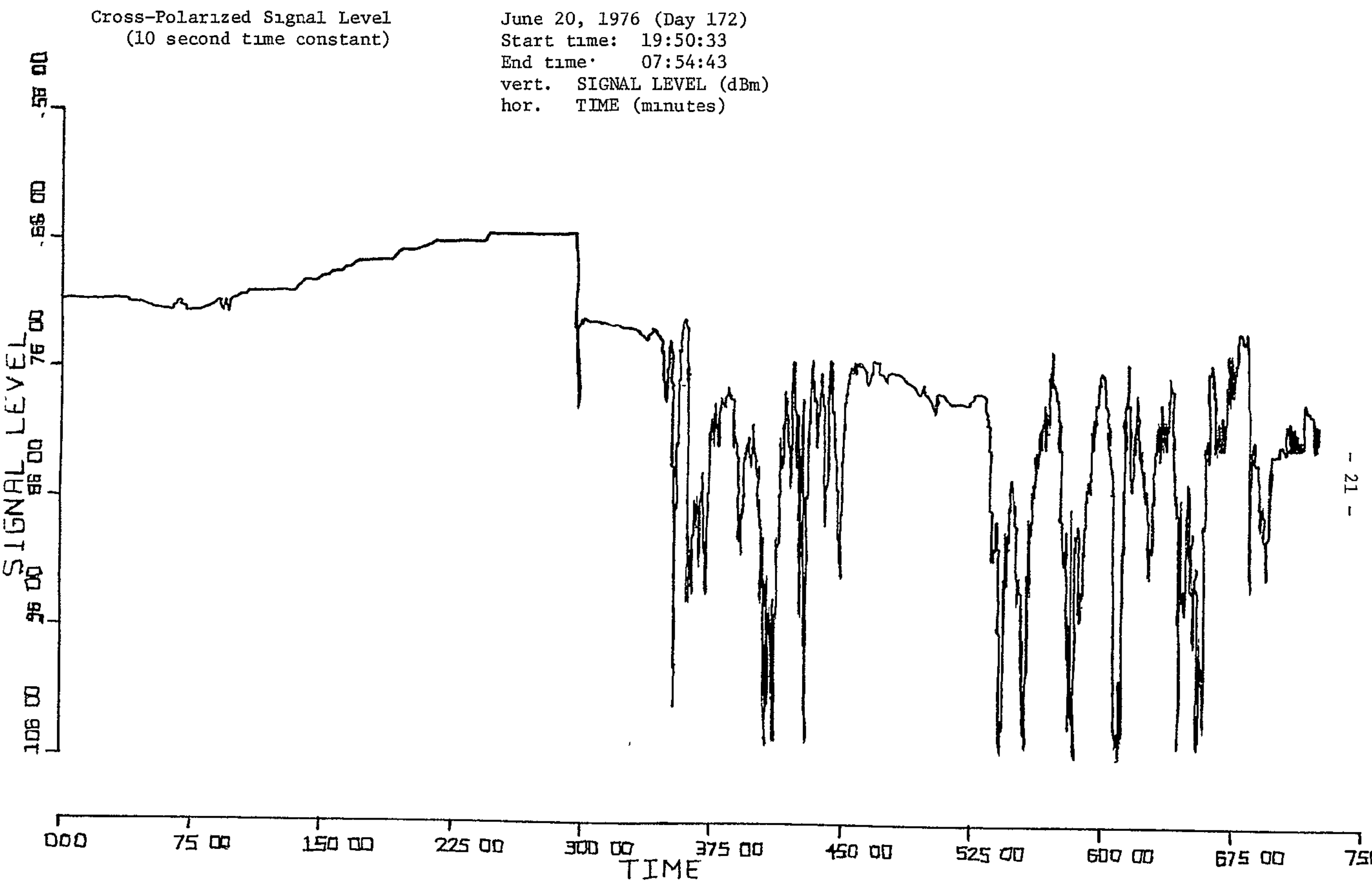

Figure 3.2-12 Cross-polarized signal level for the event of June 20, 1976.

Isolation (10 second time constant)

June 20, 1976 (Day 172)
Start time: 19:50 33
End time: 07 54.43
vert. ISOLATION (dB)
hor. TIME (minutes)

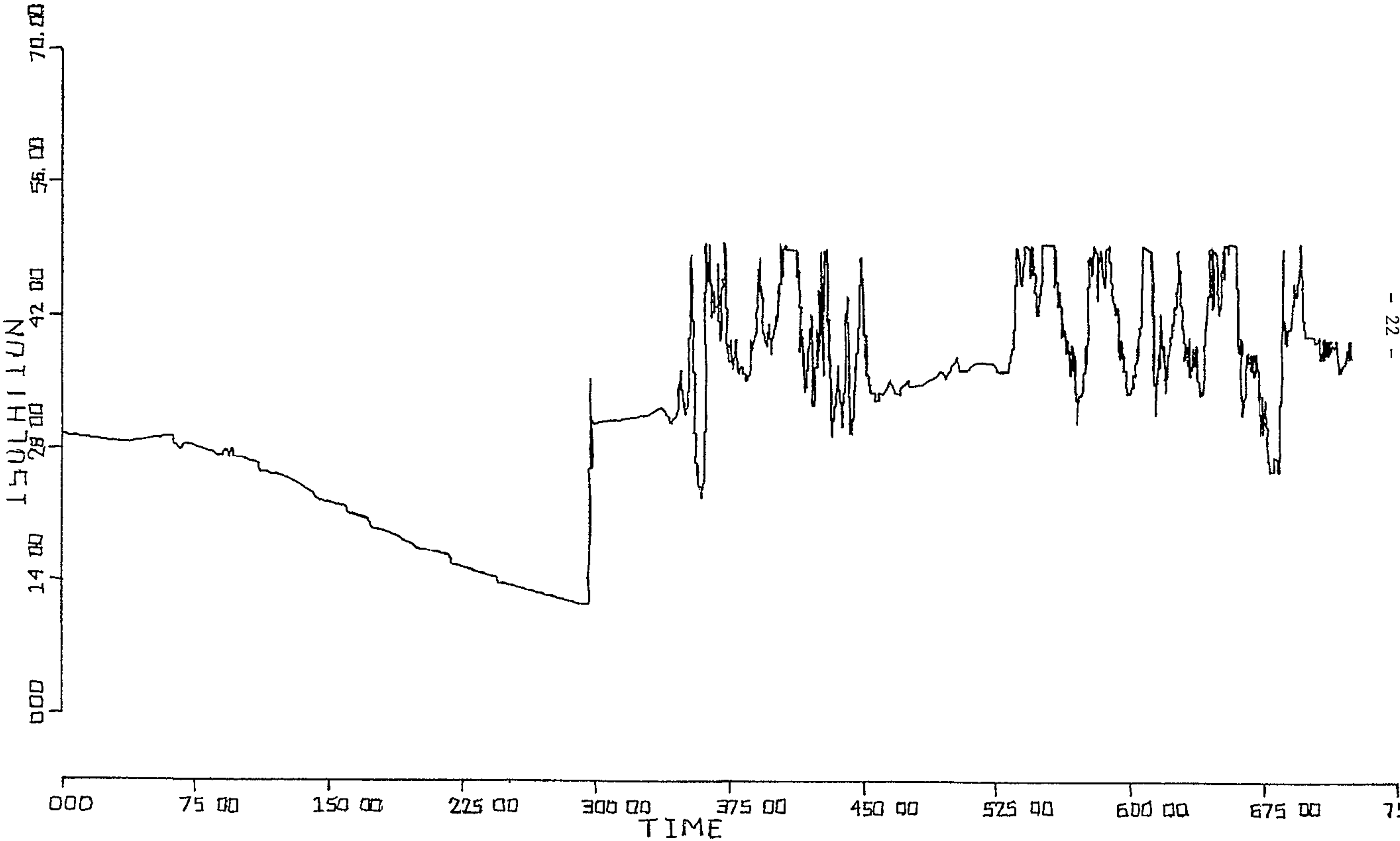

Figure 3.2-13 Isolation for the event of June 20, 1976.

The actual signals compared by the phase detector are the reference oscillator outputs from the phase locked loops in the two receiver channels. The phase locked loop in the co-polarized channel has a one-second time constant while the one in the cross-polarized channel has a 60-second time constant for increased sensitivity. This long time constant further smooths out fast phase variations and incidentally produces a temporary loss of cross-polarized phase lock during rapid changes in the differential phase. Simultaneous changes in the absolute phase of both signals do not produce this effect.

Typical phase data taken during rain are shown in Figure 3.3-1 which displays differential phase versus time for a storm on June 26, 1967. The phase starts to fluctuate when rain attenuation begins. As the fade increases, the differential phase decreases (<u>in this case</u>) and has decreased by about 150 degrees by the time the attenuation has reached 3 dB. As the fade continues to almost 13 dB there is little additional change in the phase. The phase remains relatively constant until the fade decreases to about 3 dB. From there to 0 dB it varies widely and then returns to its clear weather value when the fade is over.

Figure 3.3-2 shows a similar effect from a storm on June 20, 1967. This time the phase decreases about 150 degrees in association with a 2.5 dB fade and then returns to its clear weather value when the attenuation ends.

Figures 3.3-1 and 3.3-2 both showed the phase dropping at the beginning of a fade and saturating at attenuation levels between 2 and 3 dB. Sometimes an opposite effect occurs and the phase increases before saturating. This happened in the July 30, 1976 storm, as Figure 3.3-3 indicates. (The terraced aspect of the curve in Figure 3.3-3 is an artifact of the data

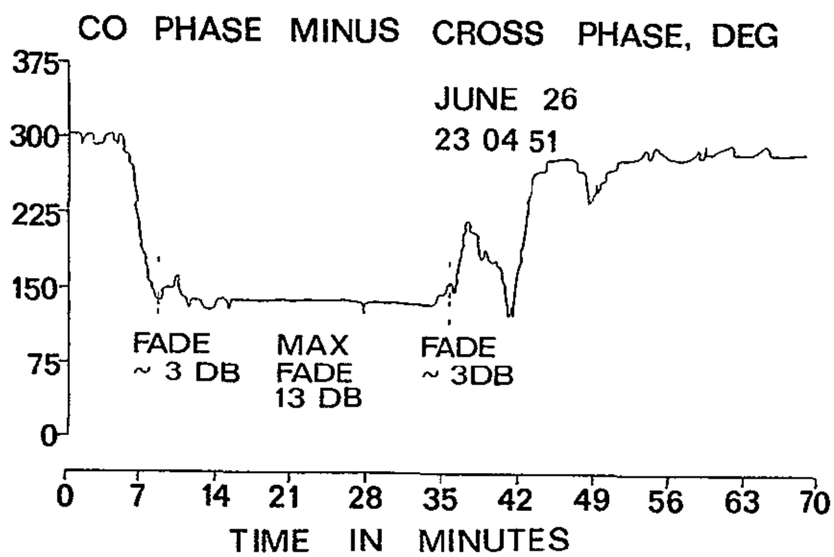

Figure 3.3-1 Differential phase behavior on June 26.

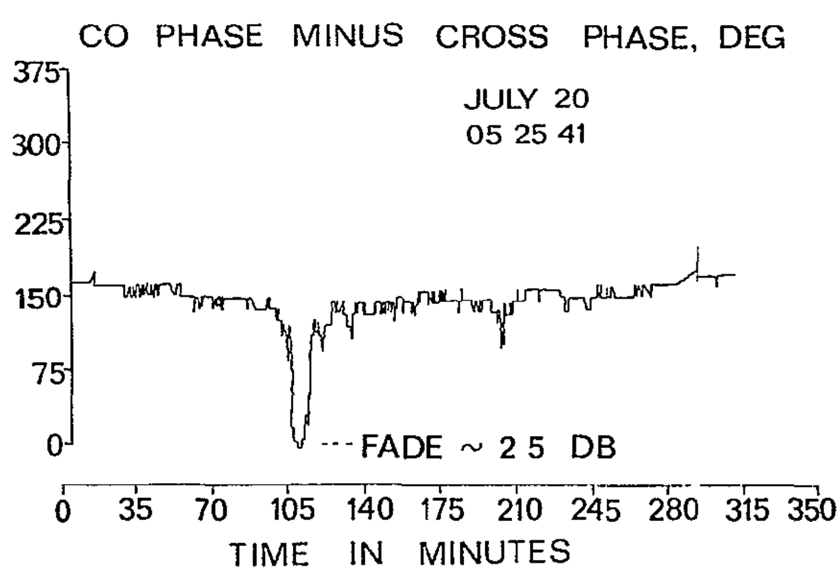

Figure 3.3-2 Differential phase behavior on July 20.

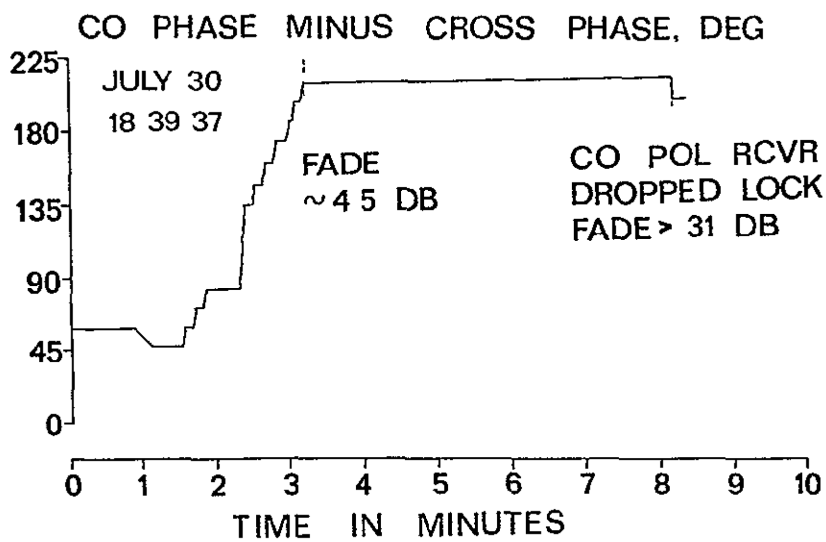

Figure 3.3-3 Differential phase behavior on July 30.

processing system and occurs when the phase change between sampling times is smaller than the minimum increment that the computer is programmed to record.) In some cases the differential phase can increase and decrease in the same storm. This is illustrated by Figure 3.3-4 where large fluctuations occurred when the attenuation was less than about 1 dB and saturation occurred twice.

At present we have no firm theoretical explanation for the phase effects that have been observed. The theory indicates that the phase should change rapidly with rain rate when the rain rate is small and then saturate as the rainfall intensity grows. The direction (decrease or increase) of the phase change is sensitive to the drop parameters and the antenna characteristics in a complicated way; a model for predicting it is yet undeveloped.

3.4 Attenuation and Isolation Statistics

Figures 3.4-1 through 3.4-3 present logarithmic percent-of-time plots for rain fall rates, attenuation, and isolation over this summer 1976 time period. Figures 3.4-4 through 3.4-6 display the same information in linear form.

The curves for attenuation show that large values of attenuation are more probable than theory would have predicted for the ground rainfall rates observed. This is consistent with our observations for individual storms as well as with those of other CTS experimenters.

3.5 Implications for Modeling

When satellite path rain depolarization and attenuation can be pre-

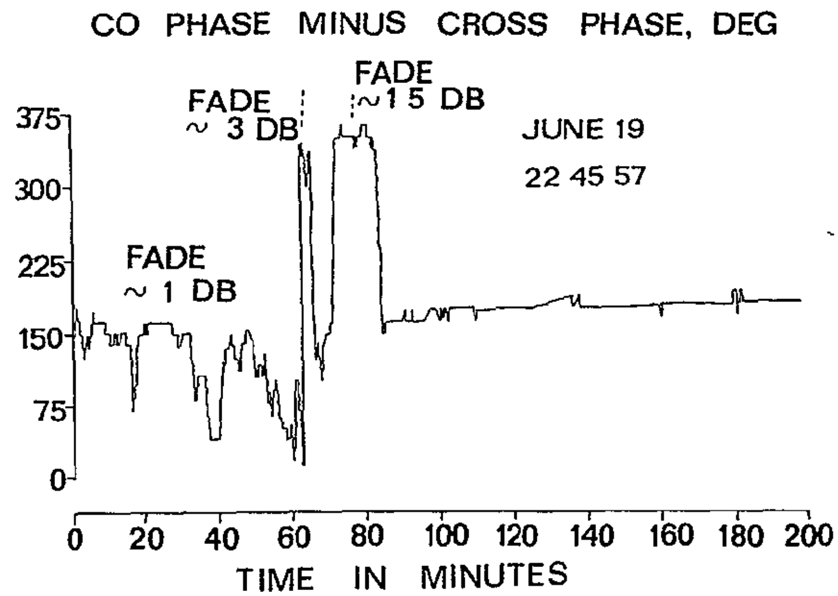

Figure 3.3-4 Differential phase behavior on June 19.

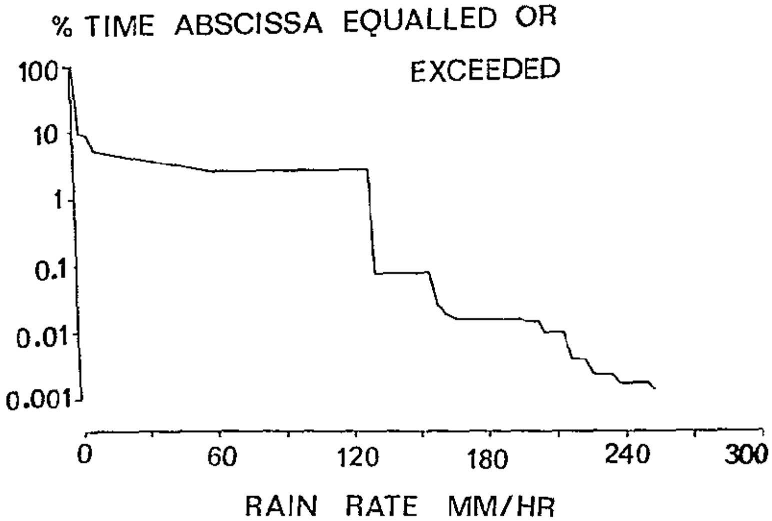

Figure 3.4-1 Logarithmic percent-of-time plot for summer 1976 rain rate data.

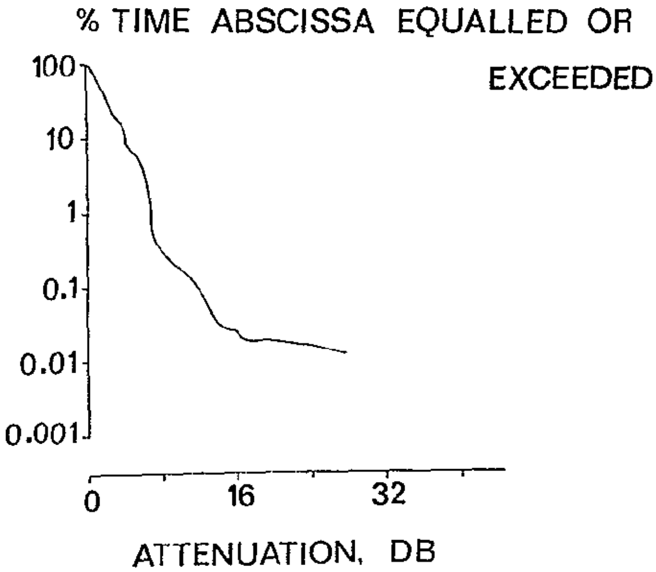

Figure 3.4-2 Logarithmic percent-of-time plot for summer 1976 attenuation data.

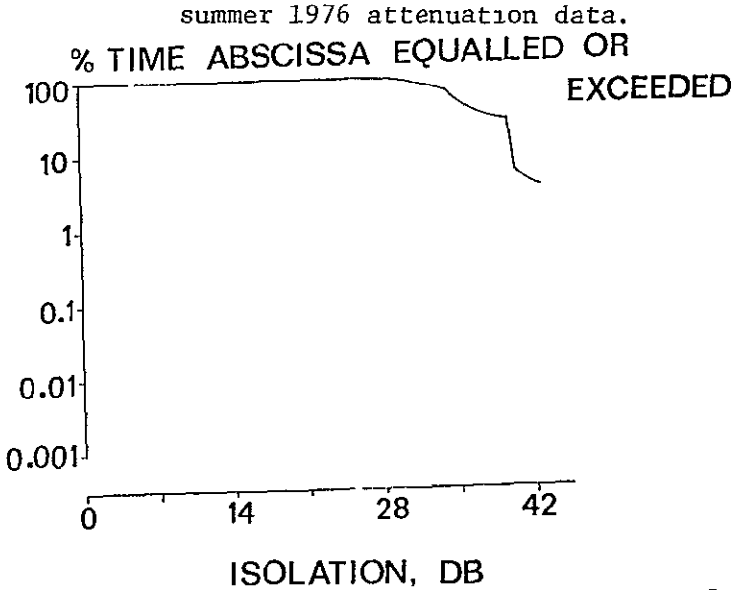

Figure 3.4-3 Logarithmic percent-of-time plot for summer 1976 isolation data.

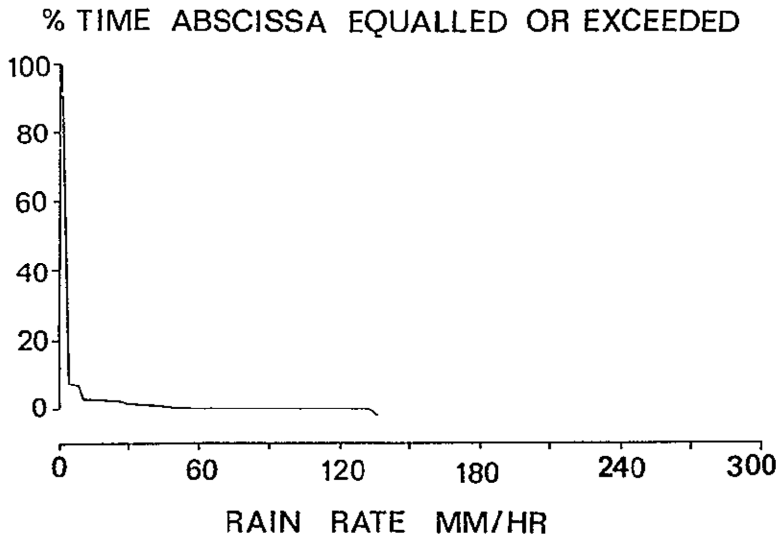

Figure 3.4-4 Linear percent-of-time plot for summer 1976 rain rate data.

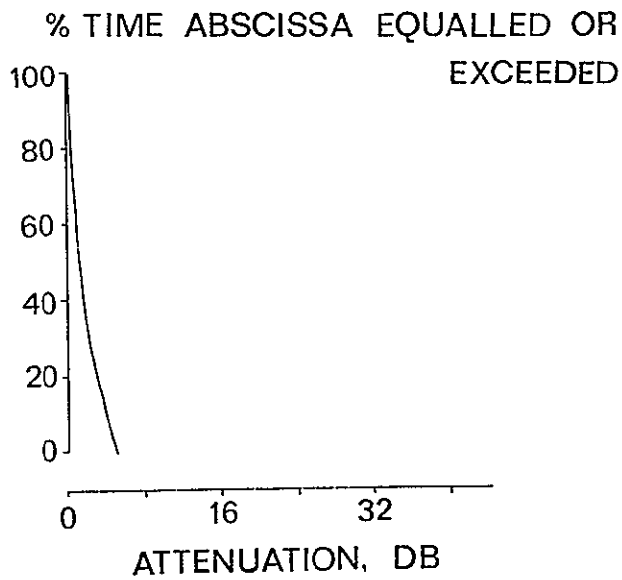

Figure 3.4-5 Linear percent-of-time plot for summer 1976 attenuation data

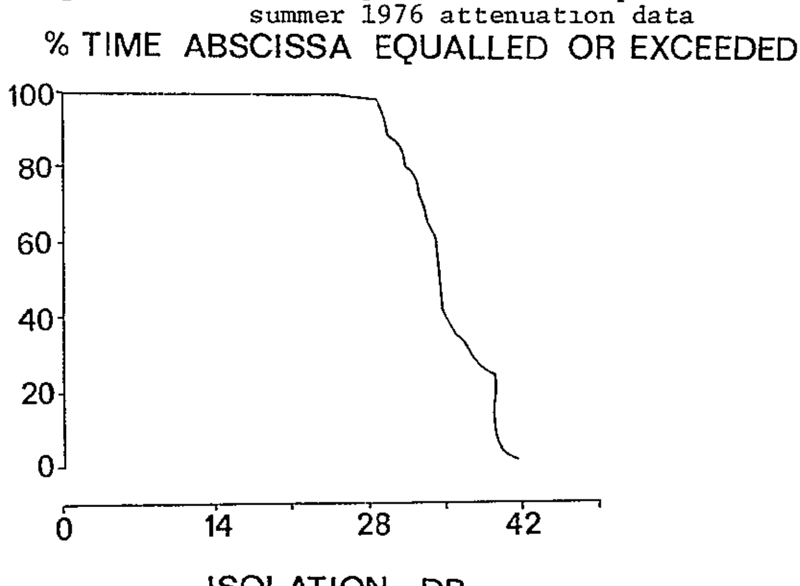

Figure 3.4-6 Linear percent-of-time plot for summer 1976 isolation data.

dicted from ground rainfall data, reliable dual-polarized millimeter wave satellite links can be designed for any earth station location For this reason, an important objective of this project is to model atmospheric propagation effects in terms of ground-based observations.

Because of the time required for raindrops to fall from the propagation path to rain gauges on the ground, no investigator has detected a meaningful correlation between simultaneous values of ground rainfall rate and attenuation. Our findings confirm this and indicate that isolation is also uncorrelated with ground rain rate. Other approaches to modeling are possible, including (1) a storm-by-storm comparison of peak rain rate, minimum isolation, and maximum isolation, (2) shifting the ground rain rate in time to compensate the time required for the drops to fall [3], and (3) comparing the attenuation and isolation statistics with the rain rate statistics. Each of these will be discussed in turn.

Figure 3.5-1 compares the maximum attenuation and the maximum observed ground rain rate for each day in the reporting period. Also plotted are the theoretical curves for a uniform rain medium discussed in Section 3.2. The effective rain medium is assumed to contain 100% oblate drops with 0° canting angle. Some points lie close to their theoretical values. The widely-scattered points probably represent rain cells in the path but beyond our rain gauge network. A 15.5 GHz radar system now in operation will analyze these during the second year's effort.

Figure 3.5-2 relates the minimum isolation and maximum rain rate for each storm. These are compared with the theoretical plot of isolation versus rain rate (antenna effects included) described in Section 3.2.

While Figures 3.5-1 and 3.5-2 indicate a general consistency between the peak ground rainfall rate and the associated propagation effects, it is

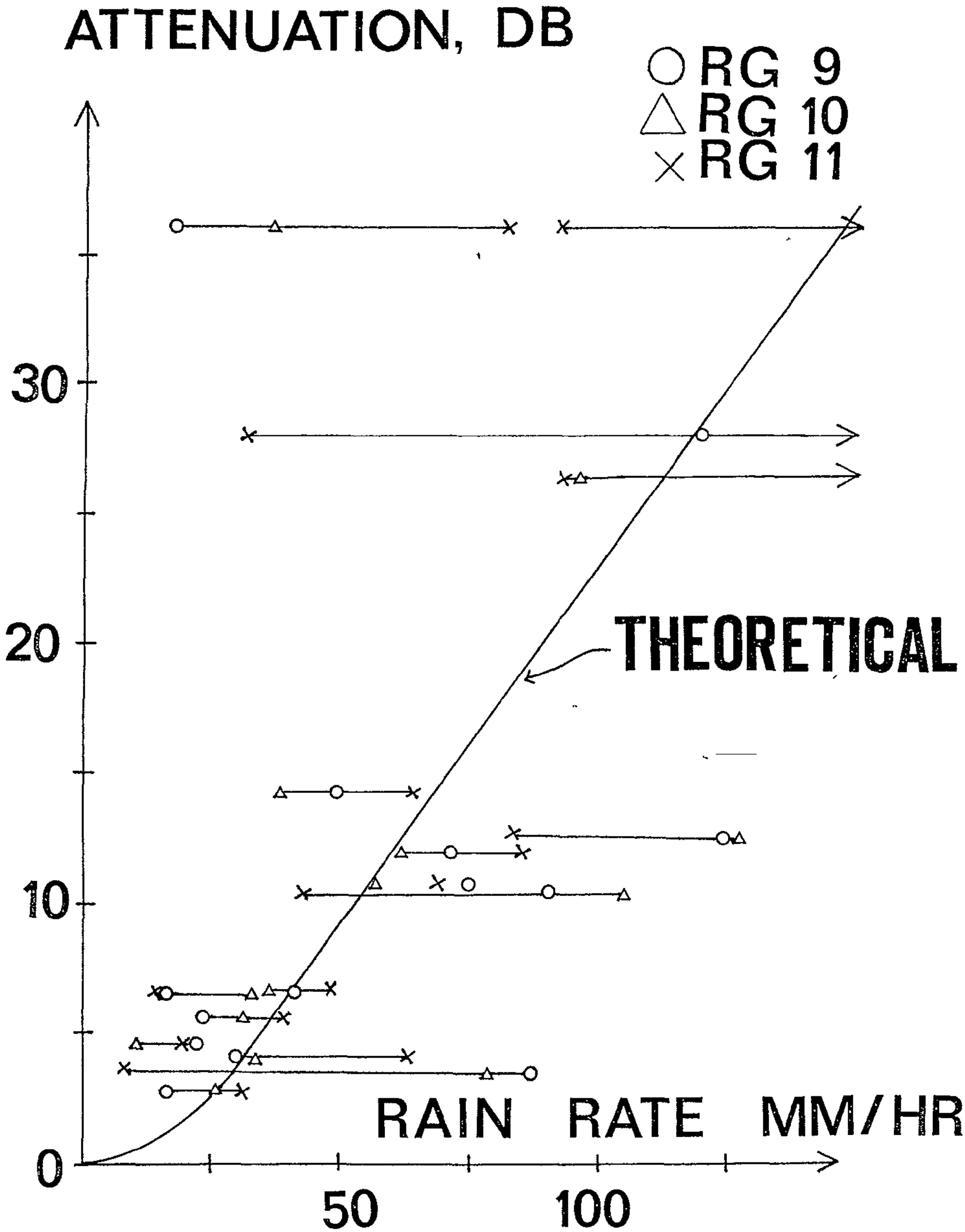

Figure 3.5-1 Maximum attenuation and maximum observed ground rainfall rate for each storm.

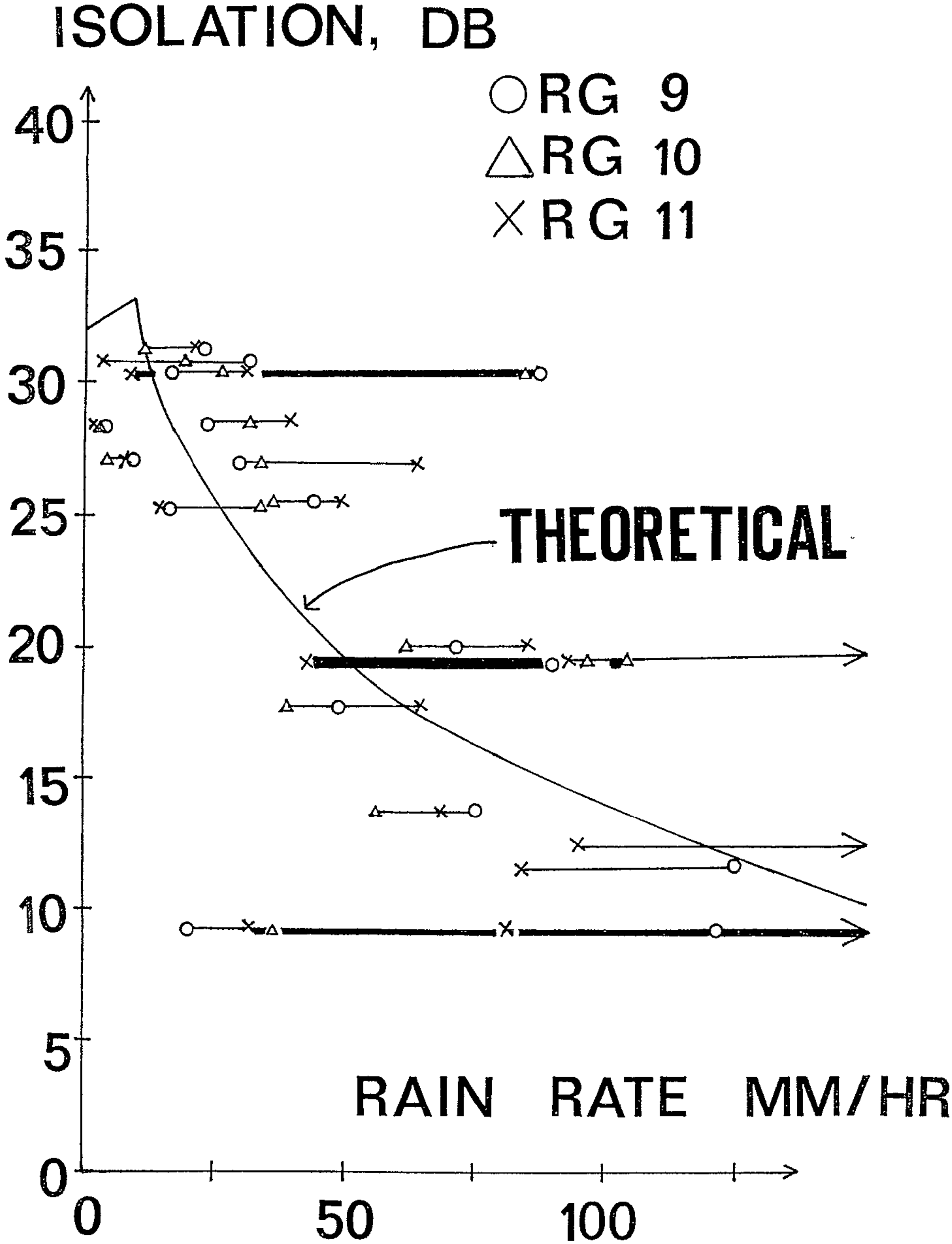

Figure 3.5-2 Minimum isolation and maximum observed ground rainfall rate for each storm.

not possible to use ground rain rate at any one gauge to predict isolation or attenuation with any useful degree of certainty. This is particularly true at the higher rain rates, where rain cells are much smaller and the variation between individual gauges is much greater.

Dixon Fang of Comsat Laboratories has developed a technique for reconstructing the drop size distribution in a satellite path from rain rate data collected on the ground. For the rain events that Fang has investigated this approach yields theoretical curves of attenuation versus ground rain rate that agree well with measured values. We intend to pursue this approach during the second year of CTS operation. Our attempts thus far to automate the procedure and adapt it to our data processing system have been unsuccessful.

Another question to be addressed in the modeling process is this: Can isolation and attenuation statistics be derived reliably from rain rate statistics? Evidence from other sites indicates that the answer is yes for attenuation, but isolation statistics are only now being accumulated. Our data base from the first year's operation is too small for a meaningful comparison, but this problem will also be addressed during the second year.

We have also begun to explore the possibility of deriving isolation statistics from attenuation statistics. If successful, this approach would permit a statistical prediction of isolation for sites where the statistics of rain attenuation are already known. Our hypothesis is that, since attenuation is directly related to rain rate and isolation is inversely related to rain rate, the isolation value equalled or exceeded P% of the time should be correlated with the attenuation value equalled or exceeded (100-P)% of the time. The corresponding values for the first year's data are as follows:

P	Isolation Equalled or Exceeded P% of Time	100-P	Attenuation Equalled or Exceeded (100-P)% of Time
99.90	13.01 dB	0.10	12.64 dB
99.75	15.40 dB	0.25	10.90 dB
99.50	21.34 dB	0.50	8.08 dB
99.00	27.01 dB	1.00	4.76 dB
98.00	28.39 dB	2.00	3.93 dB
95.00	29.46 dB	5.00	2.86 dB

These results are plotted in Figure 3.5-3 and compared with the data for the four most severe storms observed during the report period. Agreement is fair and this procedure will be pursued with the larger data base from the second year's work

3.6 Conclusions

Data collected thus far indicate that, at least during summer convective storms, attenuation at 11.7 GHz is much more severe than anticipated. Attenuation may be a more serious impediment to commercial dual-polarized satellite links at this frequency than is depolarization.

4. Data From Individual Storms

This section presents data from the significant storms which occurred during the reporting period. For each storm plots (when available) are presented in the following order.

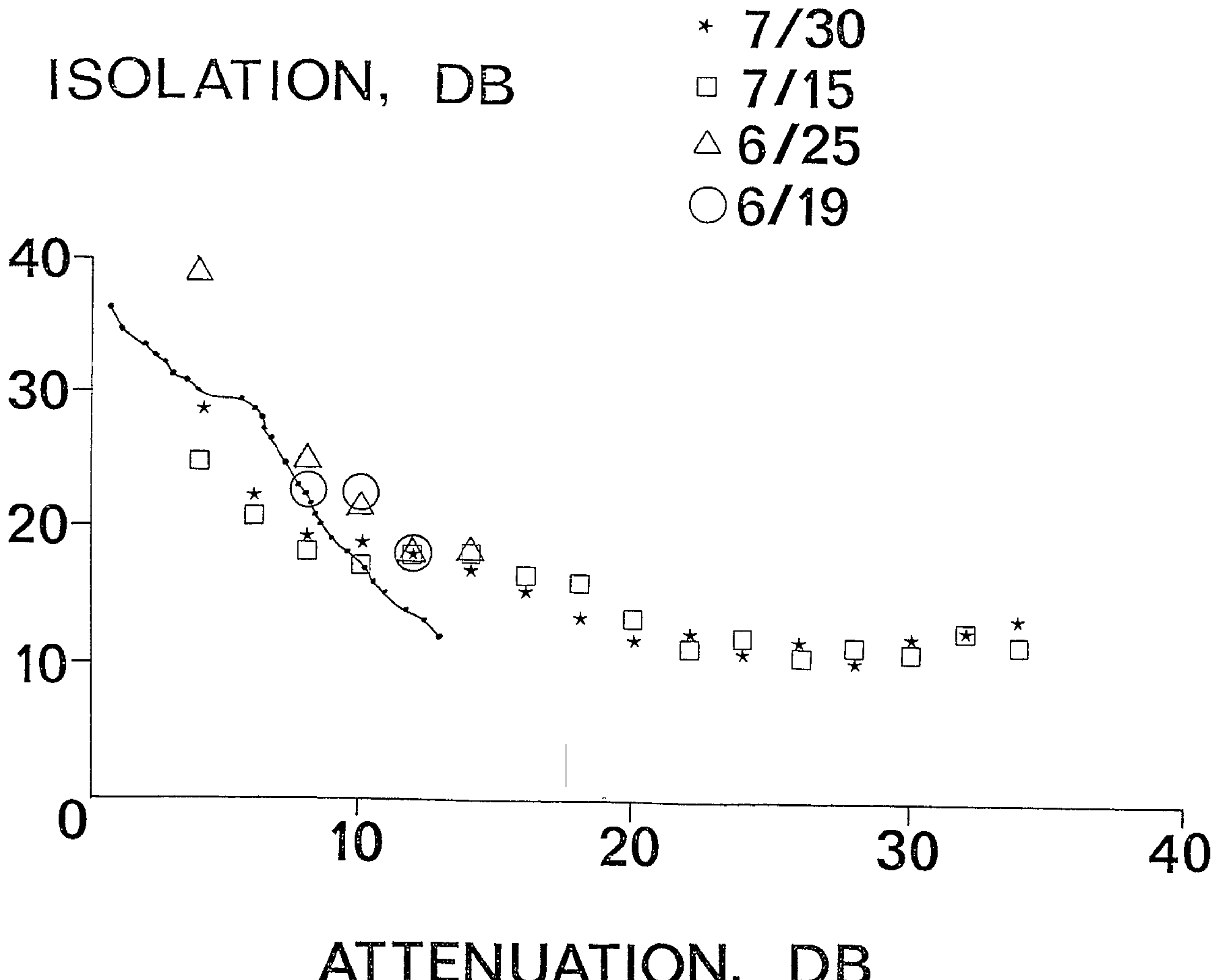

Figure 3.5-3 Statistically-related isolation and phase values for the summer of 1976 compared with measured data from the most intense storms.

Plot #	Description
1.	Rain rate at RG #9, the station rain gauge.
2.	Rain rate at RG #10, 175 meters from the receiver along the propagation path.
3.	Rain rate at RG #11, 563 meters from the receiver along the propagation path.
4.	Rain rate at RG #12, 975 meters from the receiver, 72° east of the propagation path.
5.	Rain rate at RG #13, 1400 meters from the receiver, 98° east of the propagation path.
6.	Co-polarized signal level, 0.016 Hz bandwidth.
7.	Cross-polarized signal level, 0.016 Hz bandwidth.
8.	Attenuation (0.016 Hz bandwidth).
9.	Isolation (0.016 Hz bandwidth).
10.	Isolation versus attenuation.

Plots #4 and #5 are not presented for all storms. The rain gauges involved are so far away from the path that these rain rates provide no useful information.

No phase plots are included. The computer routine for automatically plotting phase had a scaling error which could not be corrected in time for this report. All phase data were examined and significant events were plotted by hand for display in Section 3.3.

Rain Rate (RG #9 - Site Rain Gauge)

June 19-20, 1976 (Days 171 & 172)
Start time: 17:26:53
End time 05:19:06
vert. RAIN RATE (mm/hr)
hor. TIME (minutes)

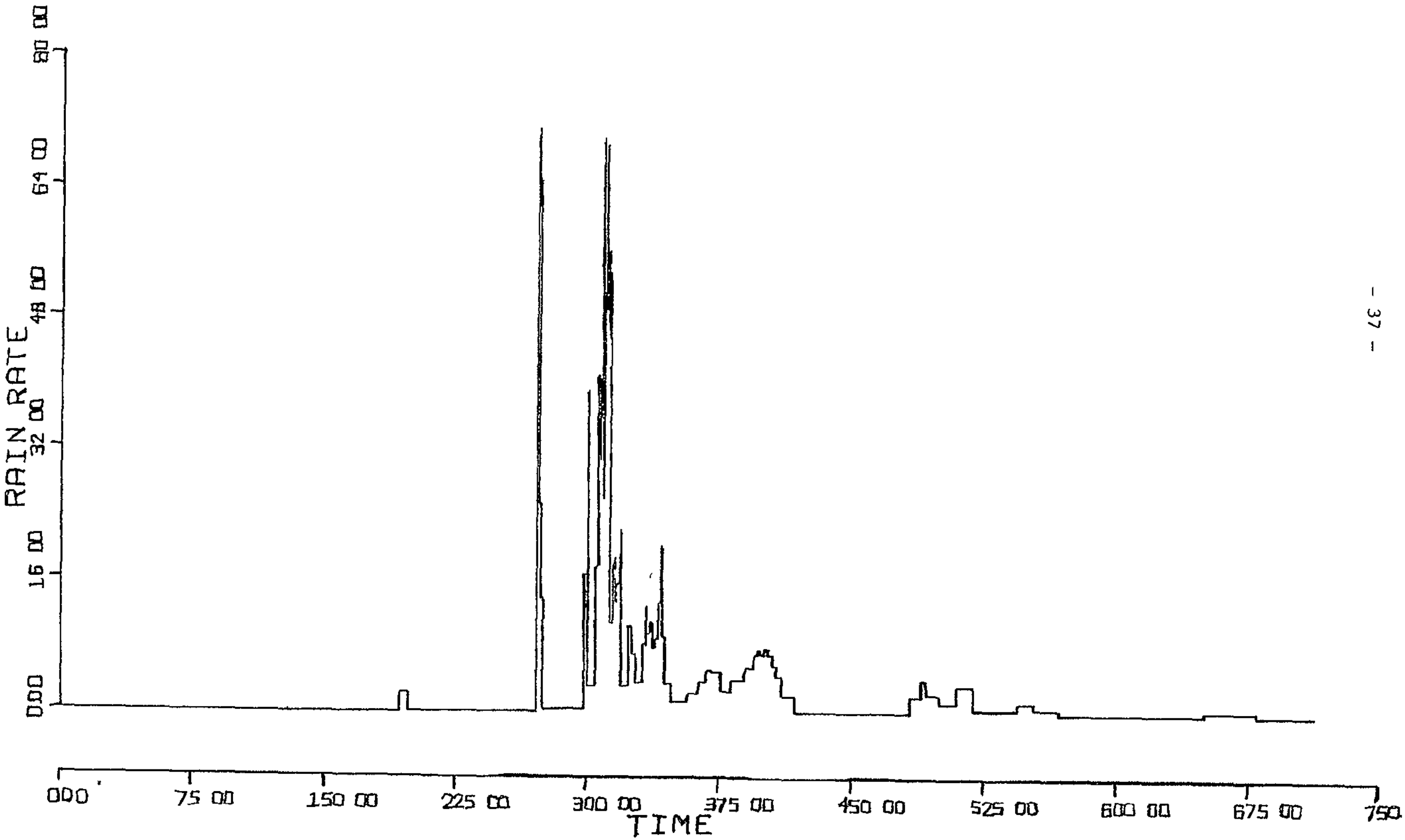

Rain Rate (RG #10 - 175 meters from receiver along path)

June 19-20, 1976 (Days 171 & 172)
Start time: 17:26:53
End time: 05:19:06
vert. RAIN RATE (mm/hr)
hor. TIME (minutes)

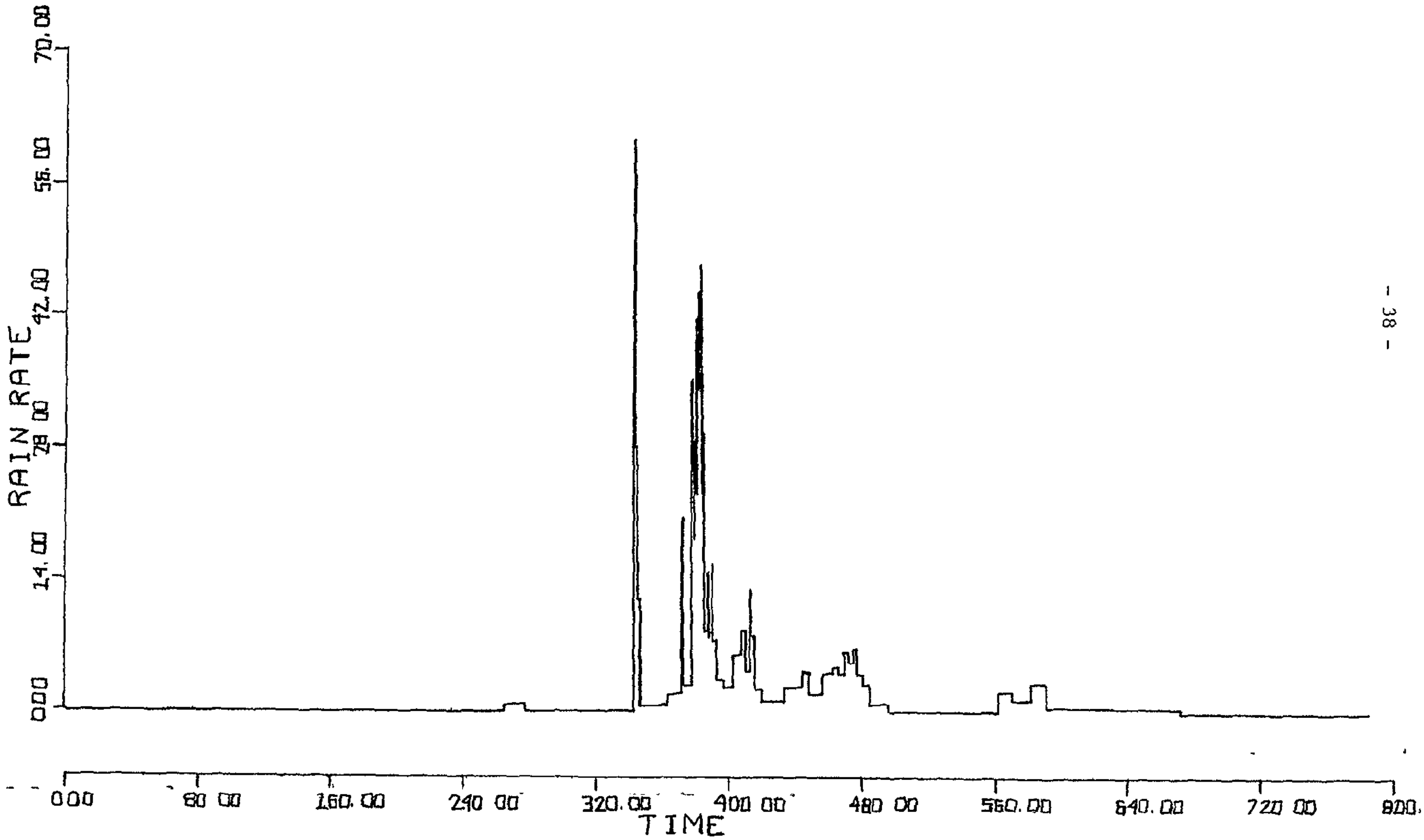

Rain Rate (RG #11 - 563 meters from receiver along path)

June 19-20, 1976 (Days 171 & 172)
Start time: 17:26.53
End time: 05:19:06
vert. RAIN RATE (mm/hr)
hor. TIME (minutes)

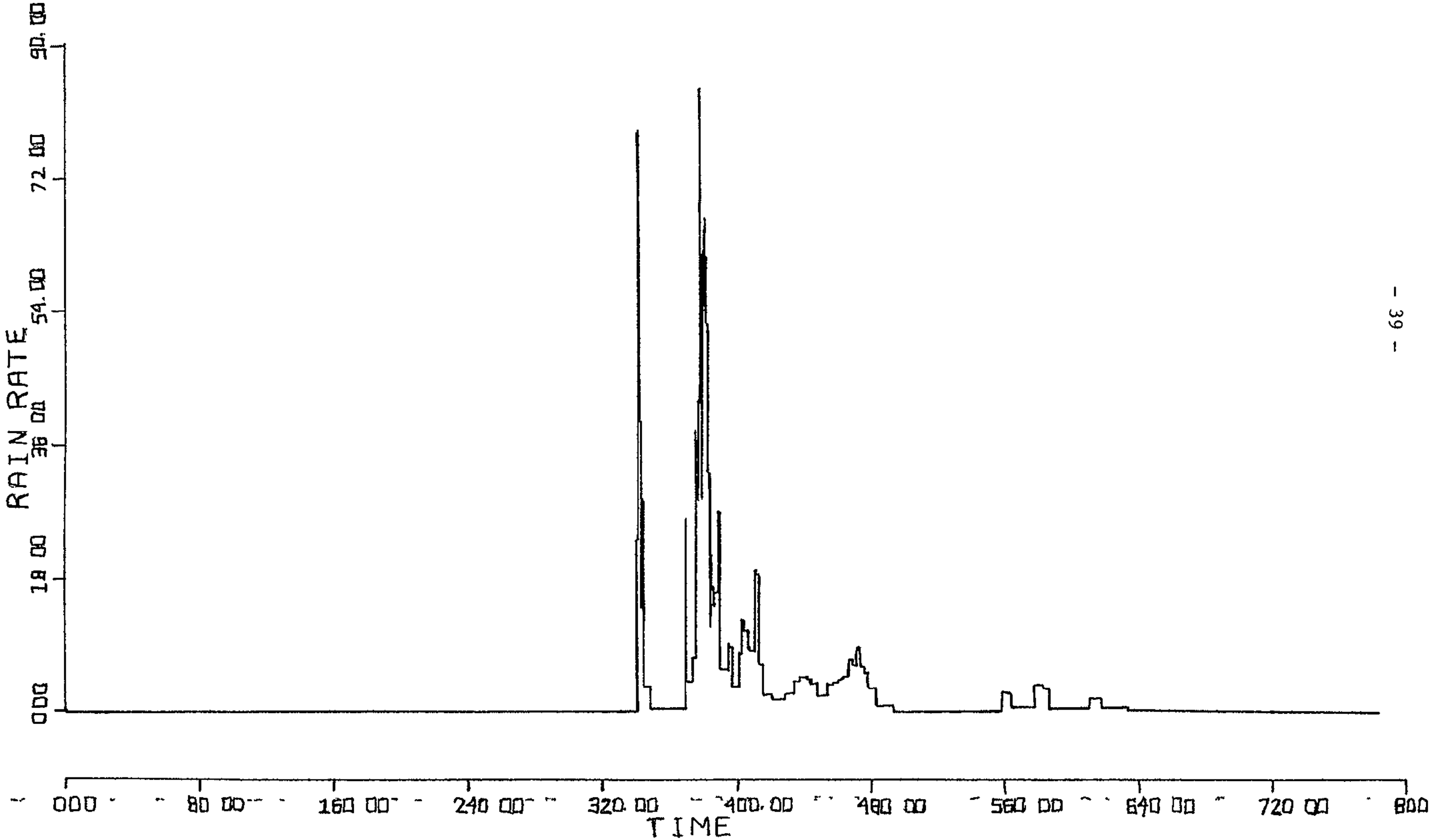

Rain Rate (RG #12 - 975 meters from
receiver, 72° east of path)

June 19-20, 1976 (Days 171 & 172)
Start time: 17:26:53
End time: 05:19 06
vert RAIN RATE (mm/hr)
hor. TIME (minutes)

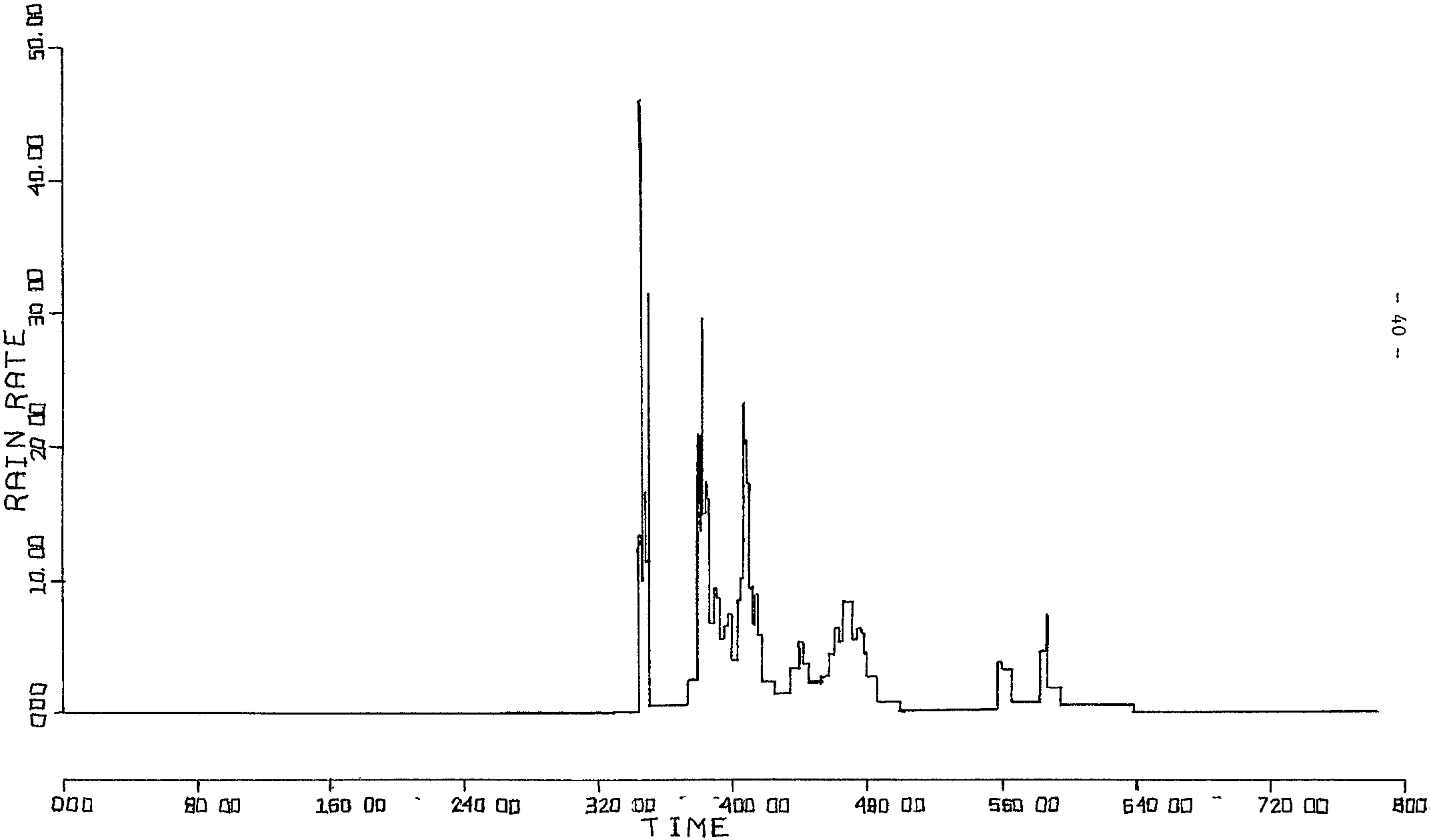

Rain Rate (RG #13 - 1400 meters from
receiver, 98° east of path)

June 19-20, 1976 (Days 171 & 172)
Start time: 17:26:53
End time: 05:19:06
vert. RAIN RATE (mm/hr)
hor. TIME (minutes)

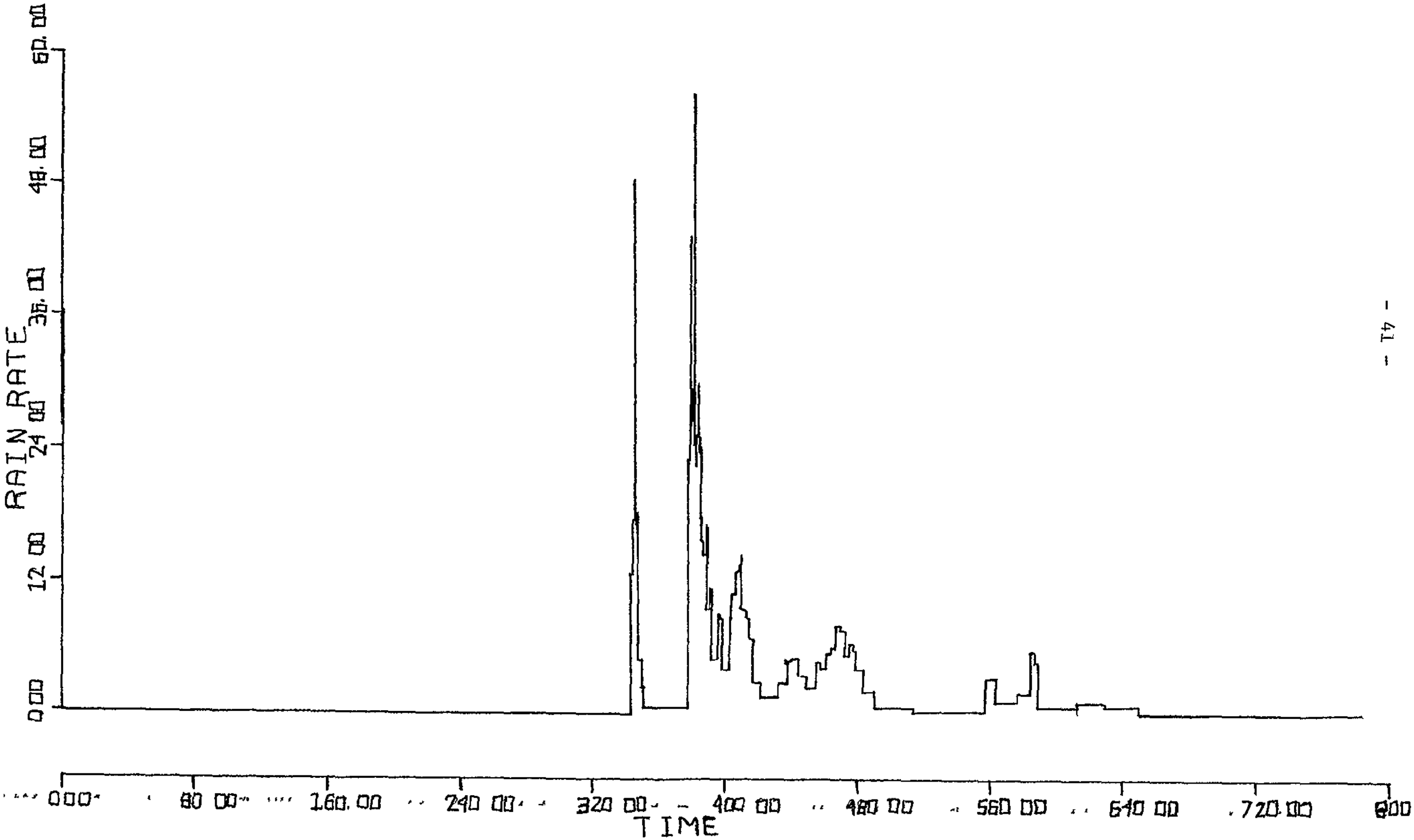

Co-Polarized Signal Level
(10 second time constant)

June 19-20, 1976 (Days 171 & 172)
Start time: 17:26:53
End time: 05:19:06
vert. SIGNAL LEVEL (dBm)
hor. TIME (minutes)

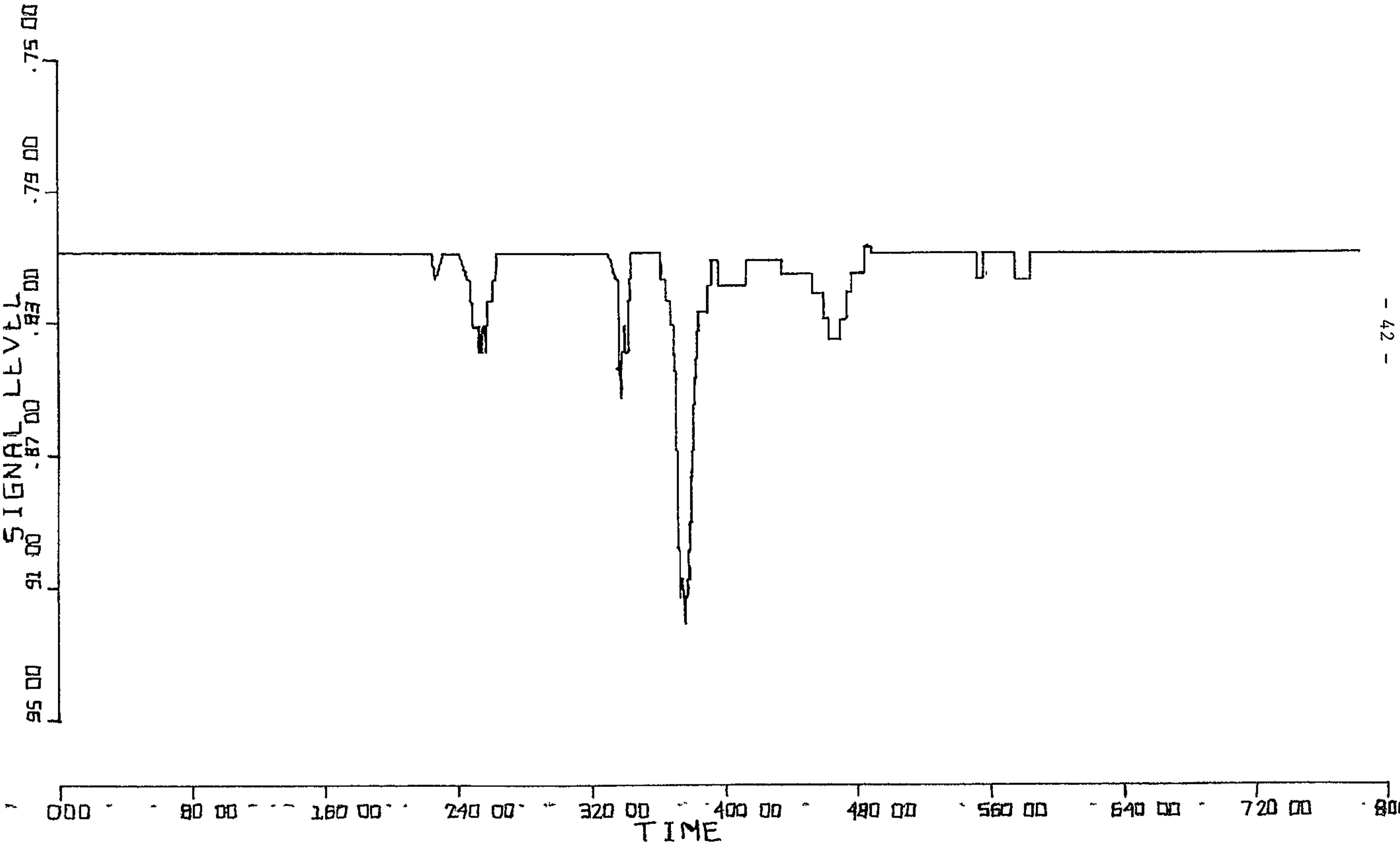

Cross-Polarized Signal Level
(10 second time constant)

June 19-20, 1976 (Days 171 & 172)
Start time: 17:26·53
End time: 05:19:06
vert. SIGNAL LEVEL (dBm)
hor. TIME (minutes)

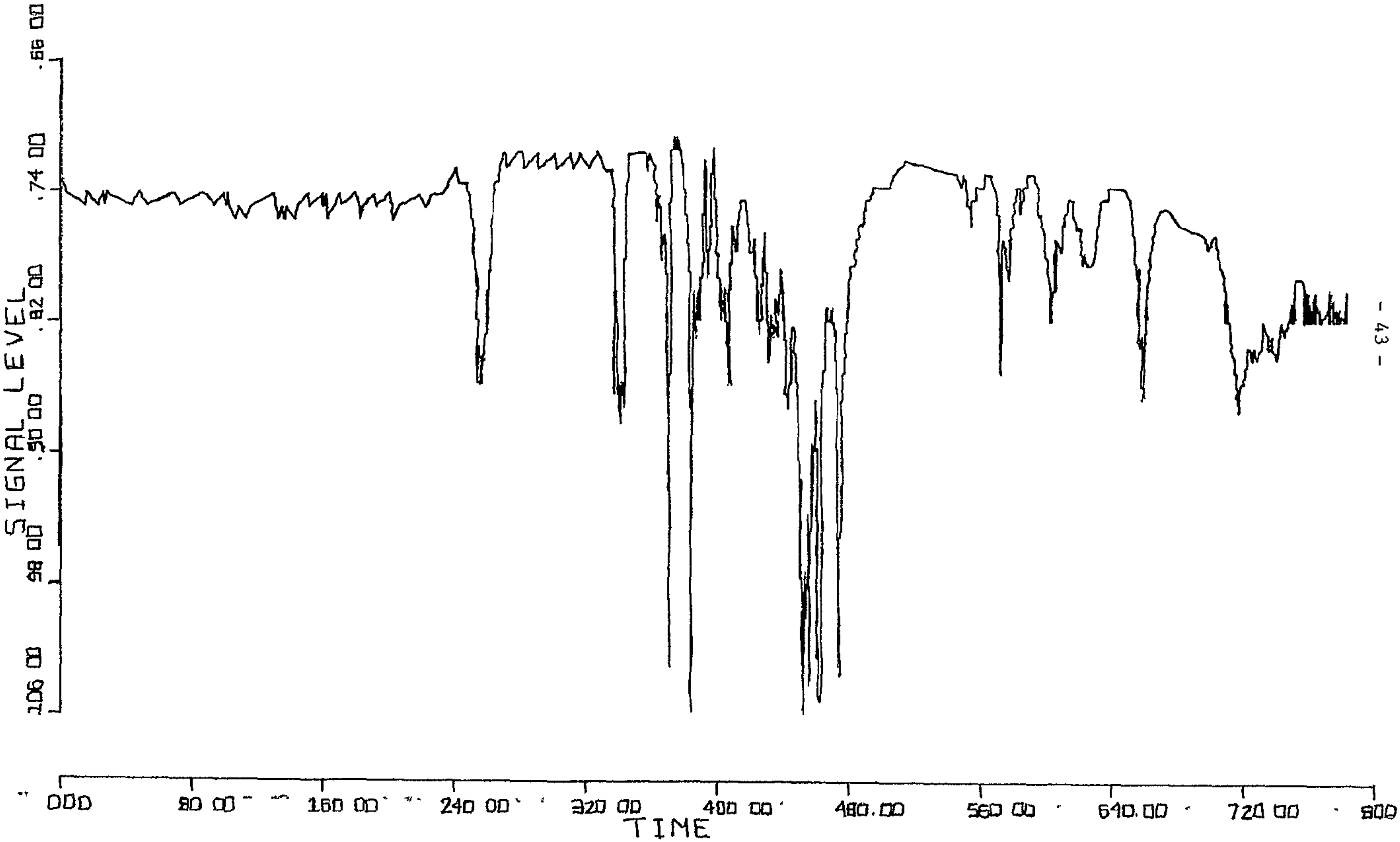

Attenuation (10 second time constant)

June 19-20, 1976 (Days 171 & 172)
Start time: 17:26:53
End time: 05:19:06
vert. ATTENUATION (dB)
hor. TIME (minutes)

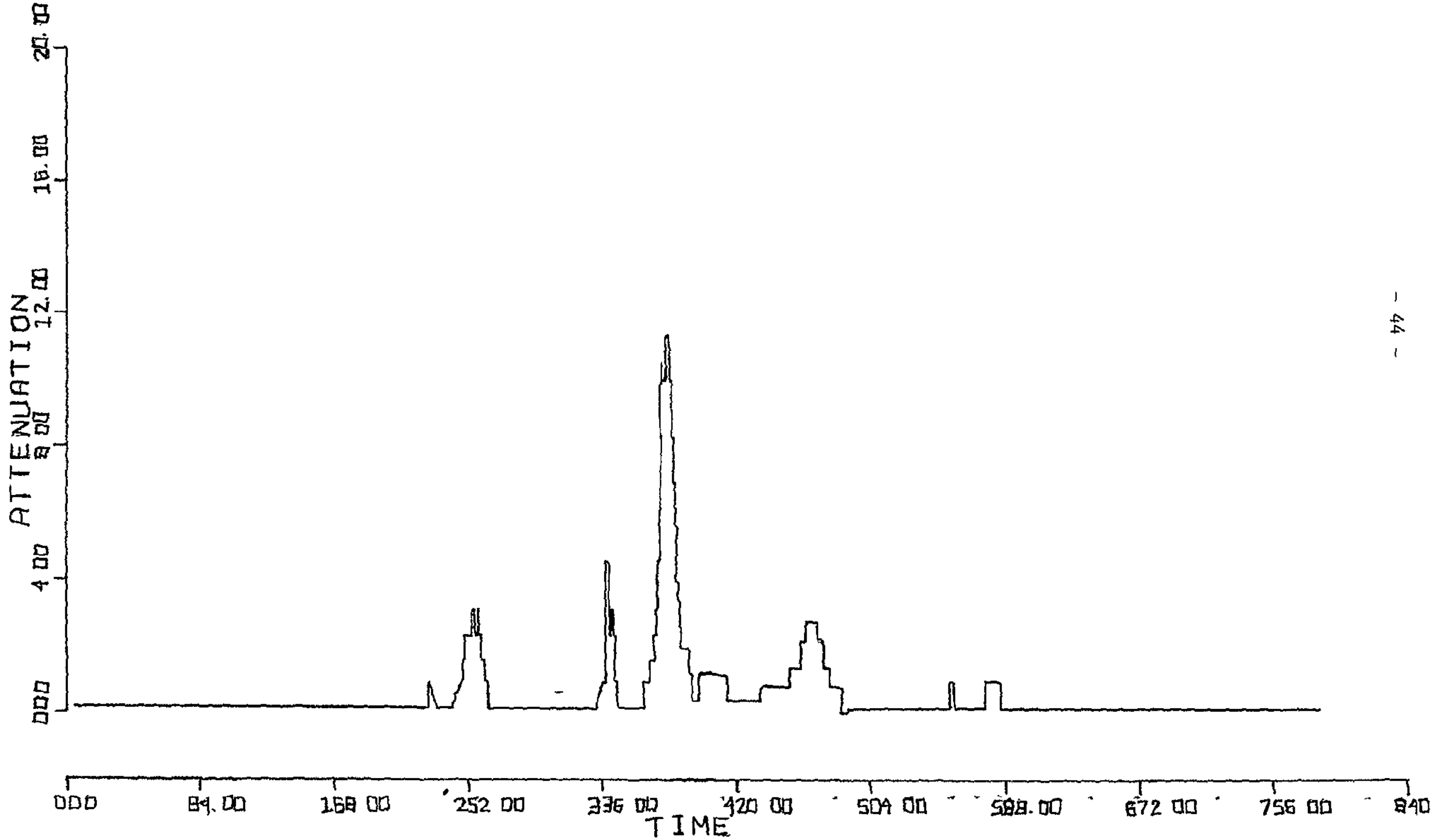

Isolation (10 second time constant)

June 19-20, 1976 (Days 171 & 172)
Start time: 17:26:53
End time: 05:19:06
vert. ISOLATION (dB)
hor. TIME (minutes)

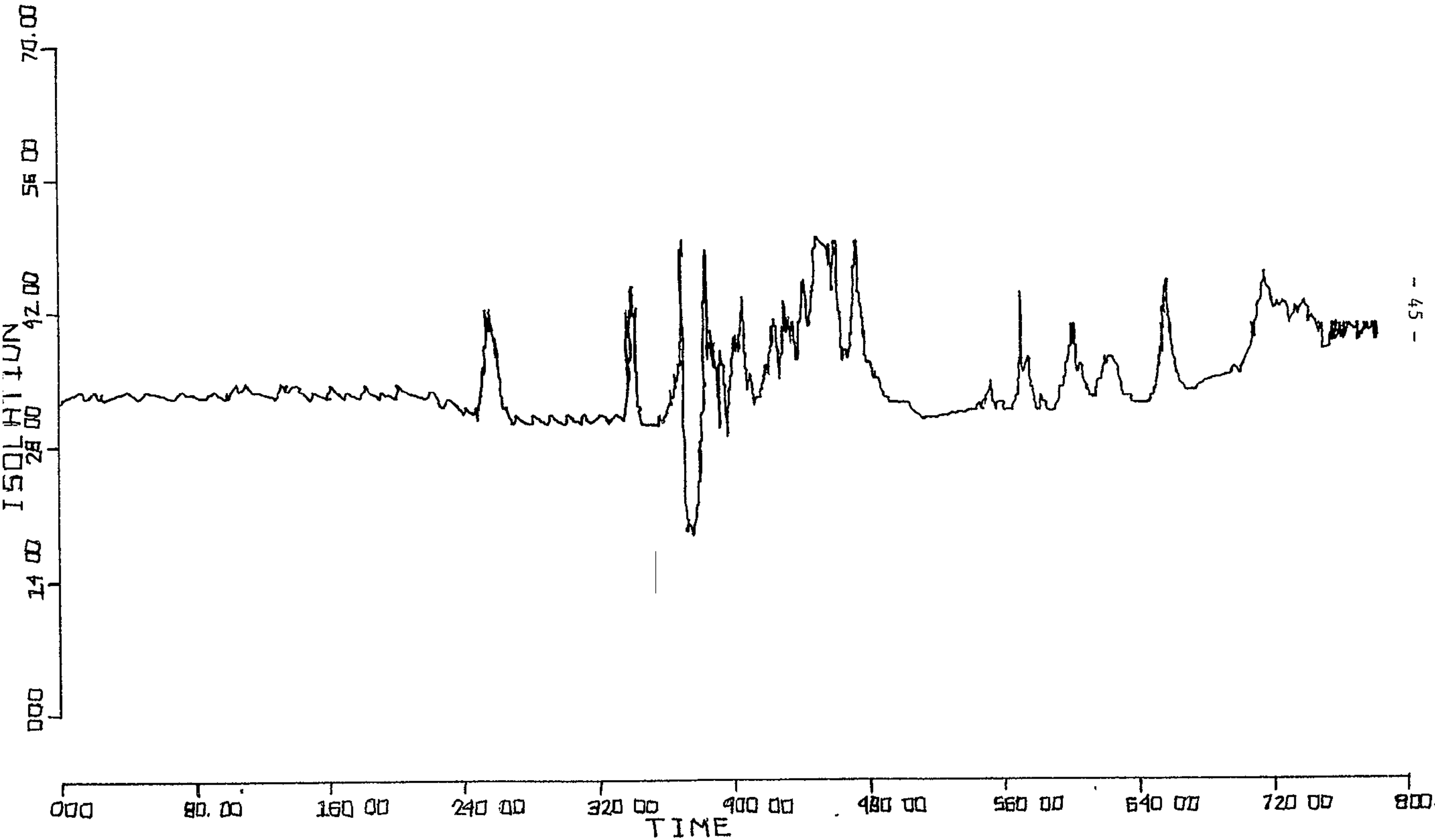

Isolation versus Attenuation
(10 second time constant)

June 19-20, 1976 (Days 171 & 172)
Start time 17:26:53
End time: 05 19:06
vert. ISOLATION (dB)
hor. ATTENUATION (dB)

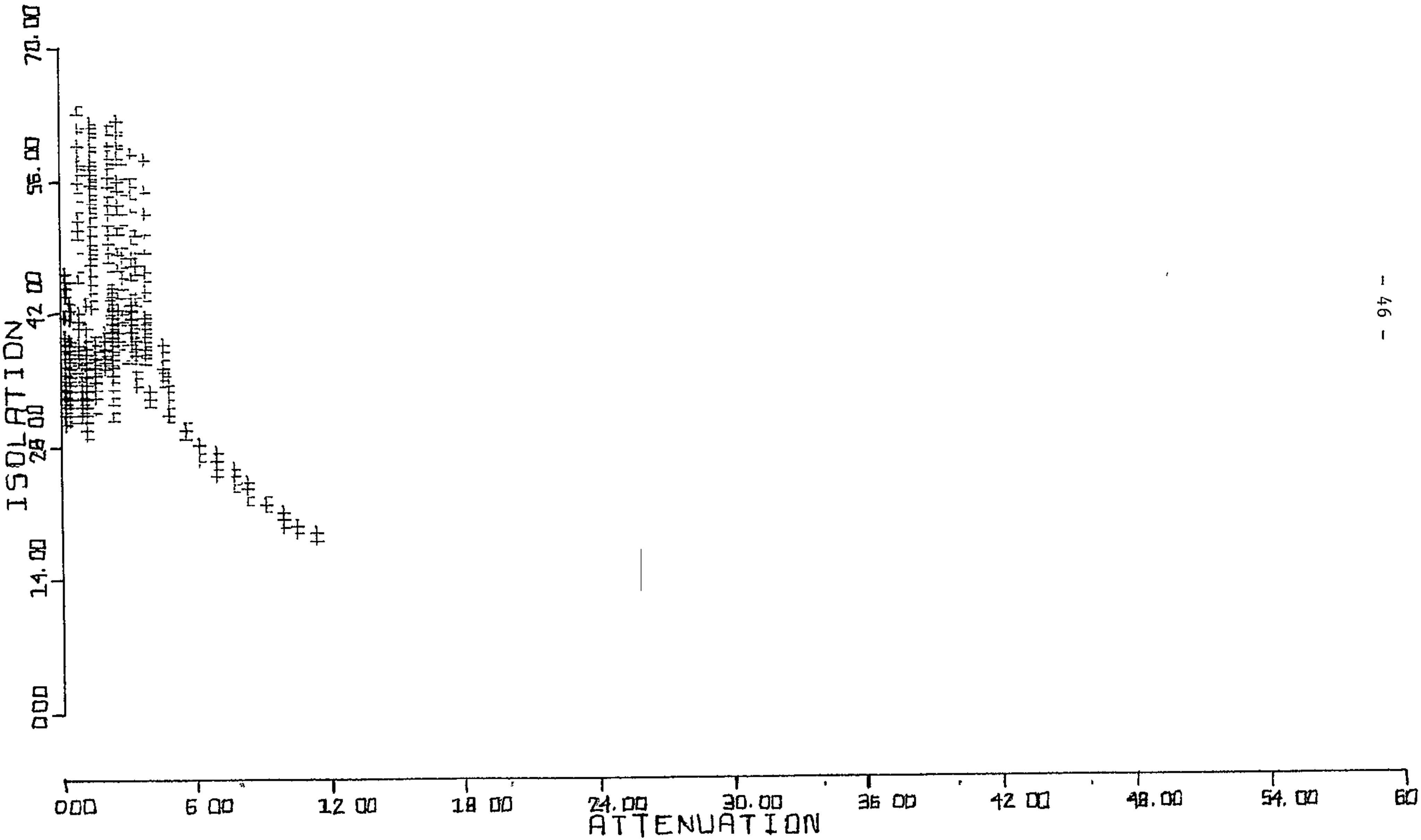

Rain Rate (RG #9 - Site Rain Gauge)

June 20, 1976 (Day 172)
Start time: 05:20:30
End time: 18:16:53
vert. RAIN RATE (mm/hr)
hor. TIME (minutes)

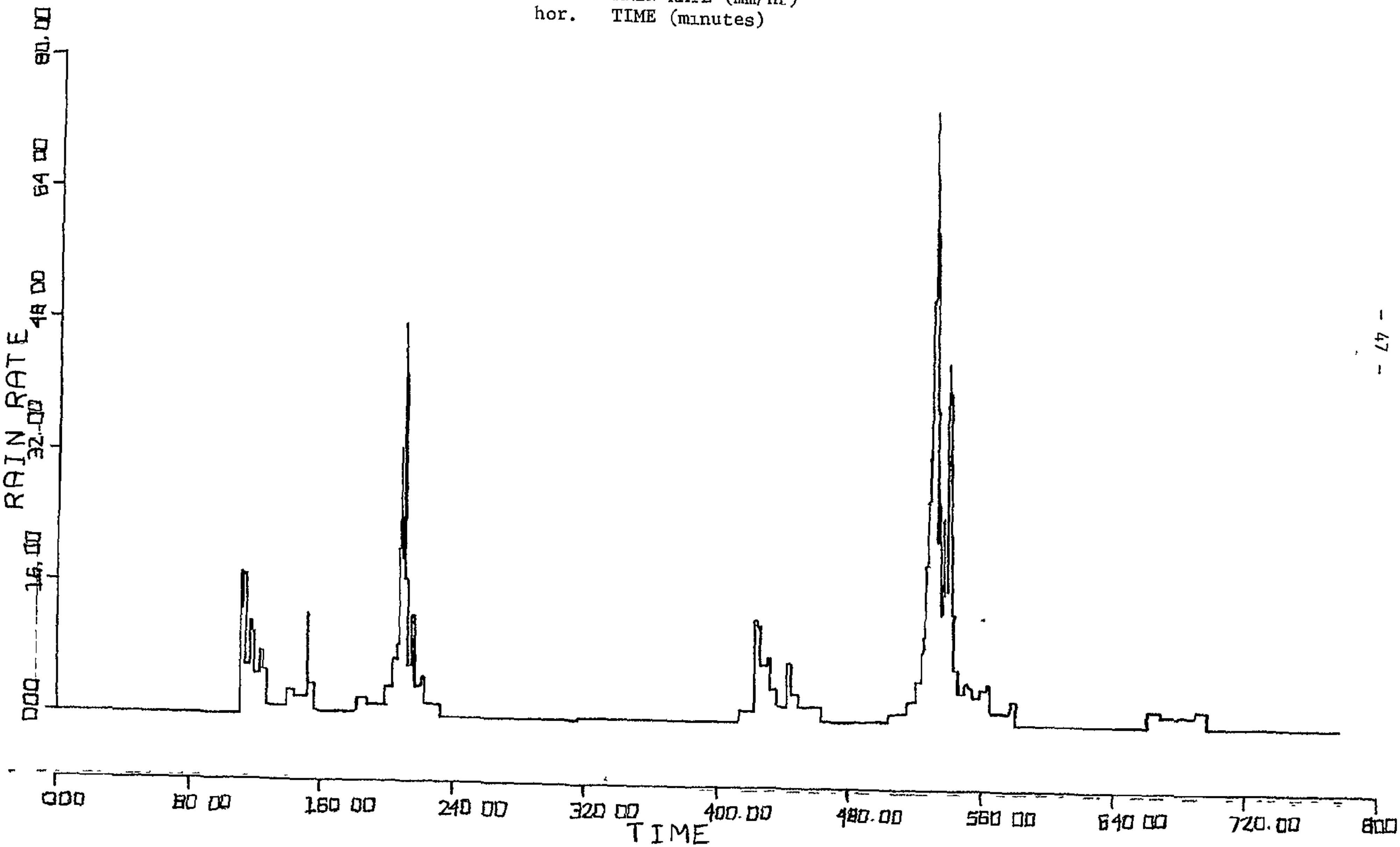

Rain Rate (RG #10 - 175 meters from receiver along path)

June 20, 1976 (Day 172)
Start time: 05:20:30
End time: 18:16:53
vert. RAIN RATE (mm/hr)
hor. TIME (minutes)

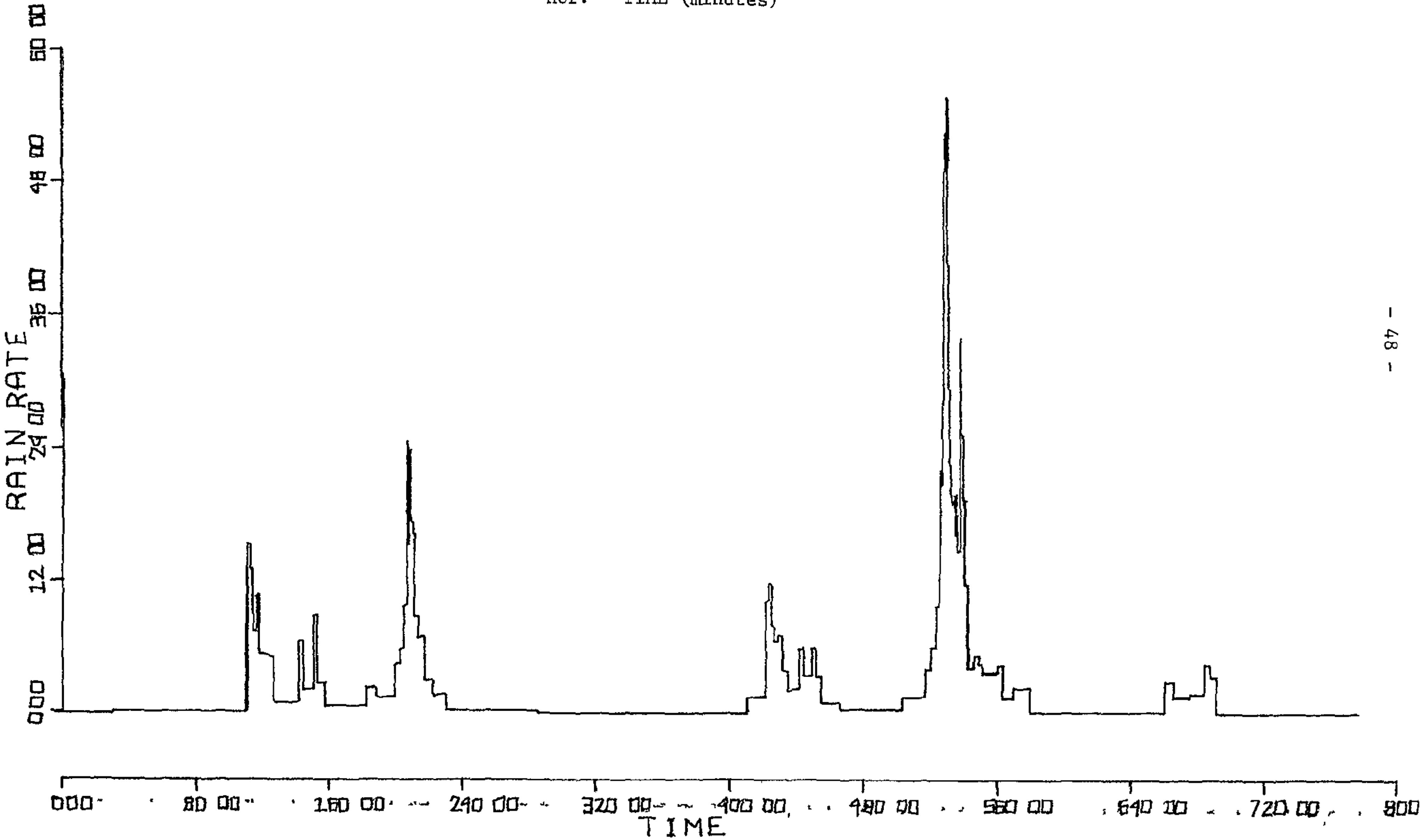

Rain Rate (RG #1 - 563 meters from receiver along path)

June 20, 1976 (Day 172)
Start time: 05:20:30
End time: 18 16:53
vert. RAIN RATE (mm/hr)
hor. TIME (minutes)

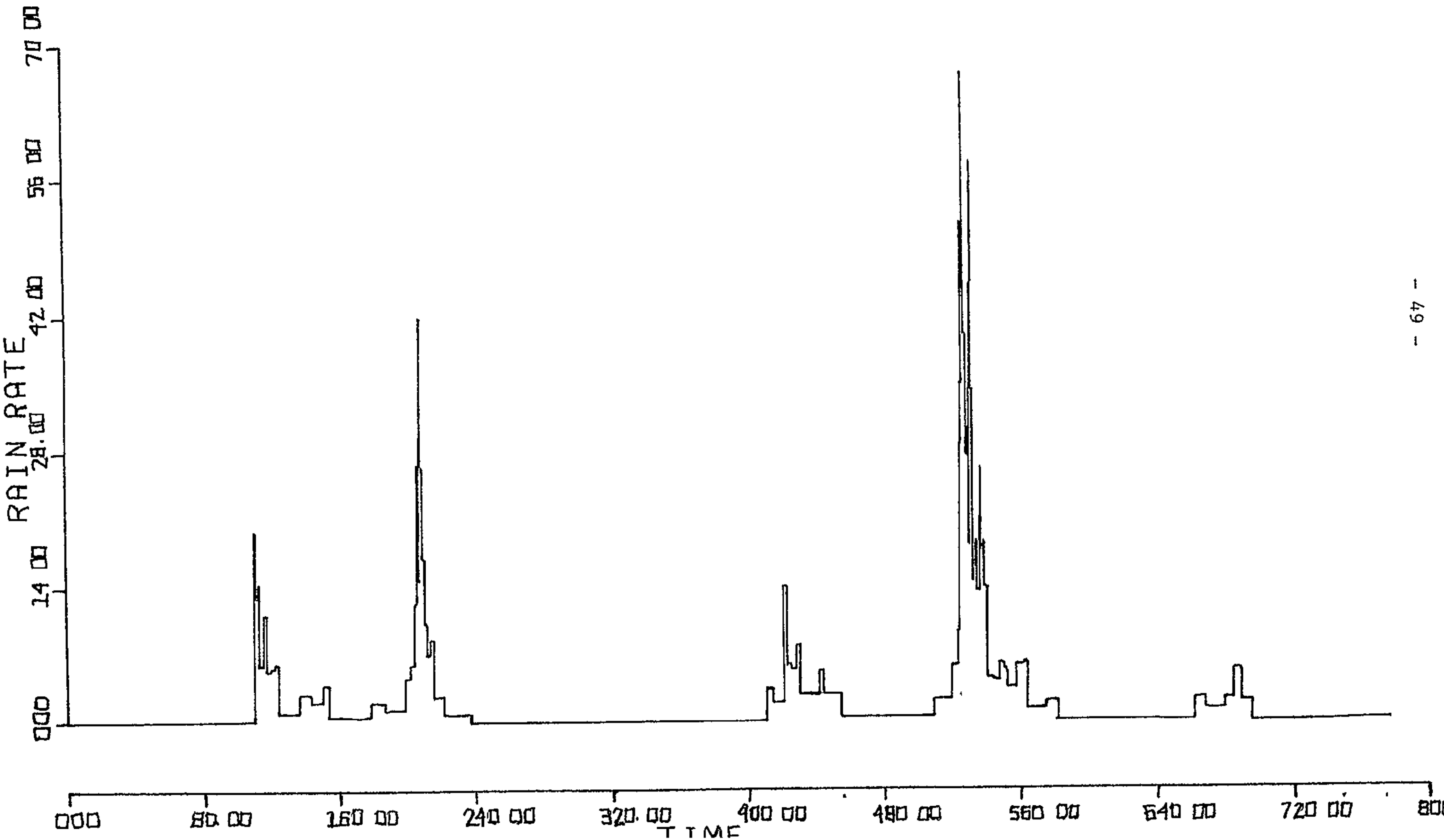

Rain Rate (RG #12 - 975 meters from
receiver, 72° east of path)

June 20, 1976 (Day 172)
Start time: 05:20:30
End time: 18:16:53
vert. RAIN RATE (mm/hr)
hor. TIME (minutes)

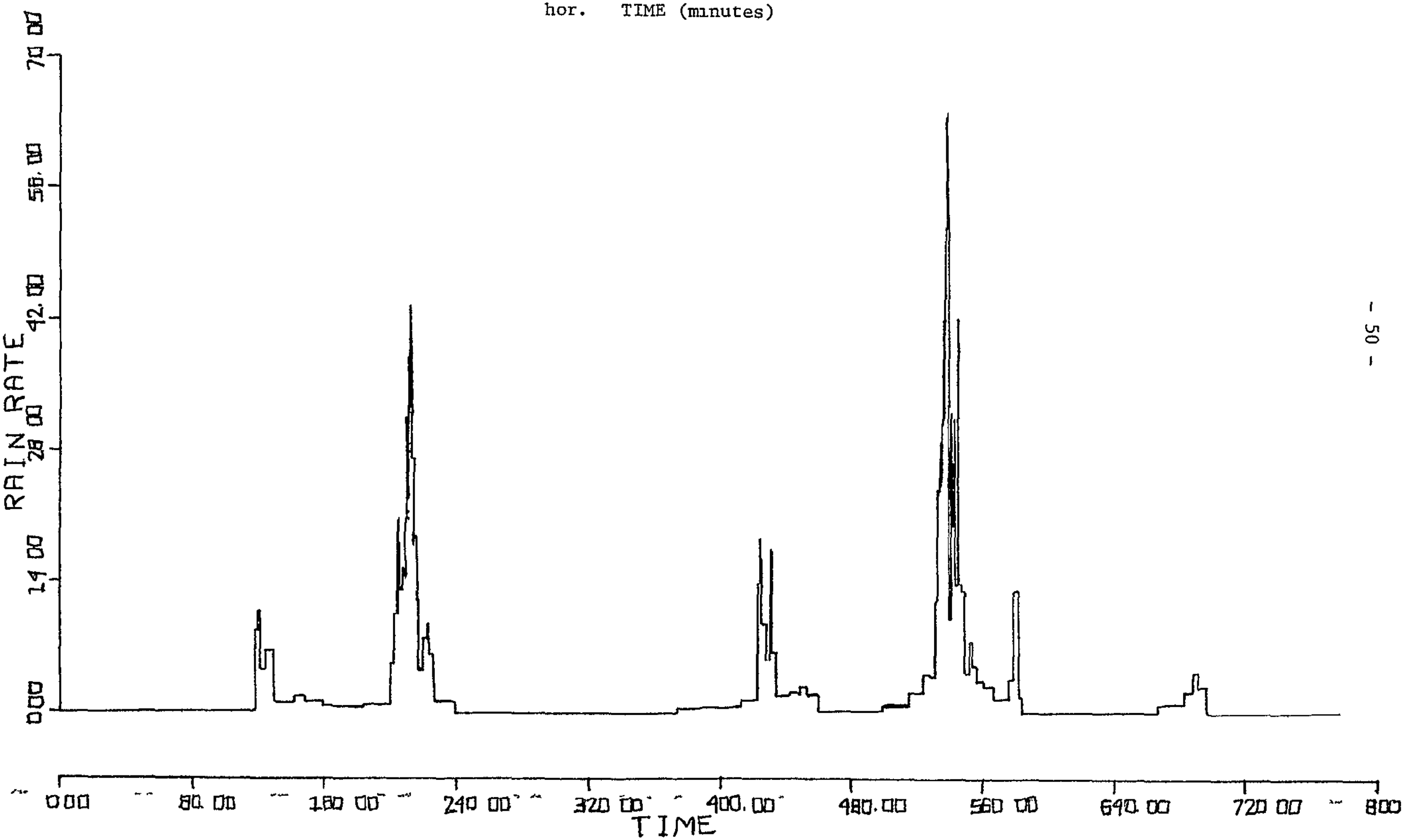

Rain Rate (RG #13 - 1400 meters from receiver, 98° east of path)

June 20, 1976 (Day 172)
Start time: 05:20:30
End time: 18:16:53
vert. RAIN RATE (mm/hr)
hor. TIME (minutes)

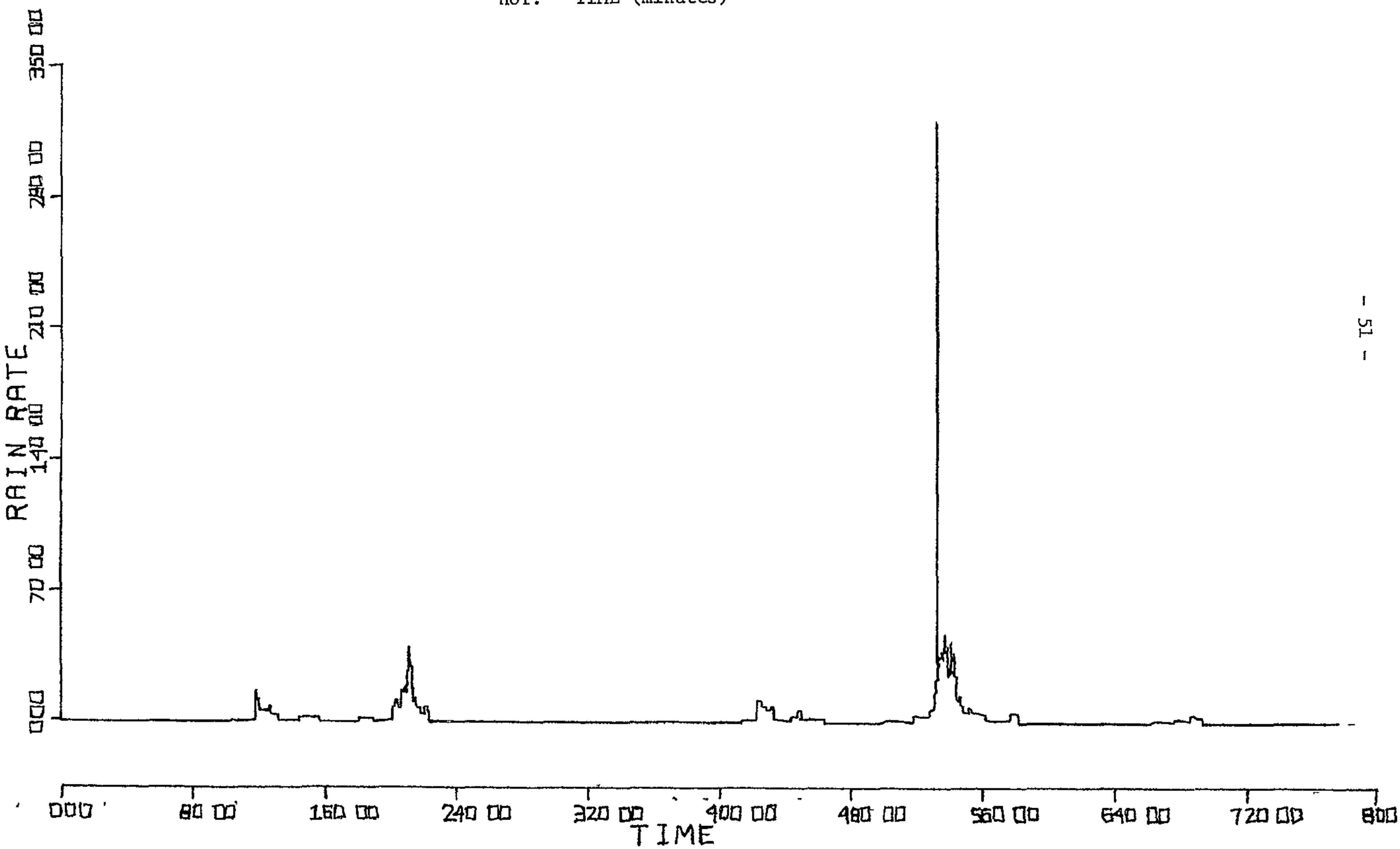

Co-Polarized Signal Level
(10 second time constant)

June 20, 1976 (Day 172)
Start time: 05:20·30
End time: 18·16:53
vert. SIGNAL LEVEL (dBm)
hor. TIME (minutes)

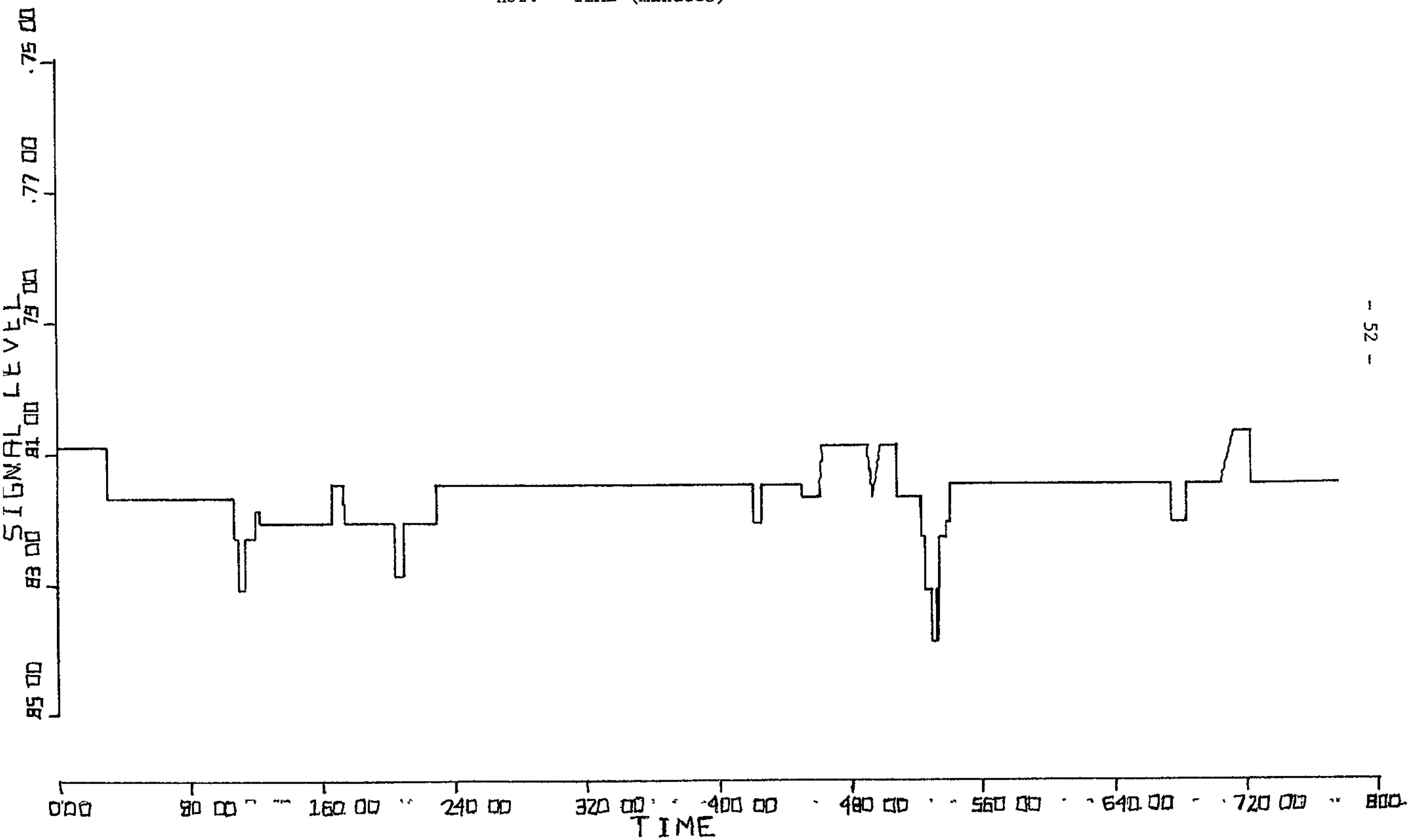

Cross-Polarized Signal Level
(10 second time constant)

June 20, 1976 (Day 172)
Start time: 05:20:30
End time: 18:16:53
vert. SIGNAL LEVEL (dBm)
hor. TIME (minutes)

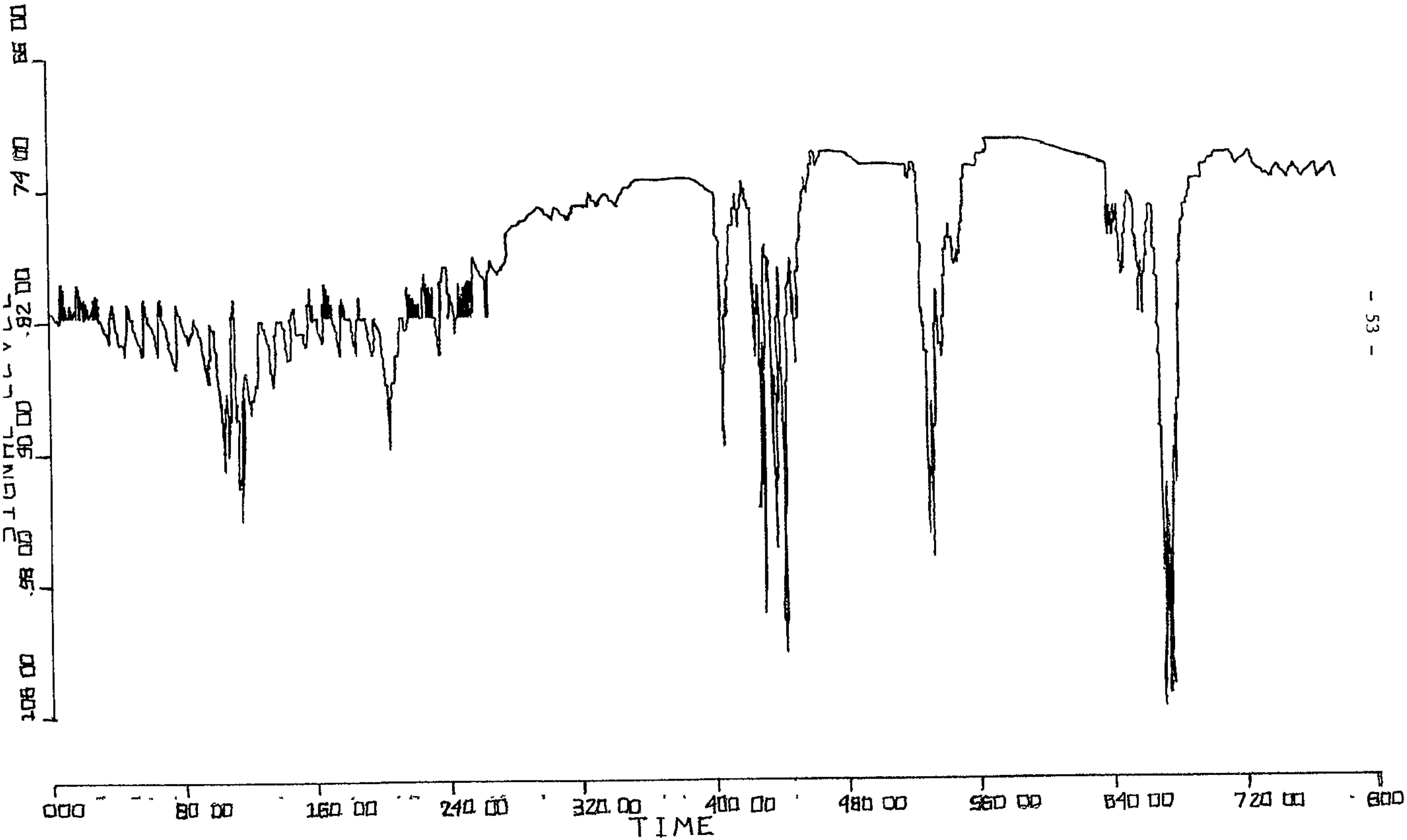

Attenuation (10 second time constant)

June 20, 1976 (Day 172)
Start time: 05 20·30
End time. 18:16:53
vert. ATTENUATION (dB)
hor. TIME (minutes)

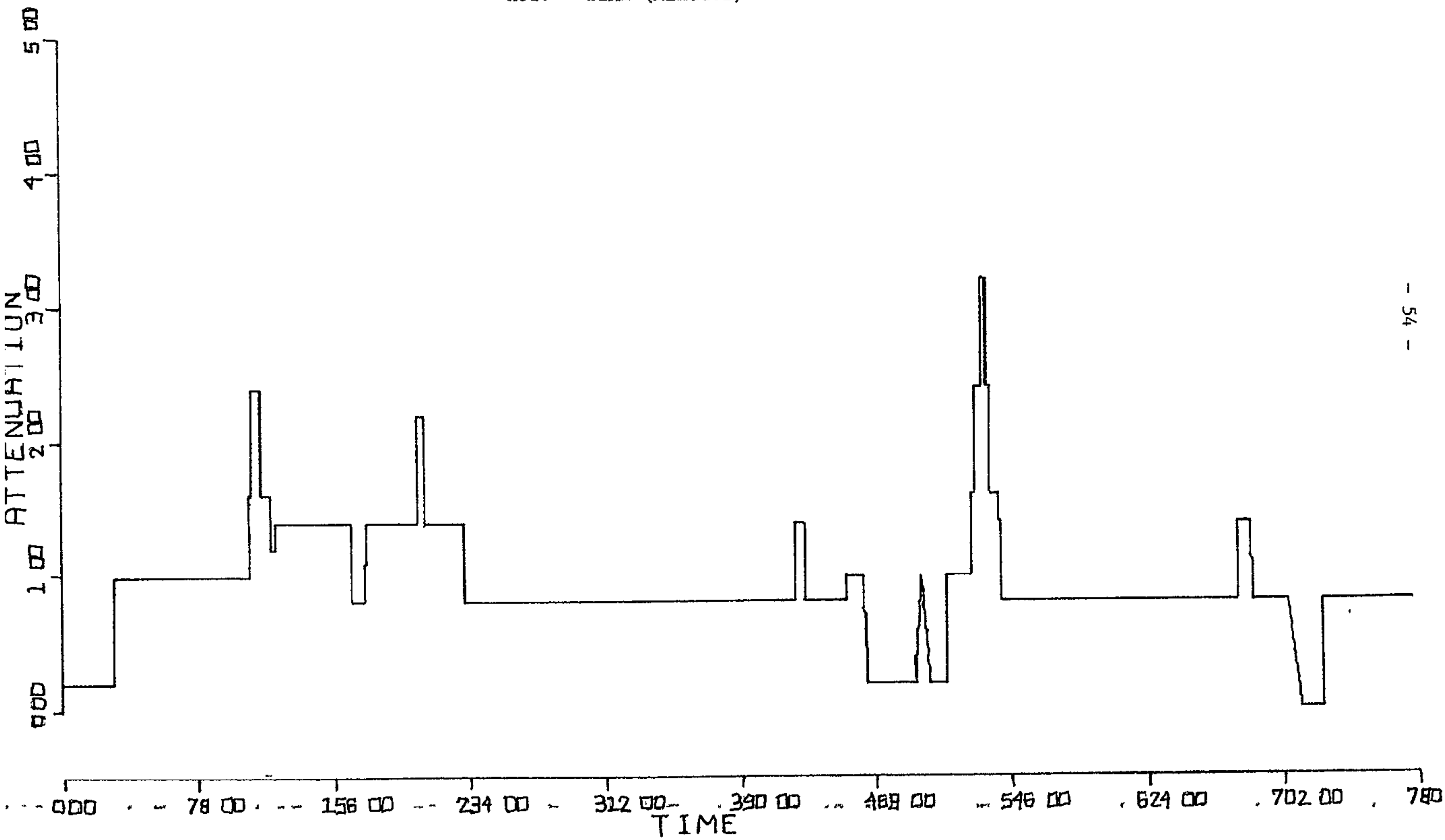

Isolation (10 second time constant)

June 20, 1976 (Day 172)
Start time: 05.20:30
End time: 18:16:53
vert. ISOLATION (dB)
hor. TIME (minutes)

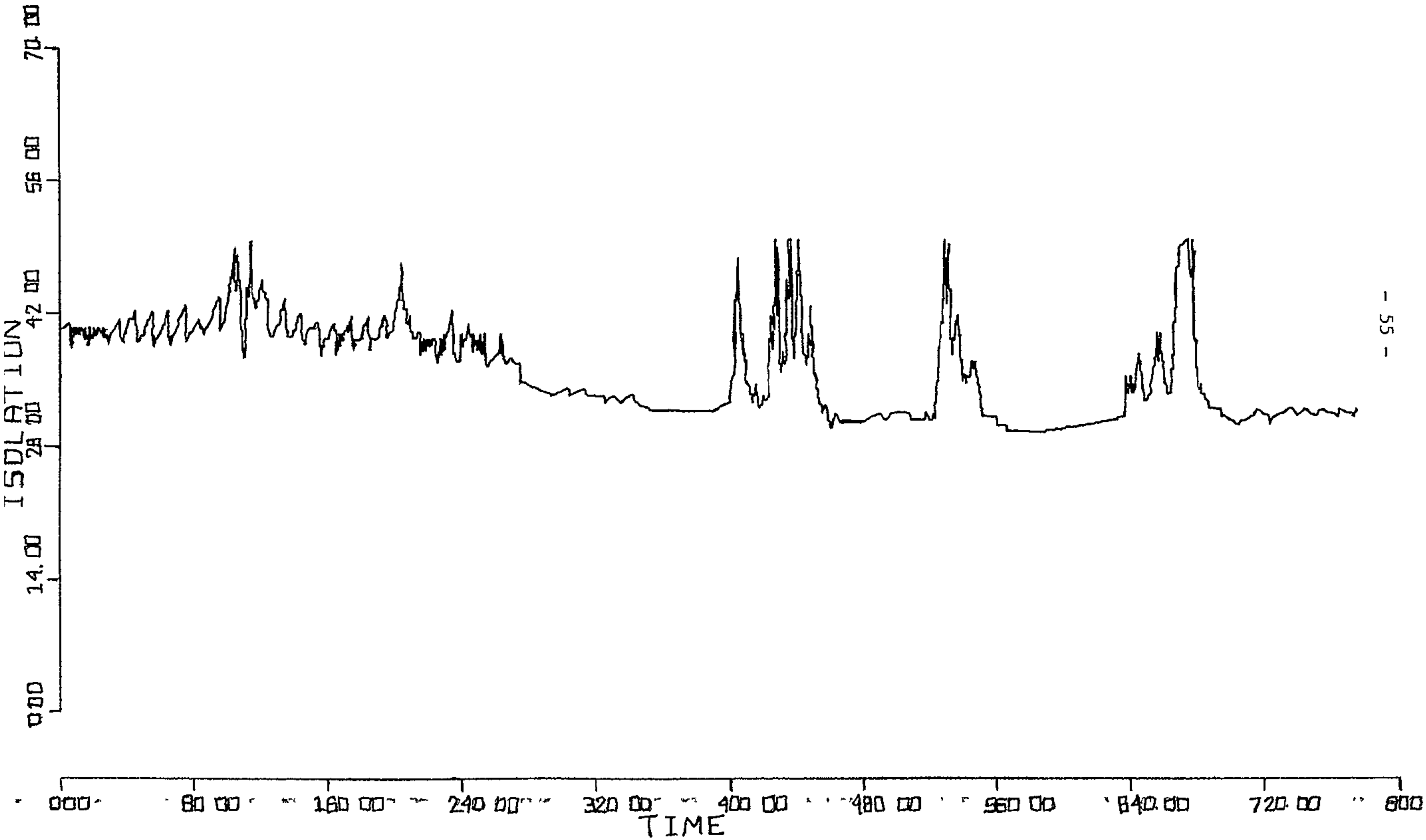

Isolation versus Attenuation
(10 second time constant)

June 20, 1976 (Day 172)
Start time: 05:20:30
End time: 18:16:53
vert. ISOLATION (dB)
hor. ATTENUATION (dB)

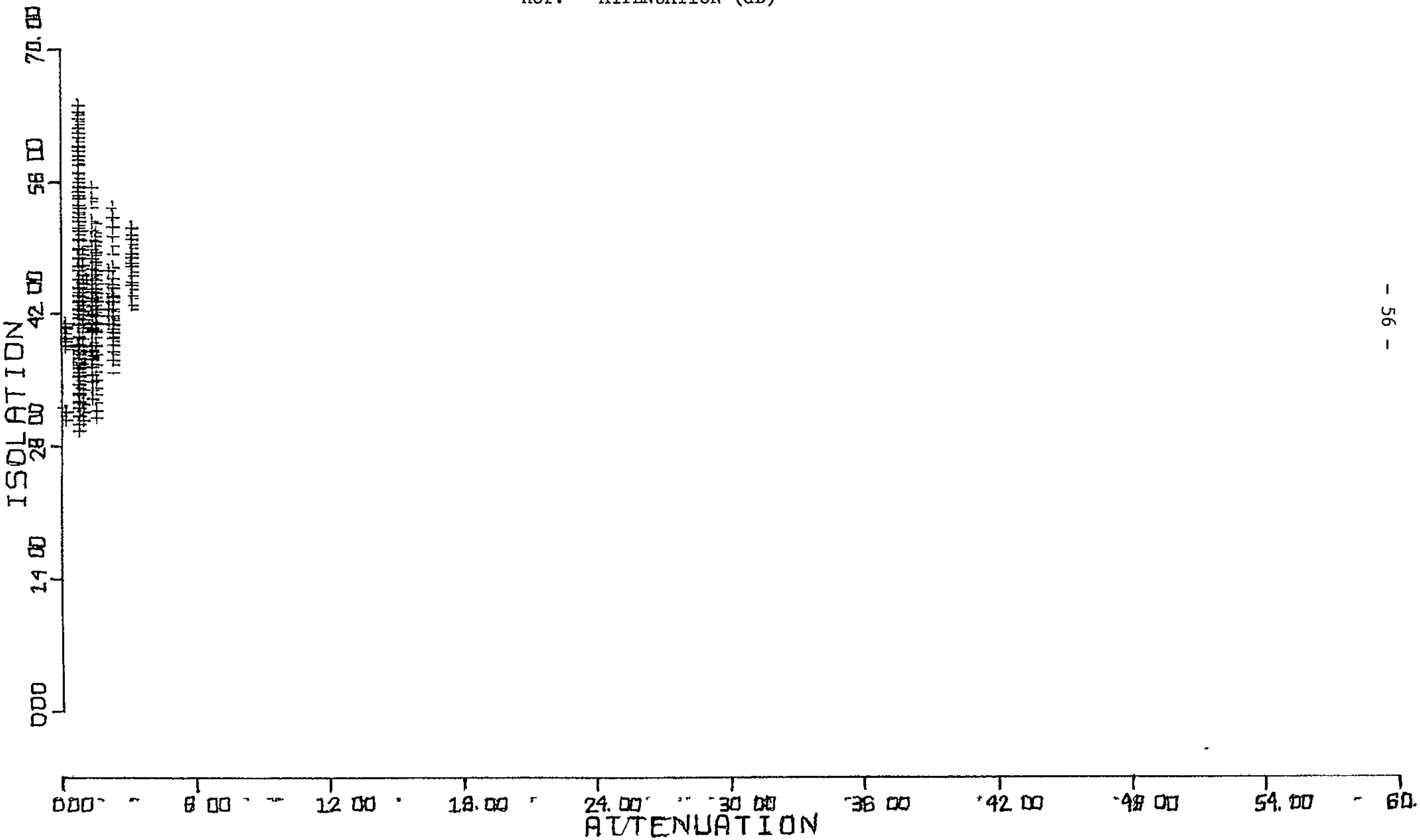

Rain Rate (RG #9 - Site Rain Gauge)

June 20, 1976 (Day 172)
Start time: 19:50:33
End time: 07.54:43
vert. RAIN RATE (mm/hr)
hor. TIME (minutes)

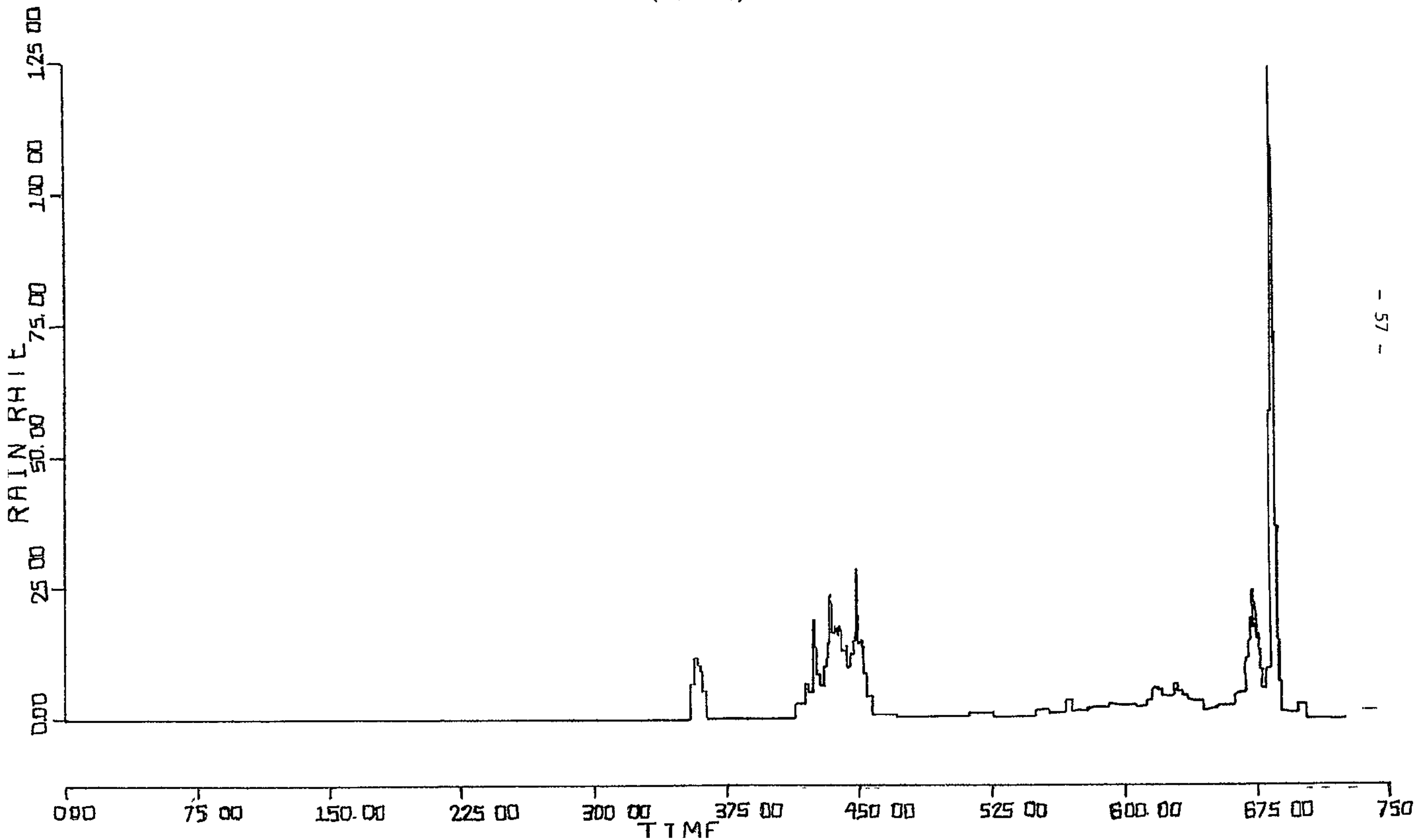

Rain Rate (RG #10 - 175 meters from receiver along path)

June 20, 1976 (Day 172)
Start time: 19:50:33
End time: 07:54:43
vert. RAIN RATE (mm/hr)
hor. TIME (minutes)

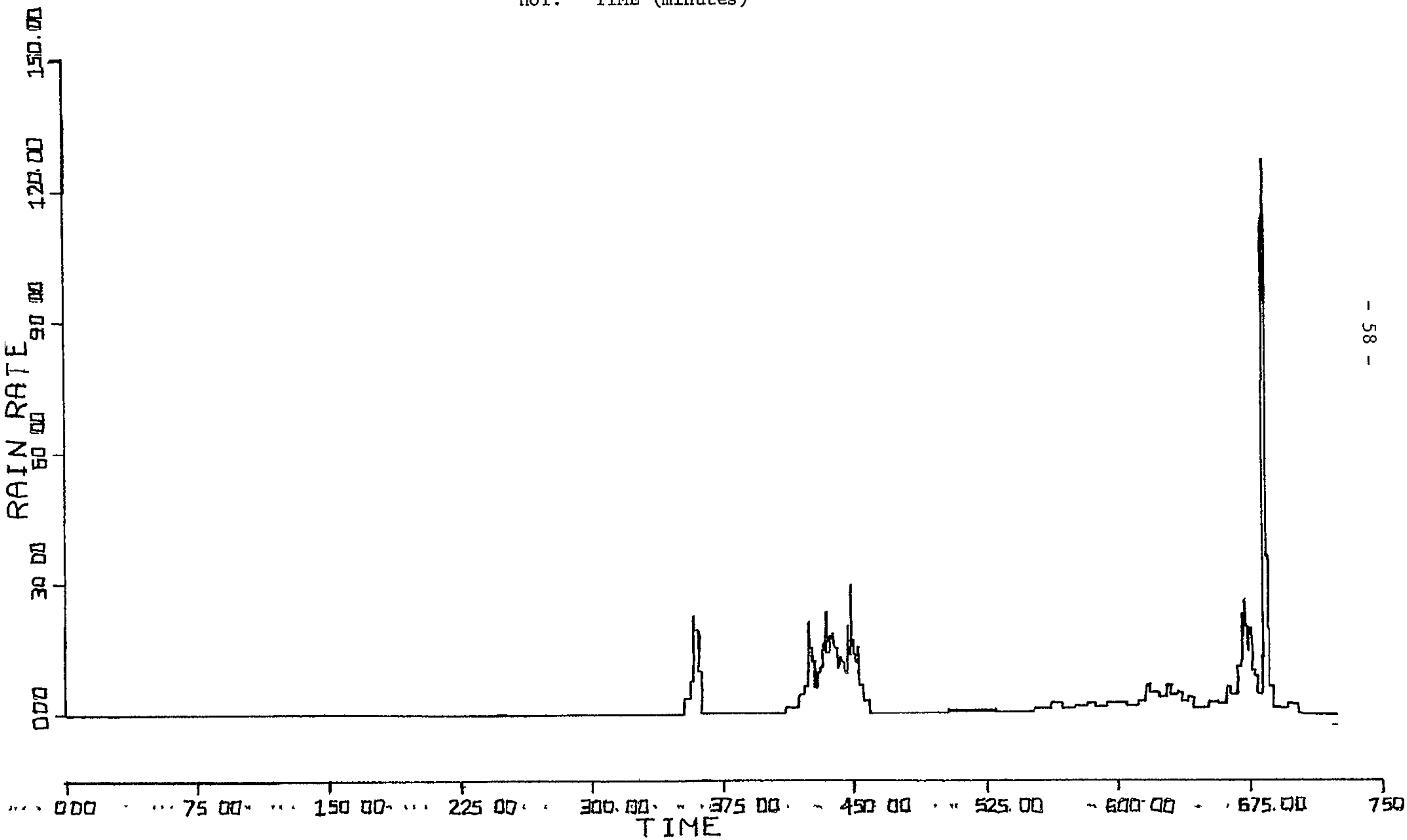

Rain Rate (RG #11 - 563 meters from receiver along path)

June 20, 1976 (Day 172)
Start time: 19:50:33
End time: 07:54:43
vert. RAIN RATE (mm/hr)
hor. TIME (minutes)

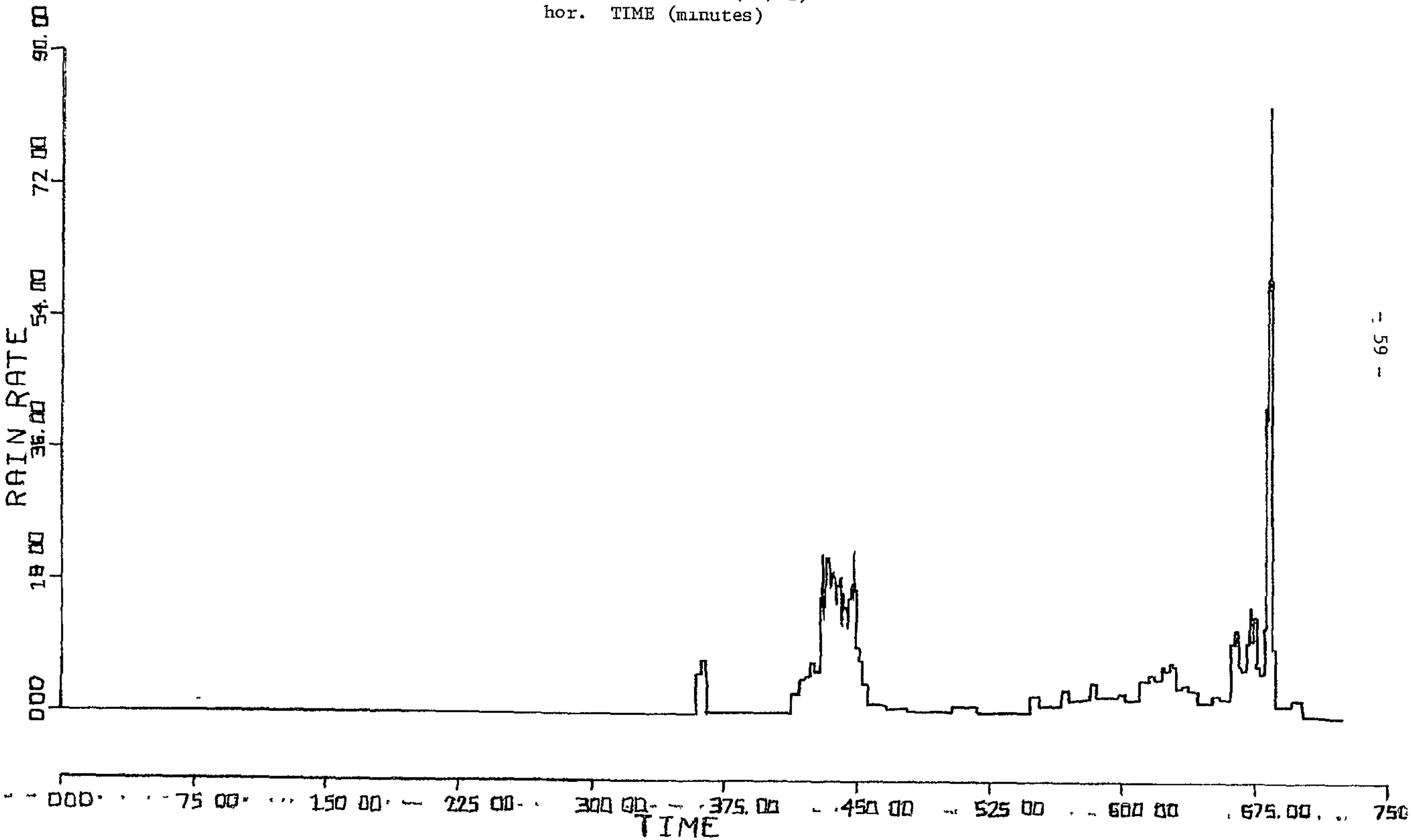

Rain Rate (RG #12 - 975 meters from receiver, 72° east of path)

June 20, 1976 (Day 172)
Start time: 19:50:33
End time. 07:54:43
vert. RAIN RATE (mm/hr)
hor. TIME (minutes)

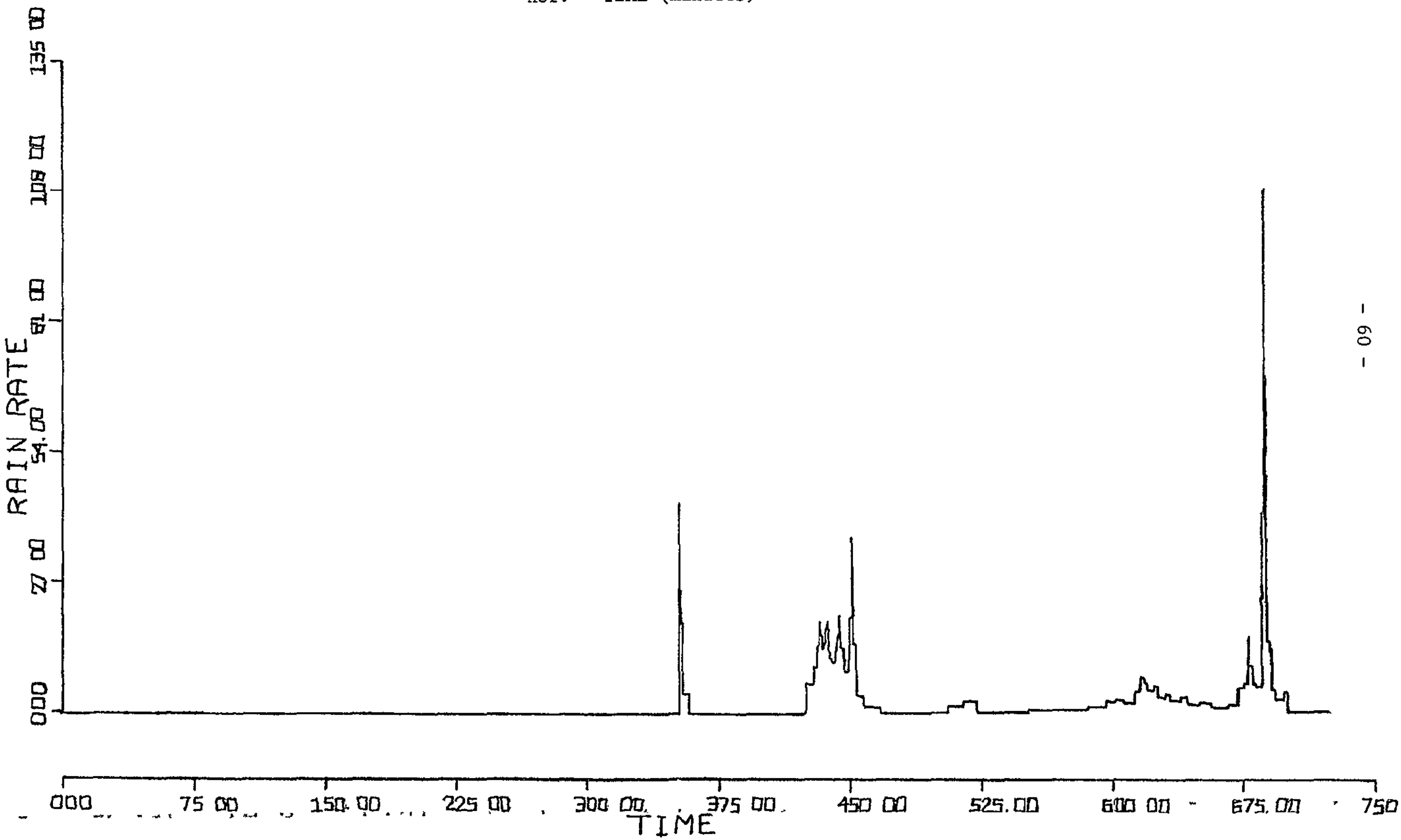

Rain Rate (RG #13 - 1400 meters from receiver, 98° east of path)

June 20, 1976 (Day 172)
Start time: 19:50:33
End time: 07:54:43
vert. RAIN RATE (mm/hr)
hor. TIME (minutes)

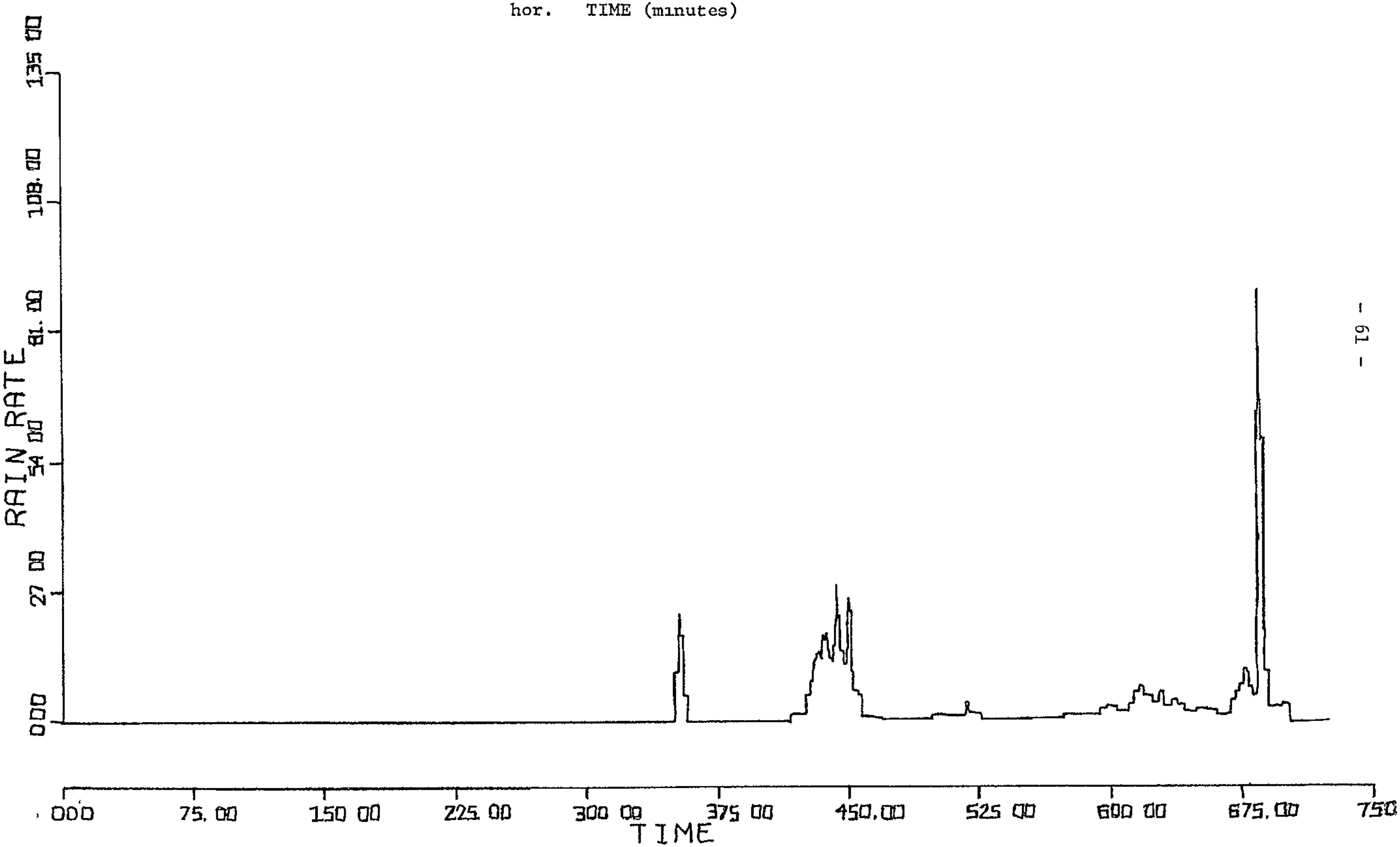

1800 211551 08 24 76 76 172 4285980 73 173 1708980

Co-Polarized Signal Level
(10 second time constant)

June 20, 1976 (Day 172)
Start time: 19:50:33
End time: 07:54:43
vert. SIGNAL LEVEL (dBm)
hor. TIME (minutes)

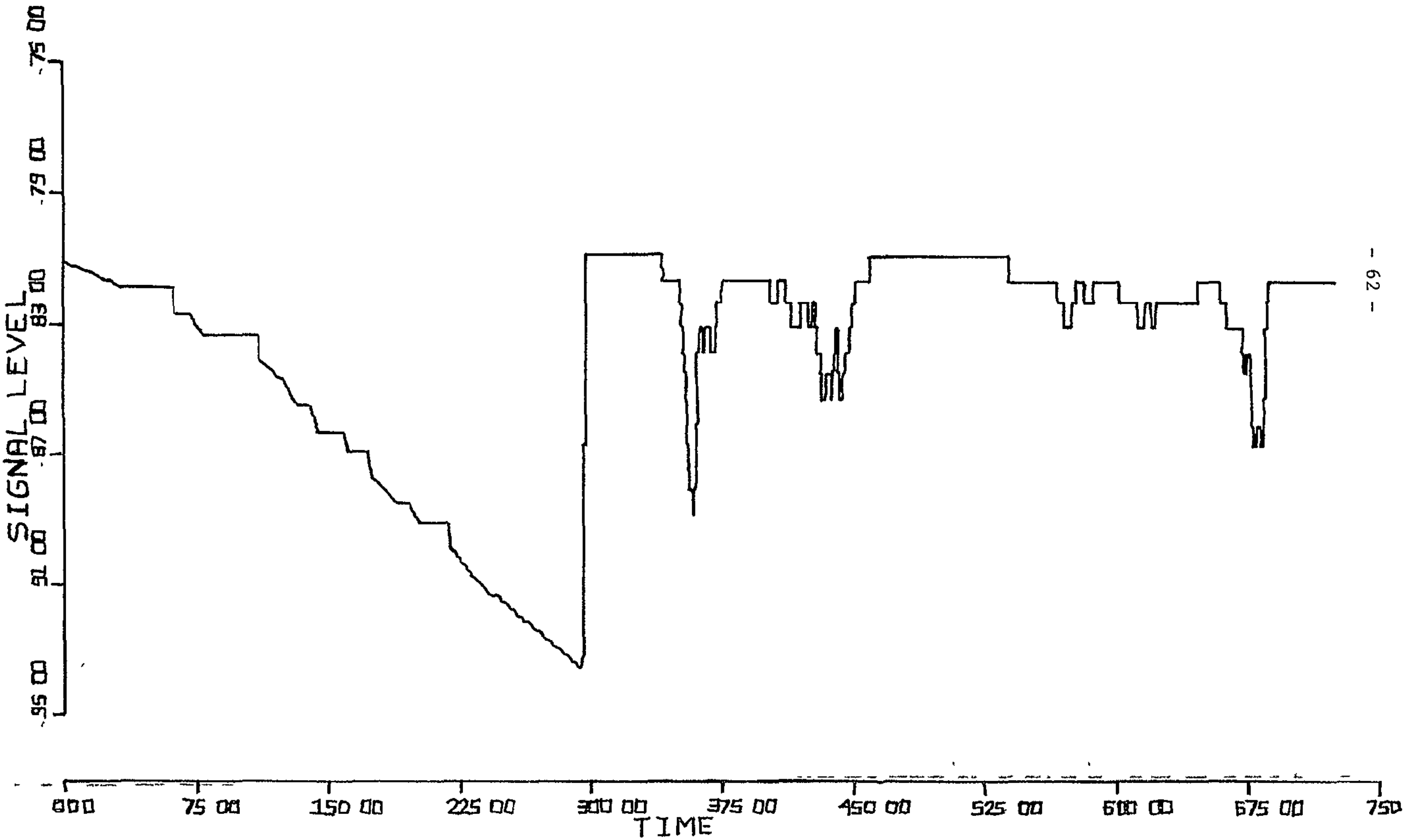

[redacted] [redacted] [redacted] [redacted] 08 [redacted] 24 76 76 172 4285980 76 173 1708980

Cross-Polarized Signal Level
(10 second time constant)

June 20, 1976 (Day 172)
Start time: 19:50:33
End time: 07:54:43
vert. SIGNAL LEVEL (dBm)
hor. TIME (minutes)

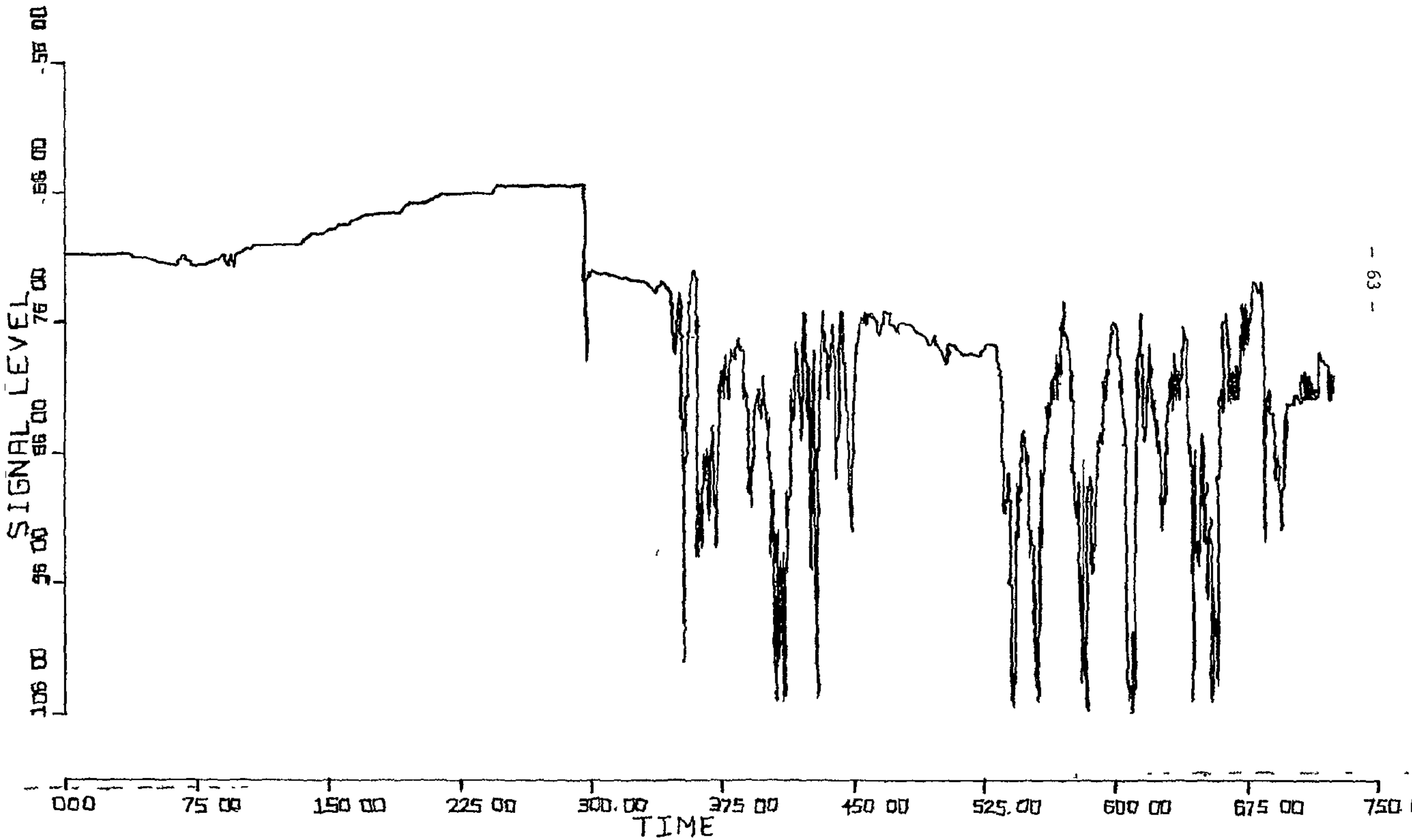

Attenuation (10 second time constant)

June 20, 1976 (Day 172)
Start time. 19:50:33
End time: 07 54:43
vert. ATTENUATION (dB)
hor TIME (minutes)

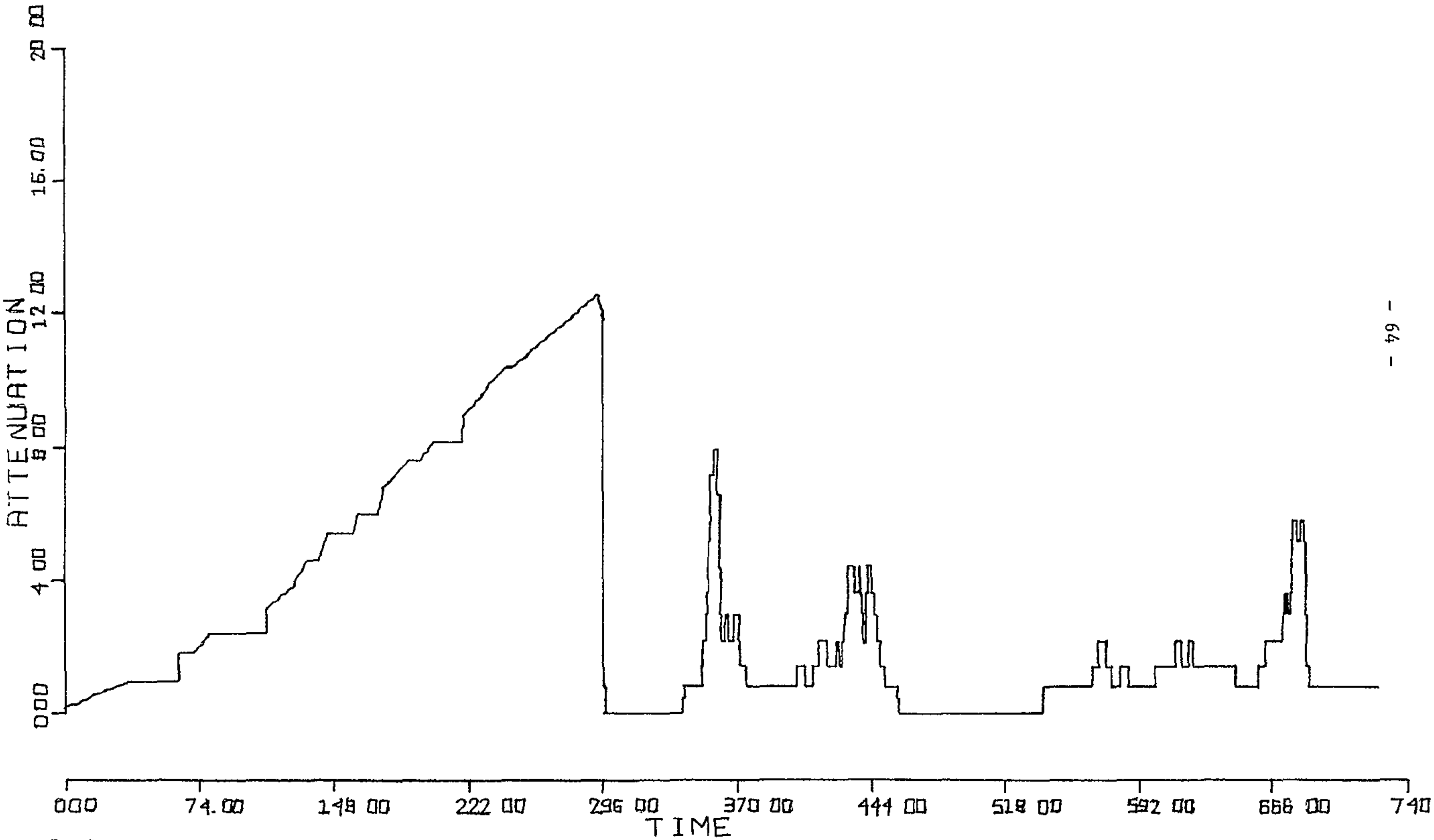

Isolation (10 second time constant)

June 20, 1976 (Day 172)
Start time: 19:50:33
End time: 07:54:43
vert. ISOLATION (dB)
hor. TIME (minutes)

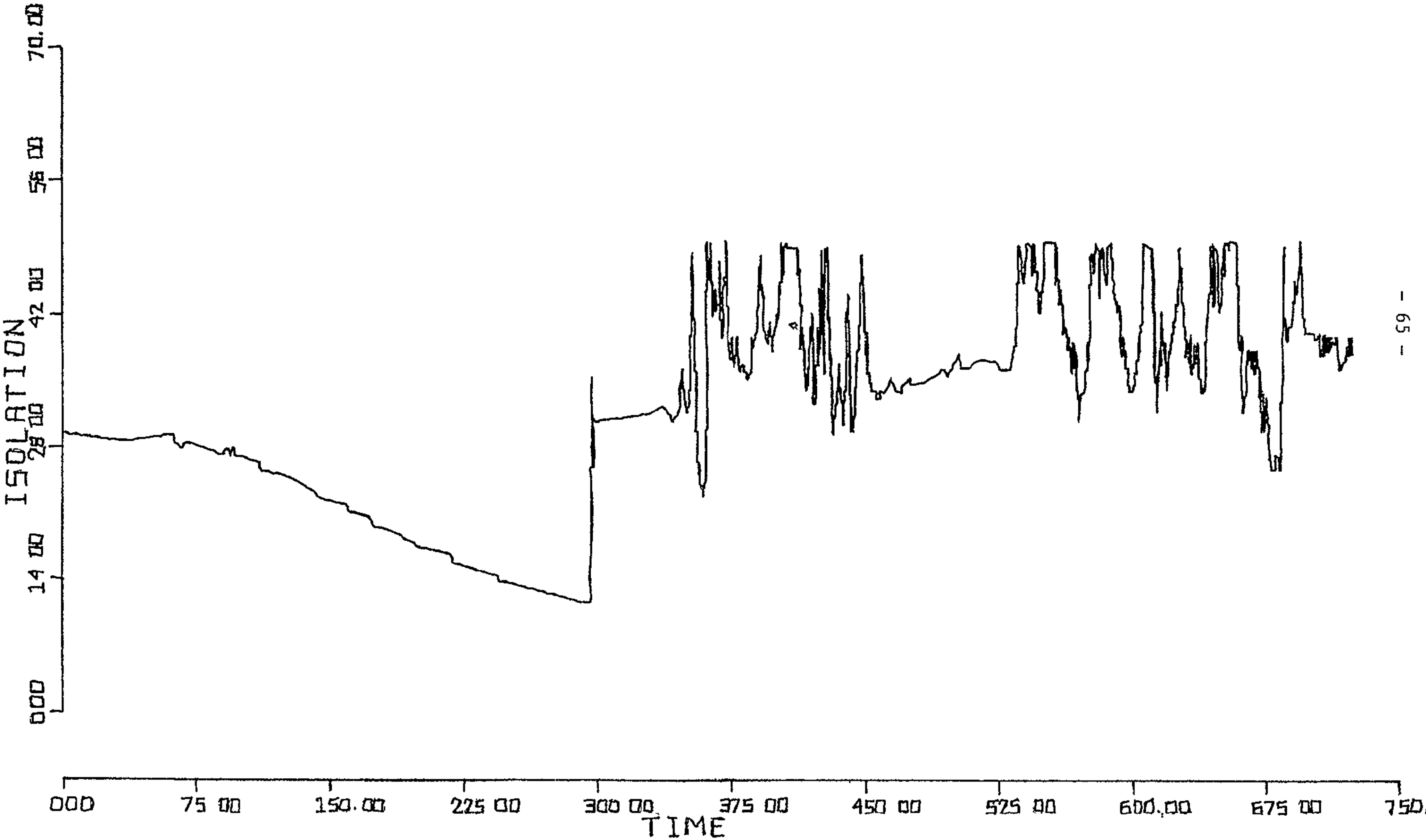

Isolation versus Attenuation
(10 second time constant)

June 20, 1976 (Day 172)
Start time: 19:50:33
End time: 07:54:43
vert. ISOLATION (dB)
hor. ATTENUATION (dB)

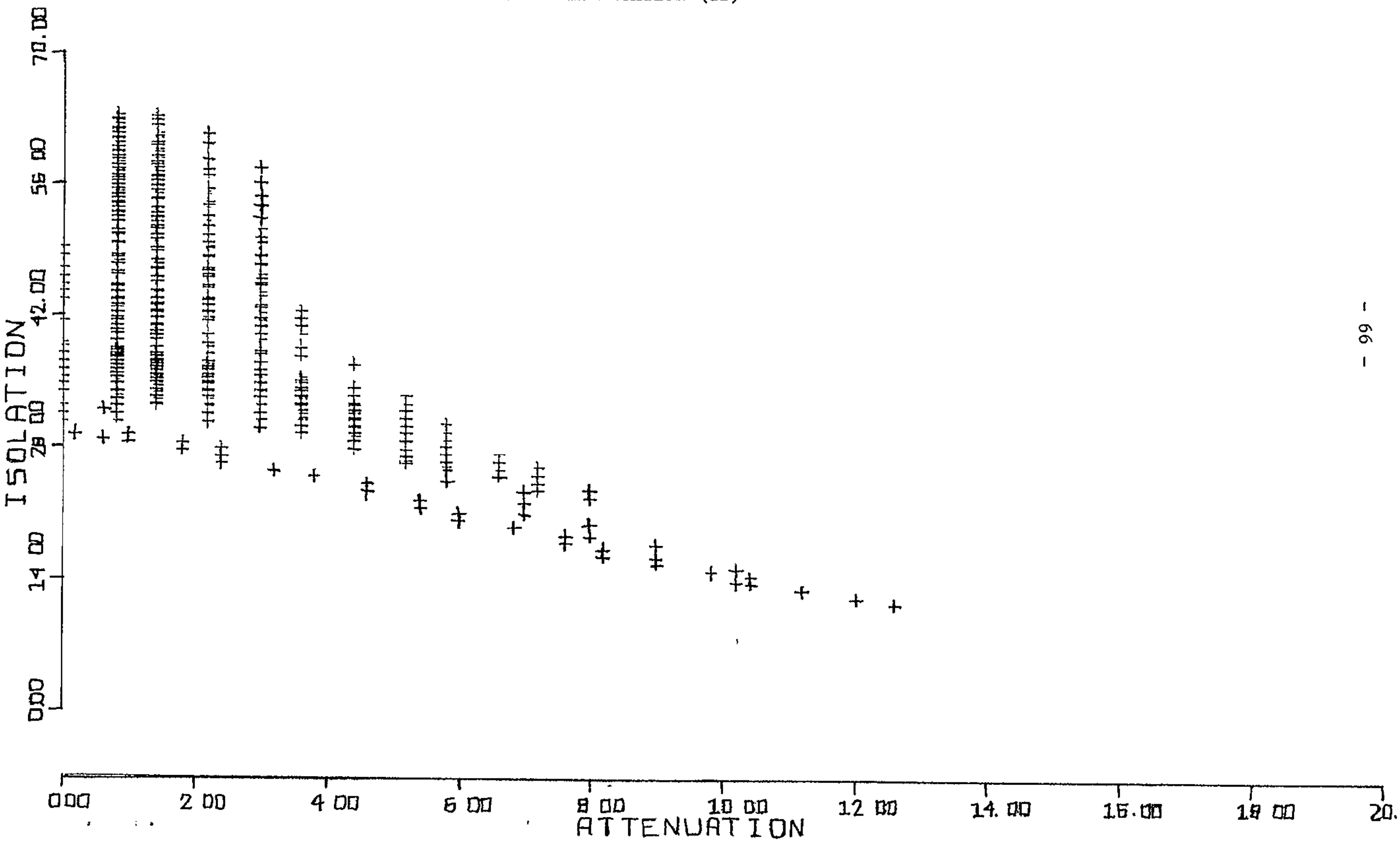

Rain Rate (RG #9 - Site Rain Gauge)

June 25, 1976 (Day 177)
Start time: 21:15:11
End time: 04:39 06
vert. RAIN RATE (mm/hr)
hor. TIME (minutes)

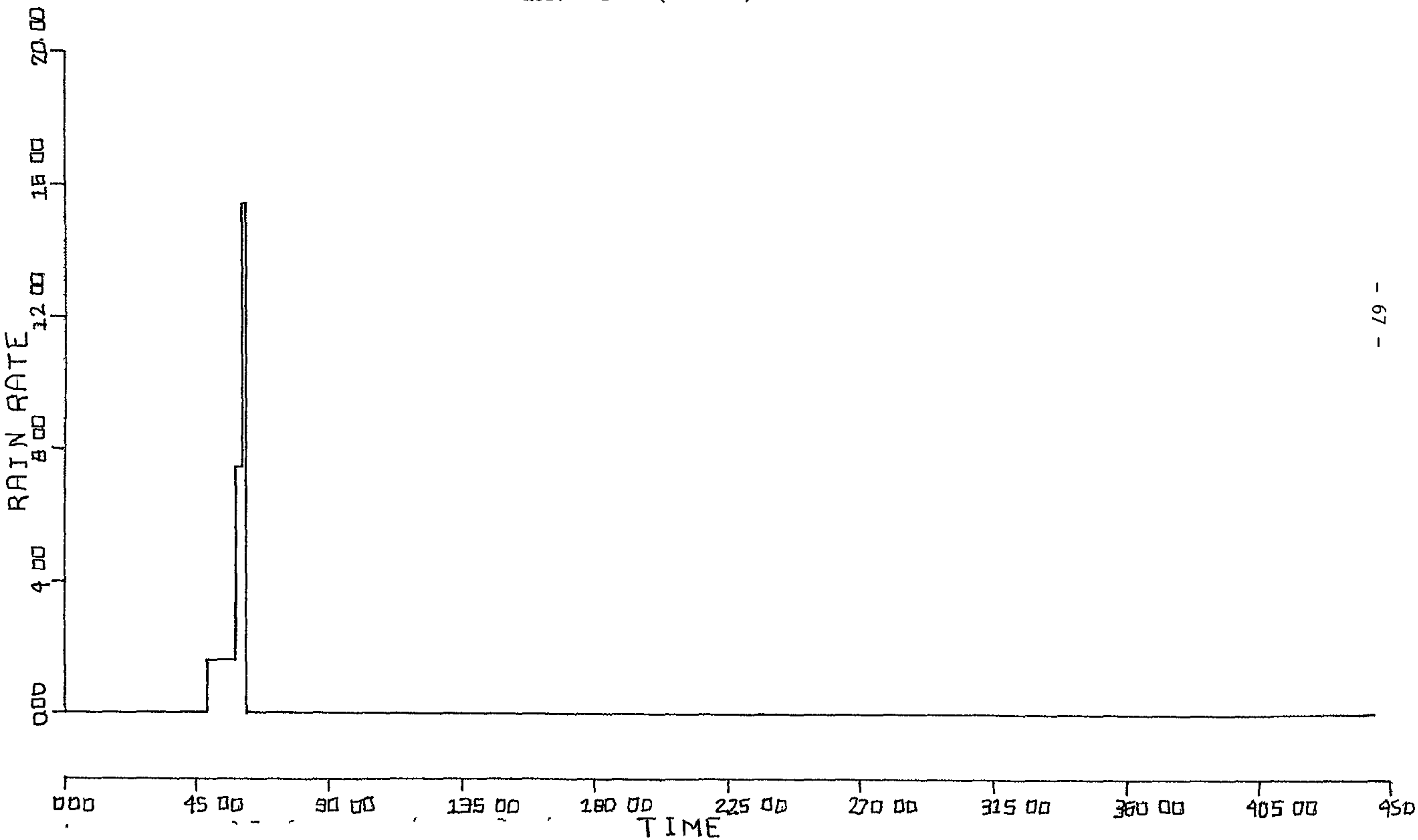

Rain Rate (RG #10 - 175 meters from receiver along path)

June 25, 1976 (Day 177)
Start time: 21:15:11
End time. 04:39:06
vert. RAIN RATE (mm/hr)
hor. TIME (minutes)

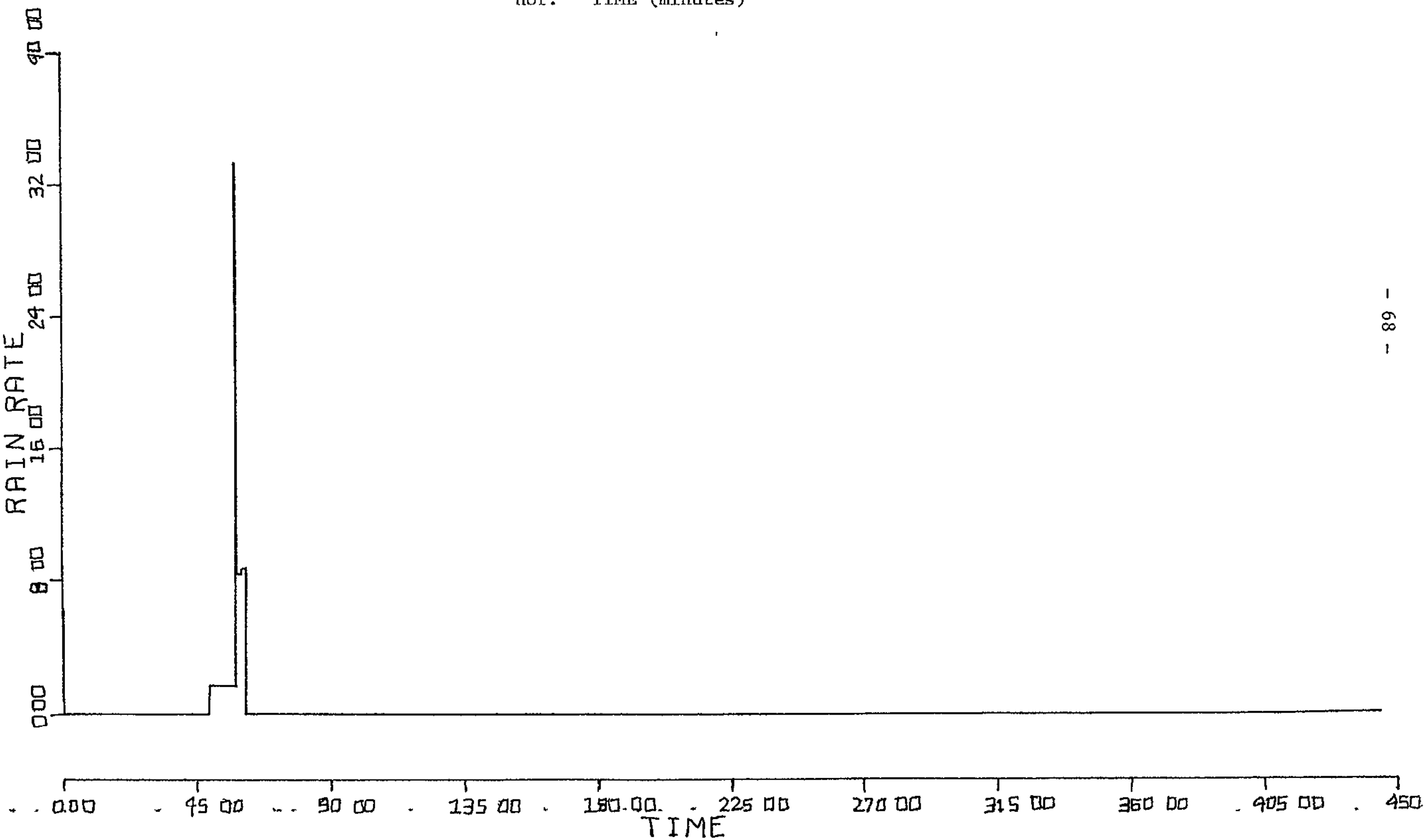

Rain Rate (RG #11 - 563 meters from receiver along path)

June 25, 1976 (Day 177)
Start time: 21:15:11
End time 04.39:06
vert. RAIN RATE (mm/hr)
hor. TIME (minutes)

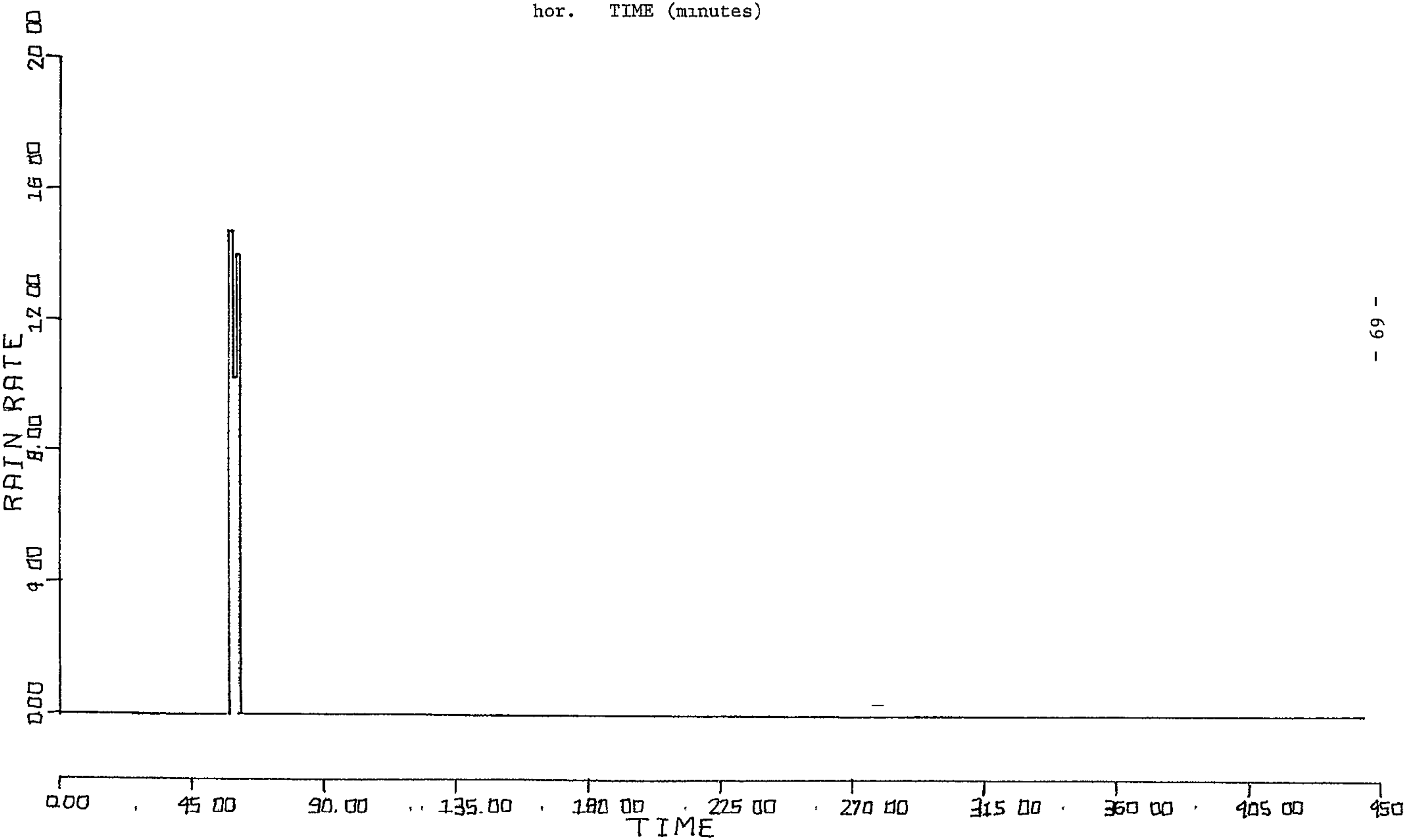

Co-Polarized Signal Level
(10 second time constant)

June 25, 1976 (Day 177)
Start time: 21:15:11
End time: 04.39:06
vert. SIGNAL LEVEL (dBm)
hor. TIME (minutes)

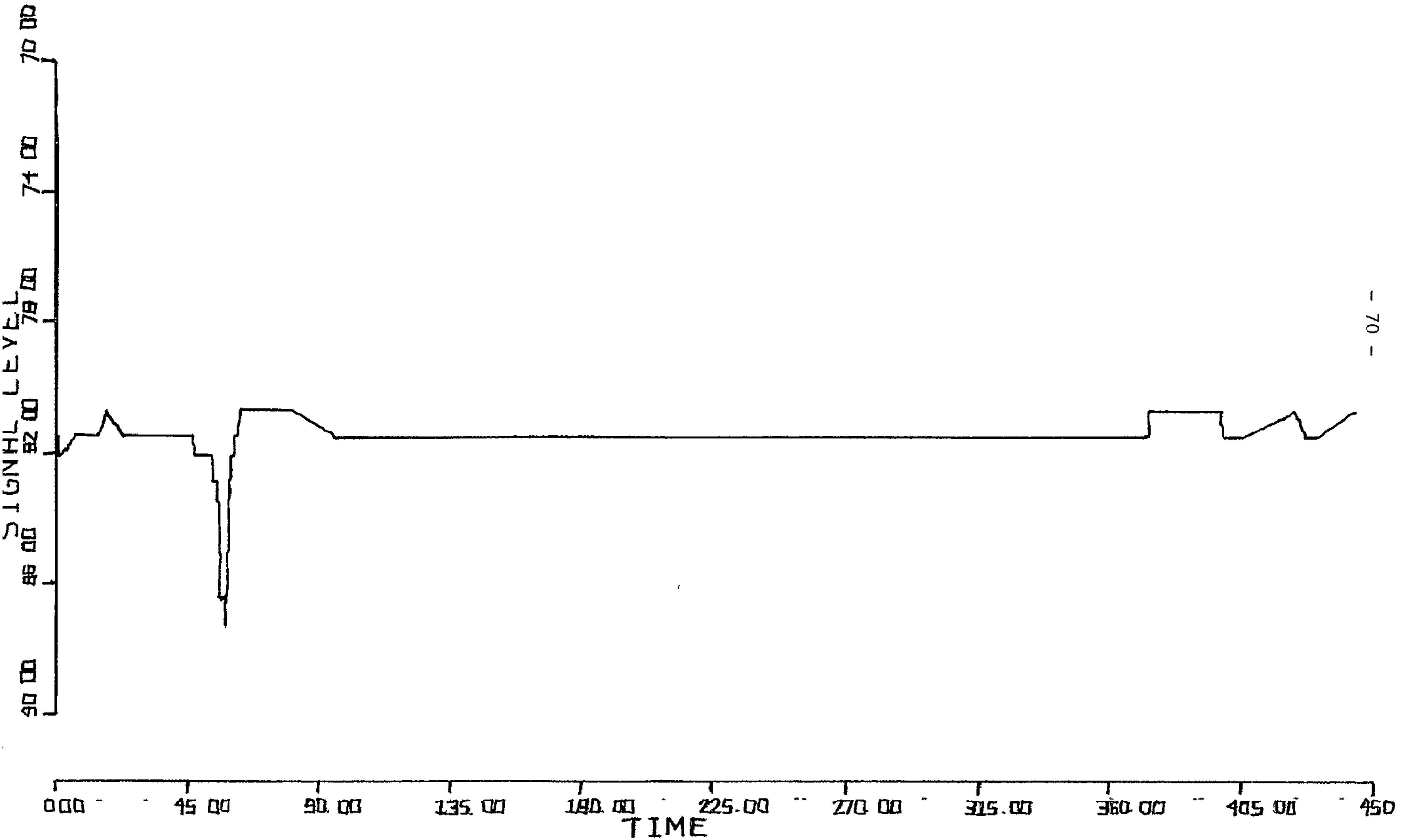

Cross-Polarized Signal Level
(10 second time constant)

June 25, 1976 (Day 177)
Start time: 21:15:11
End time: 04:39:06
vert. SIGNAL LEVEL (dBm)
hor. TIME (minutes)

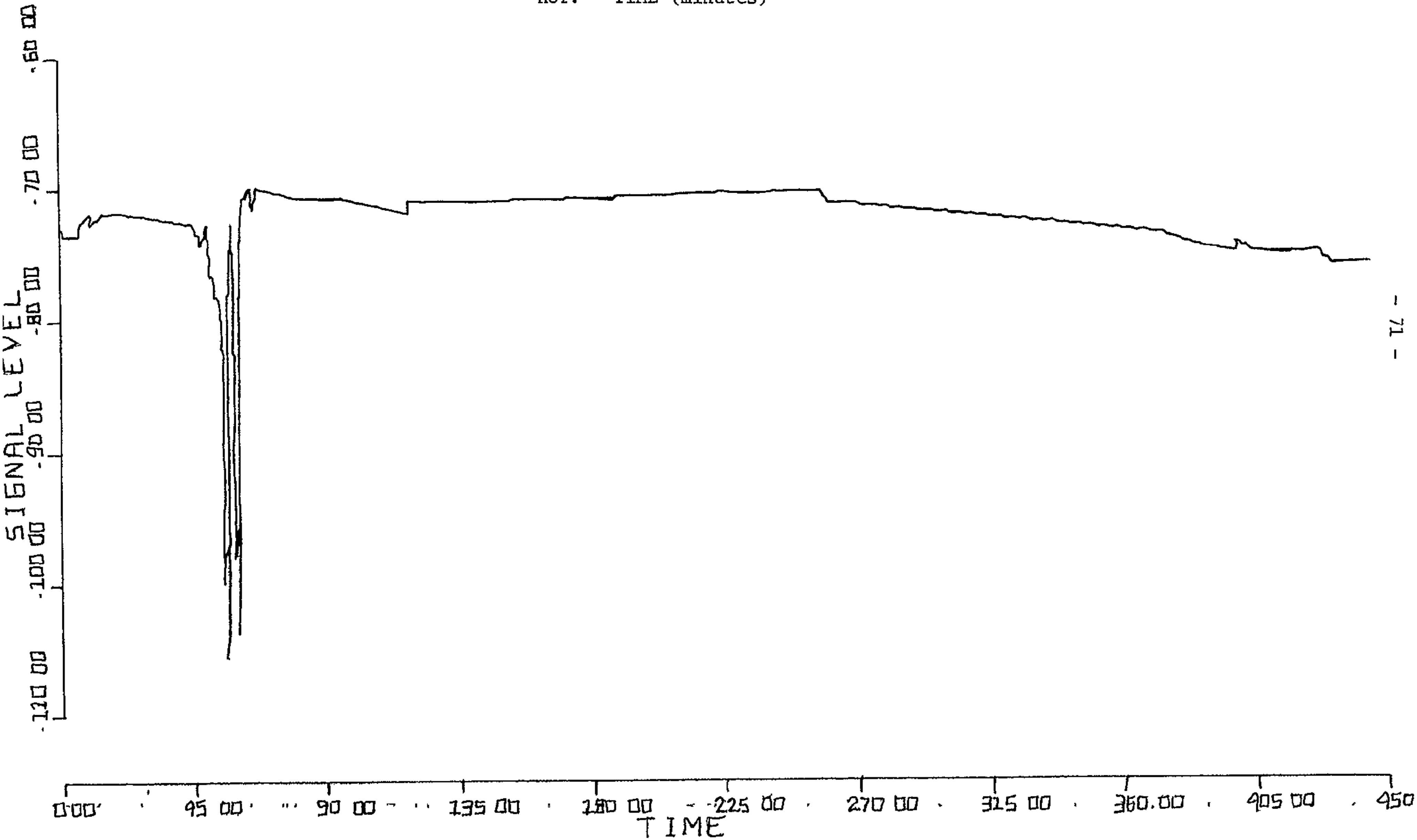

Attenuation (10 second time constant)

June 25, 1976 (Day 177)
Start time: 21:15:11
End time: 04:39:06
vert. ATTENUATION (dB)
hor. TIME (minutes)

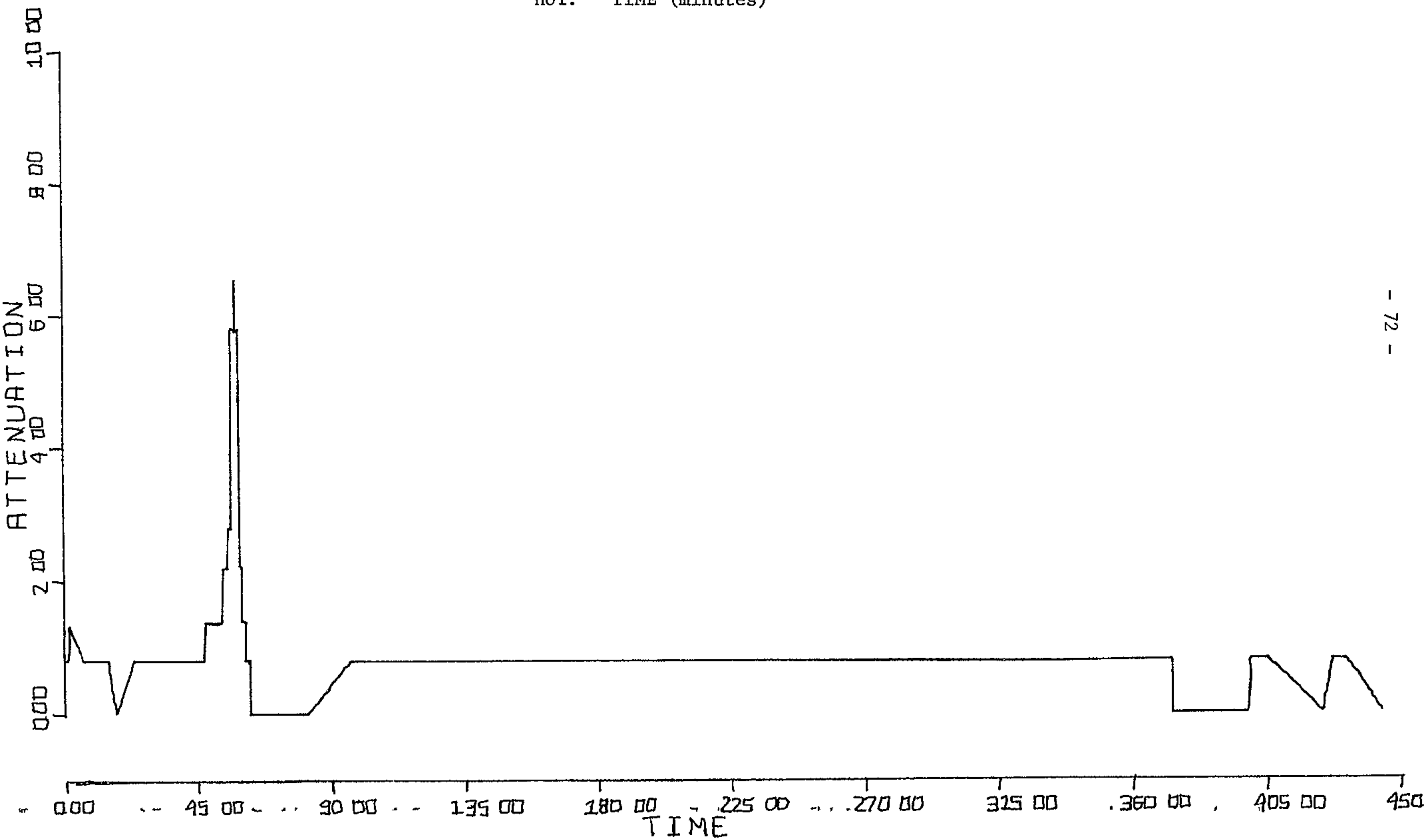

Isolation (10 second time constant)

June 25, 1976 (Day 177)
Start time: 21 15 11
End time: 04.39:06
vert. ISOLATION (dB)
hor. TIME (minutes)

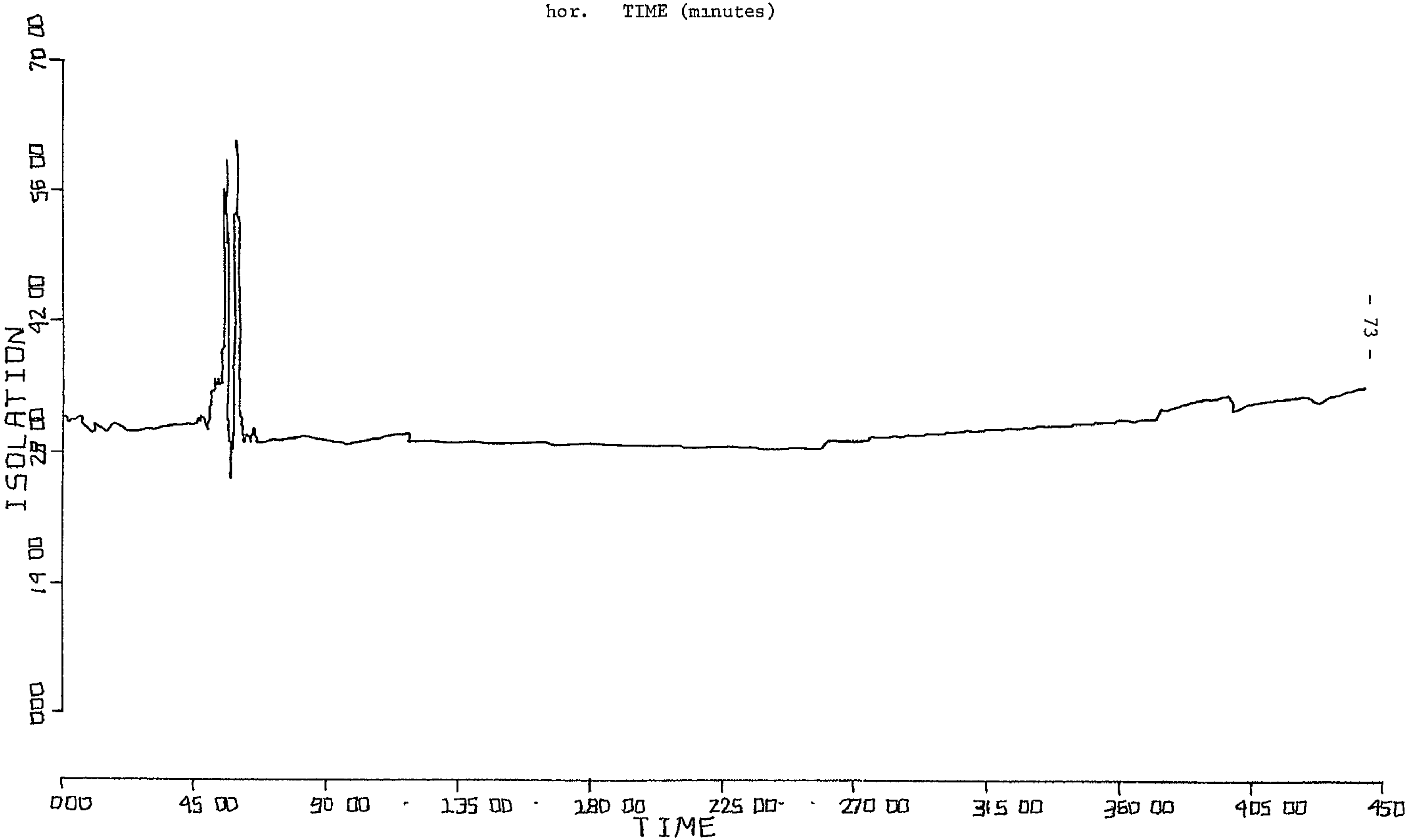

Isolation versus Attenuation
(10 second time constant)

June 25, 1976 (Day 177)
Start time: 21:15:11
End time: 04:39:06
vert. ISOLATION (dB)
hor. ATTENUATION (dB)

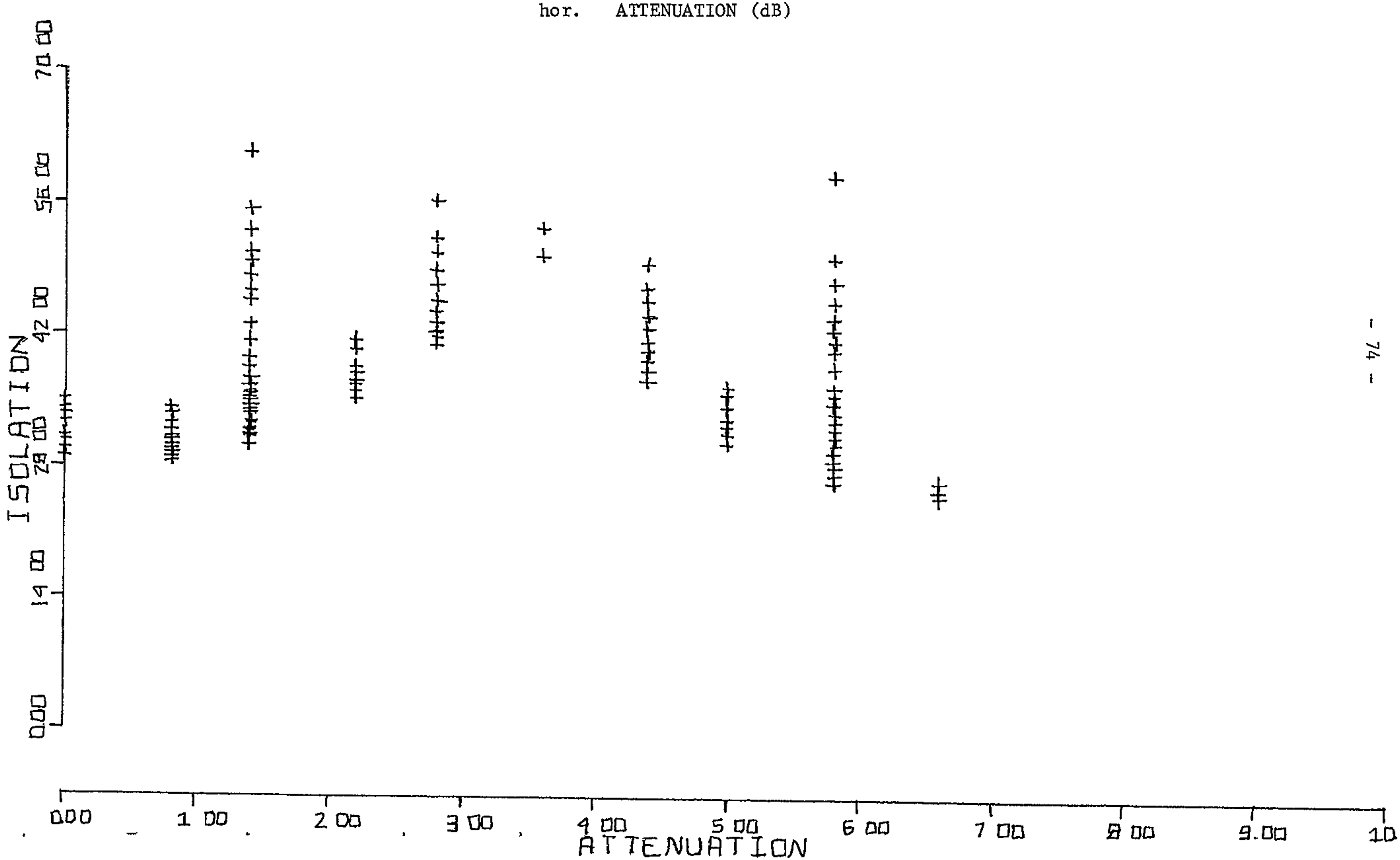

Rain Rate (RG #9 - Site Rain Gauge)

June 26, 1976 (Day 178)
Start time: 23:04:51
End time. 00:53:19
vert. RAIN RATE (mm/hr)
hor. TIME (minutes)

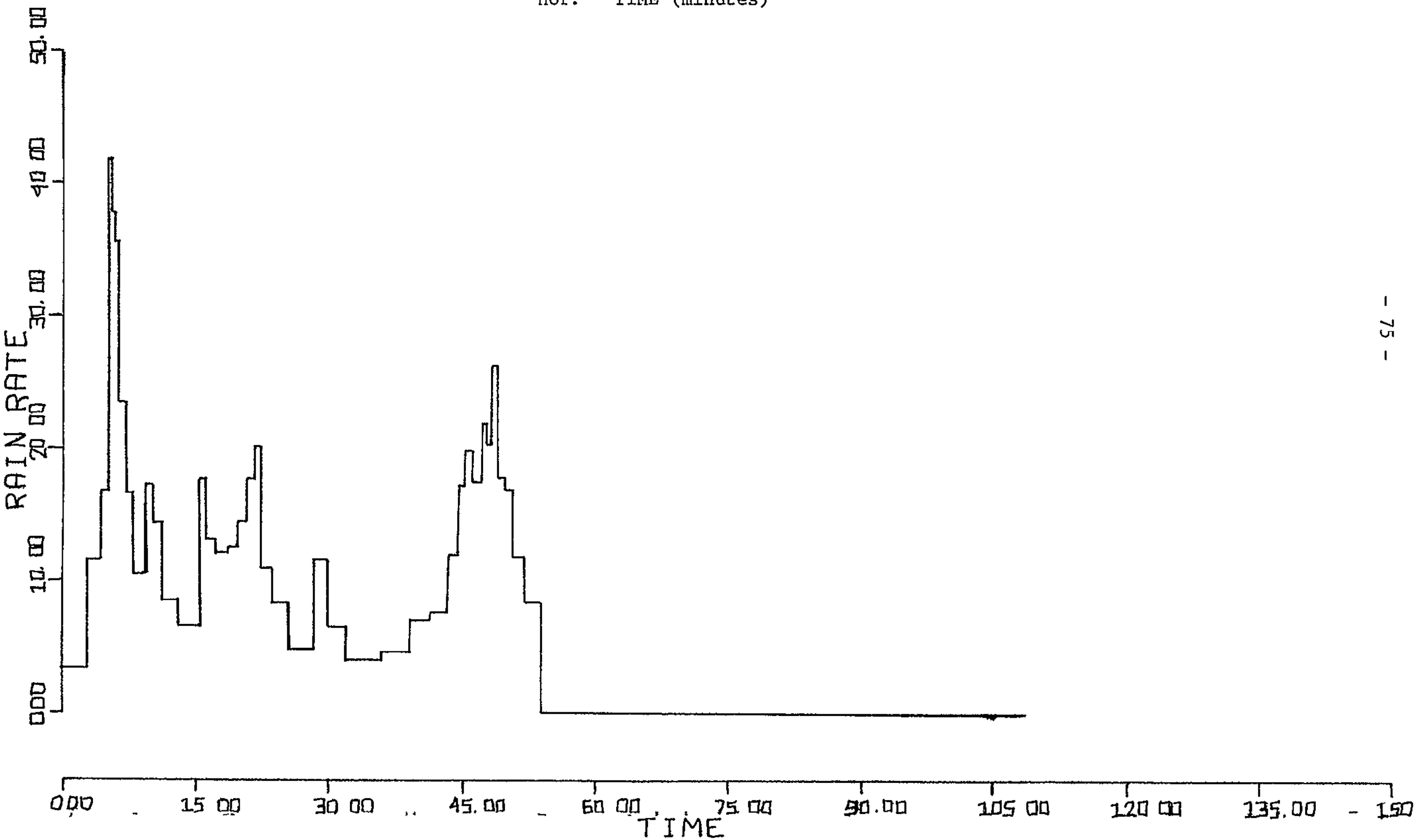

Rain Rate (RG #10 - 175 meters from receiver along path)

June 26, 1976 (Day 178)
Start time: 23·04:51
End time: 00:53·19
vert. RAIN RATE (mm/hr)
hor. TIME (minutes)

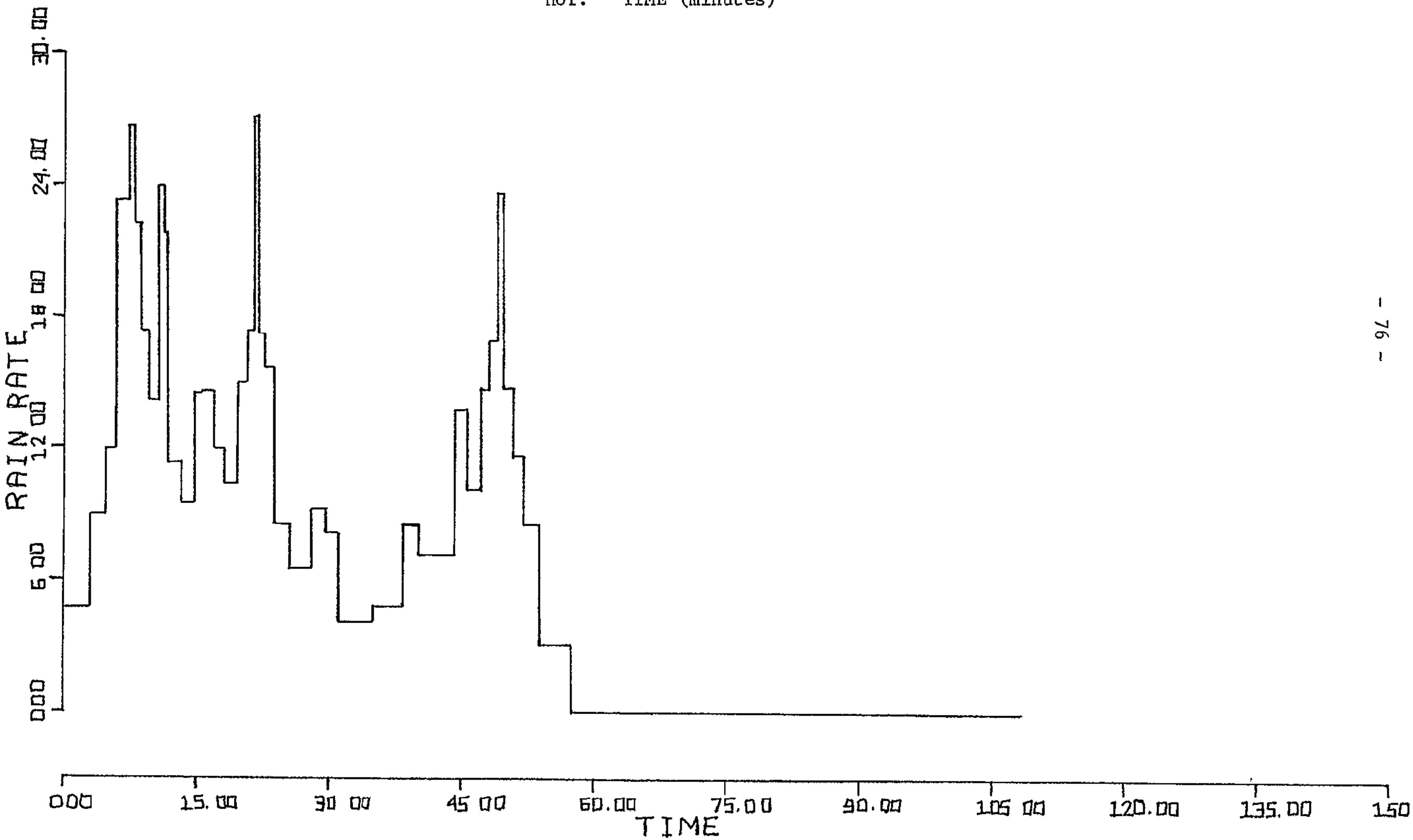

Rain Rate (RG #11 - 563 meters from receiver along path)

June 26, 1976 (Day 178)
Start time. 23:04:51
End time. 00:53:19
vert. RAIN RATE (mm/hr)
hor. TIME (minutes)

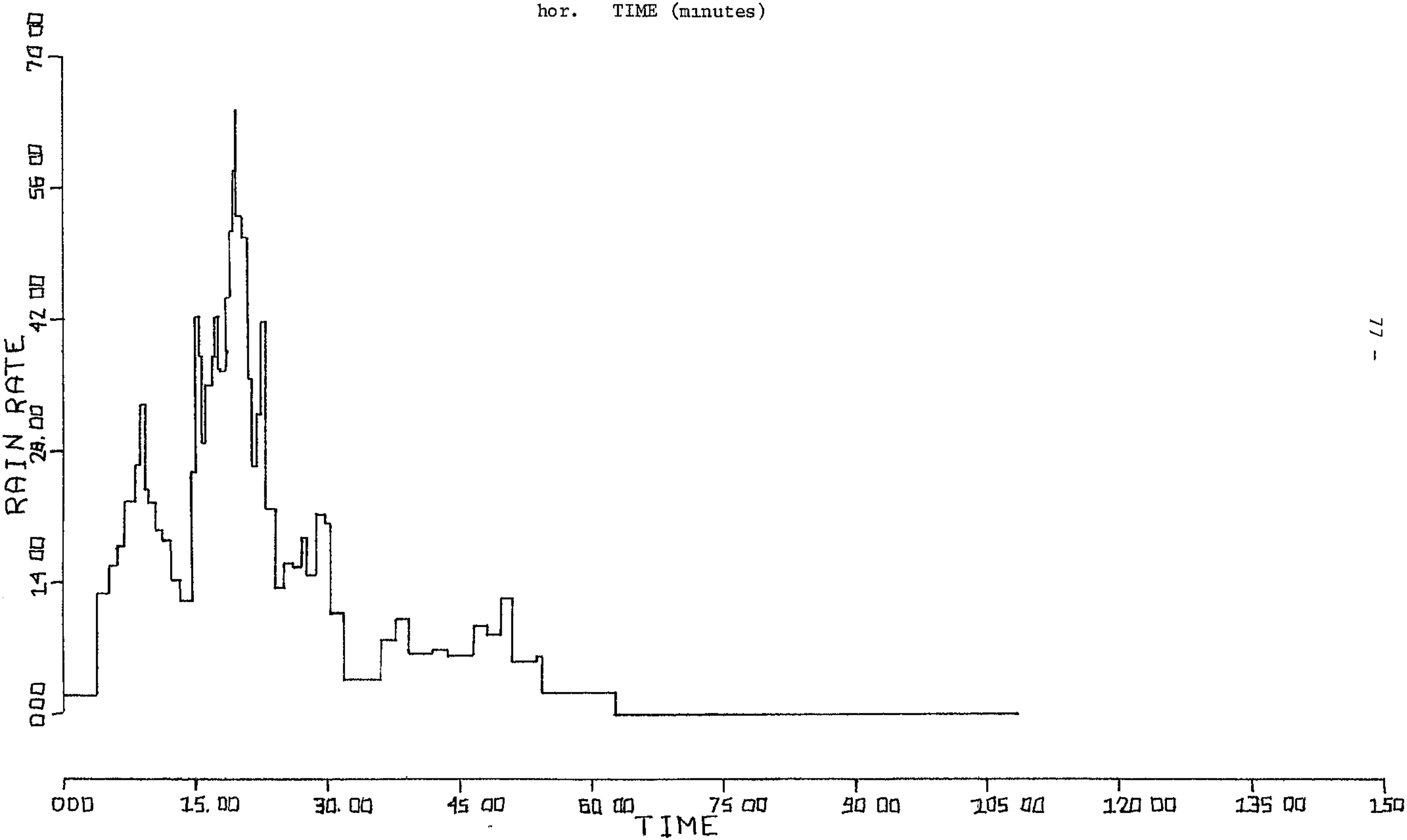

Co-Polarized Signal Level
(10 second time constant)

June 26, 1976 (Day 178)
Start time: 23:04.51
End time: 00:53.19
vert. SIGNAL LEVEL (dBm)
hor. TIME (minutes)

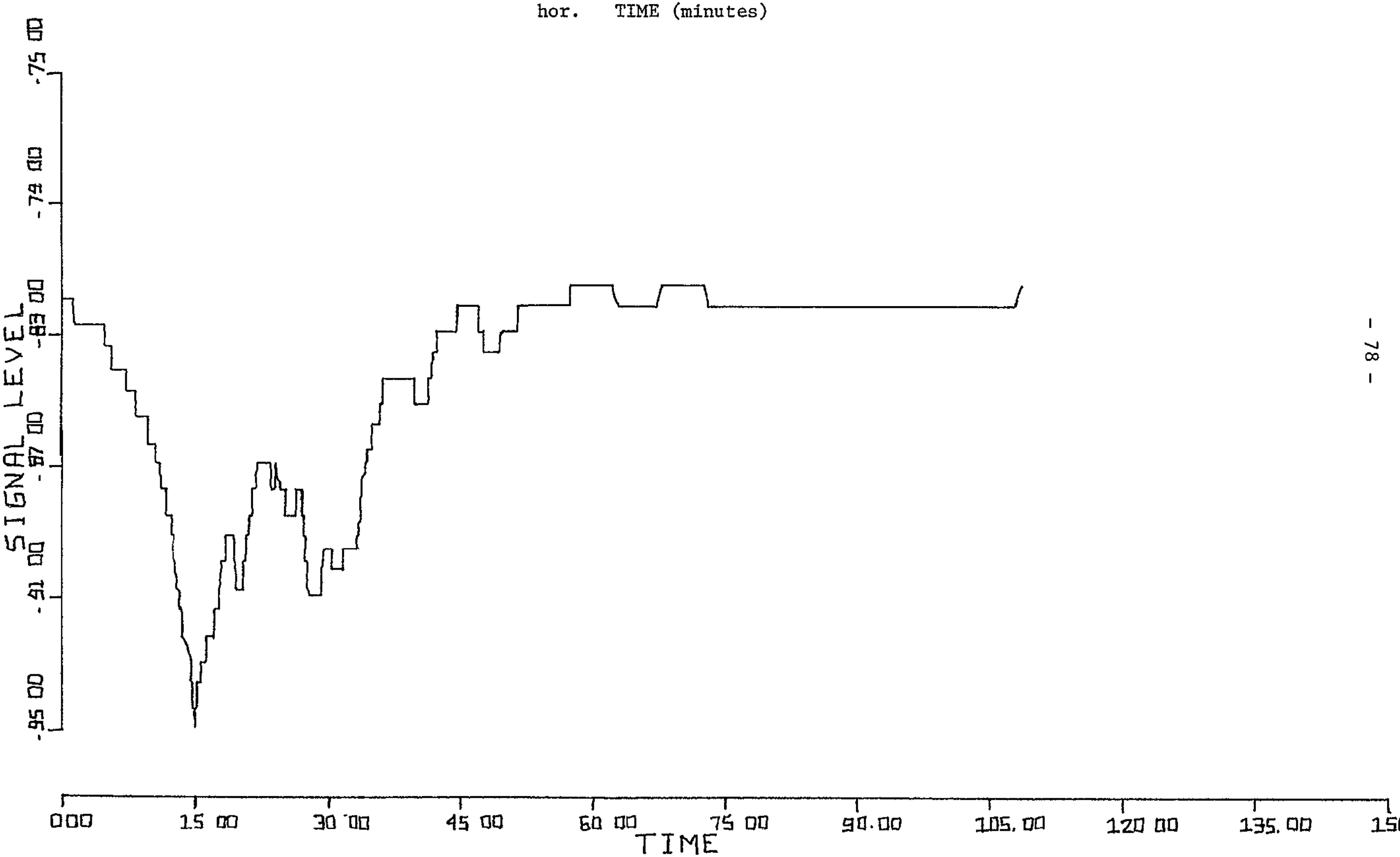

Cross-Polarized Signal Level
(10 second time constant)

June 26, 1976 (Day 178)
Start time: 23 04:51
End time: 00:53 19
vert. SIGNAL LEVEL (dBm)
hor. TIME (minutes)

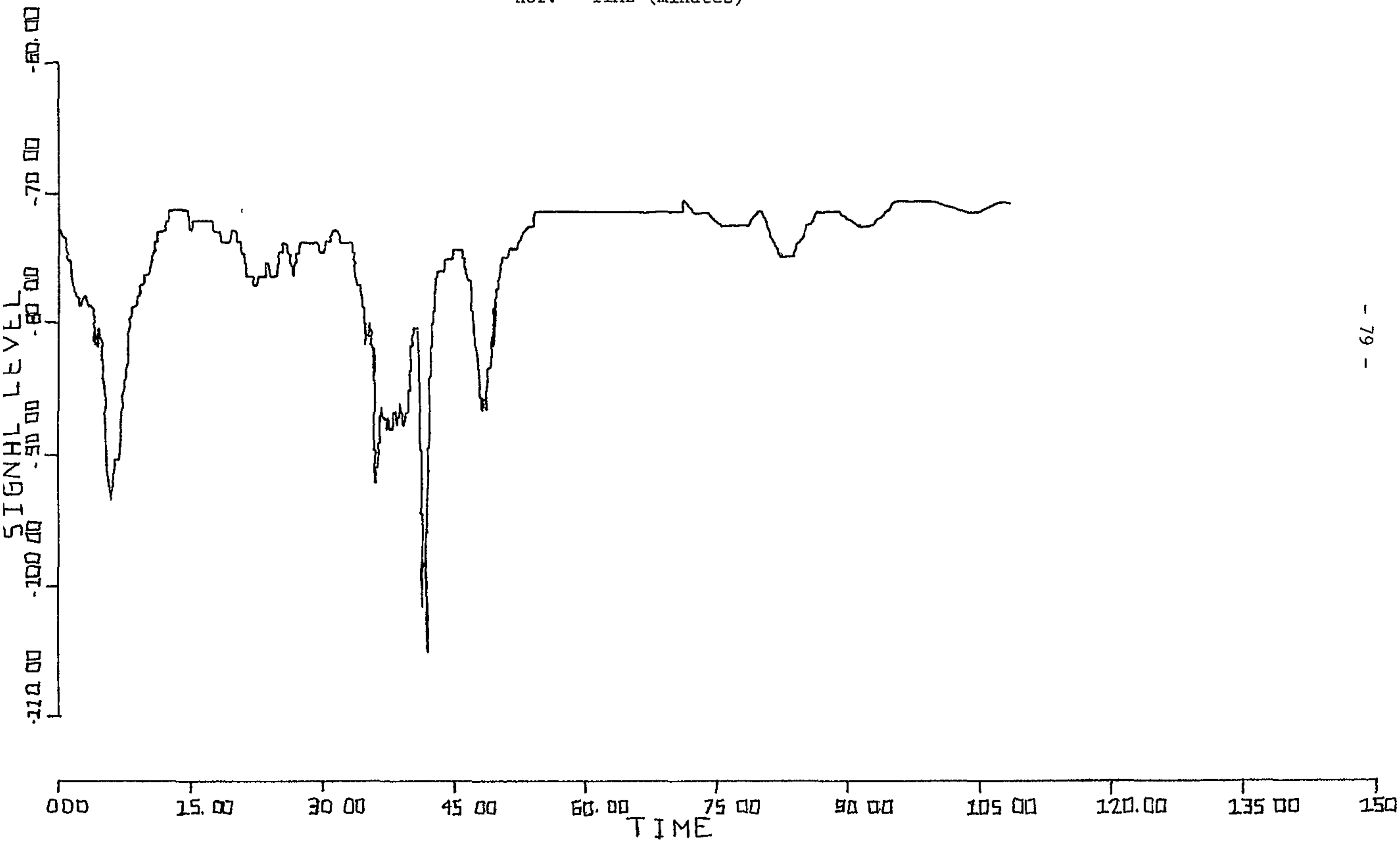

Attenuation (10 second time constant)

June 26, 1976 (Day 178)
Start time: 23:04:51
End time: 00·53:19
vert. ATTENUATION (dB)
hor. TIME (minutes)

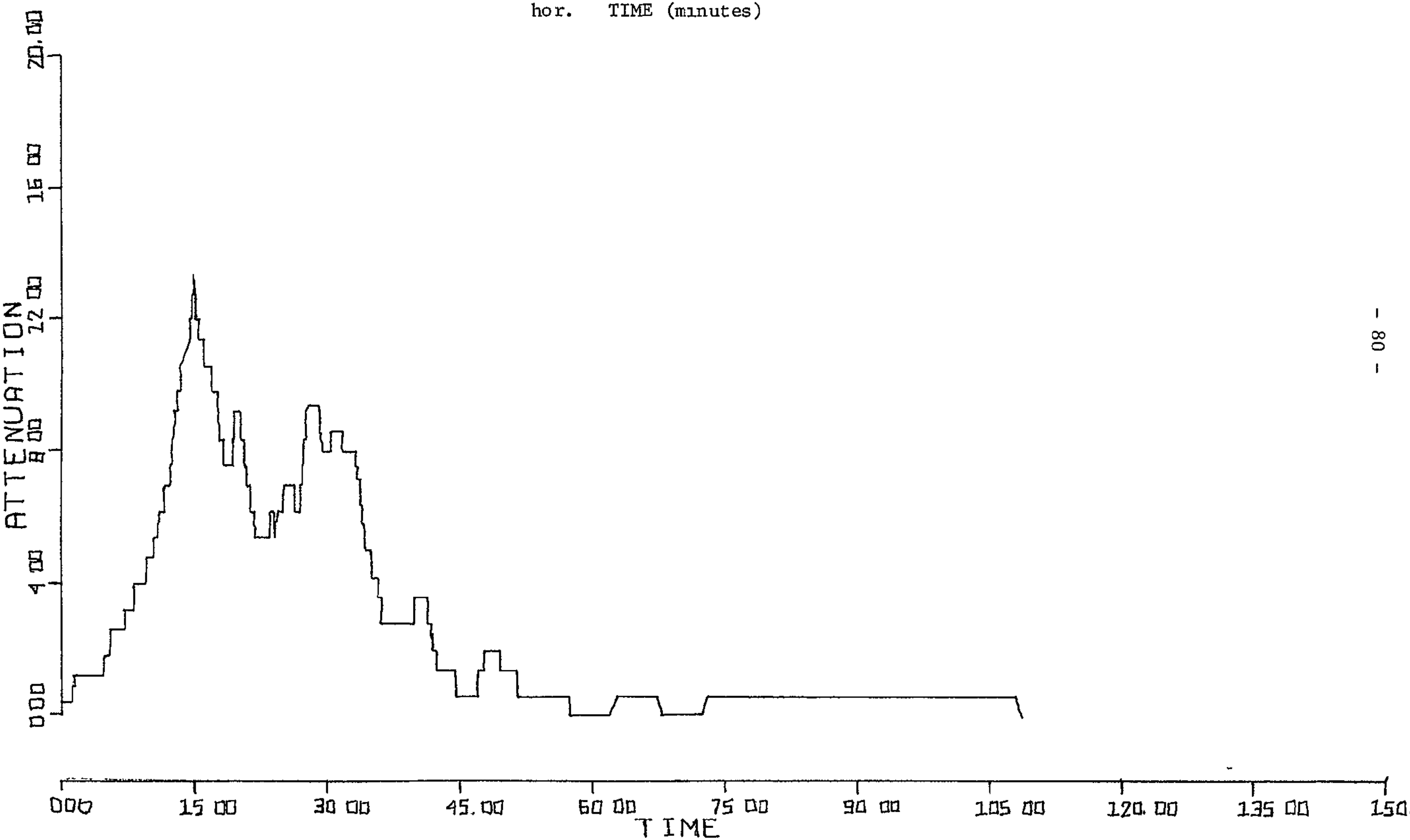

Isolation (10 second time constant)

June 26, 1976 (Day 178)
Start time: 23:04:51
End time: 00:53:19
vert. ISOLATION (dB)
hor. TIME (minutes)

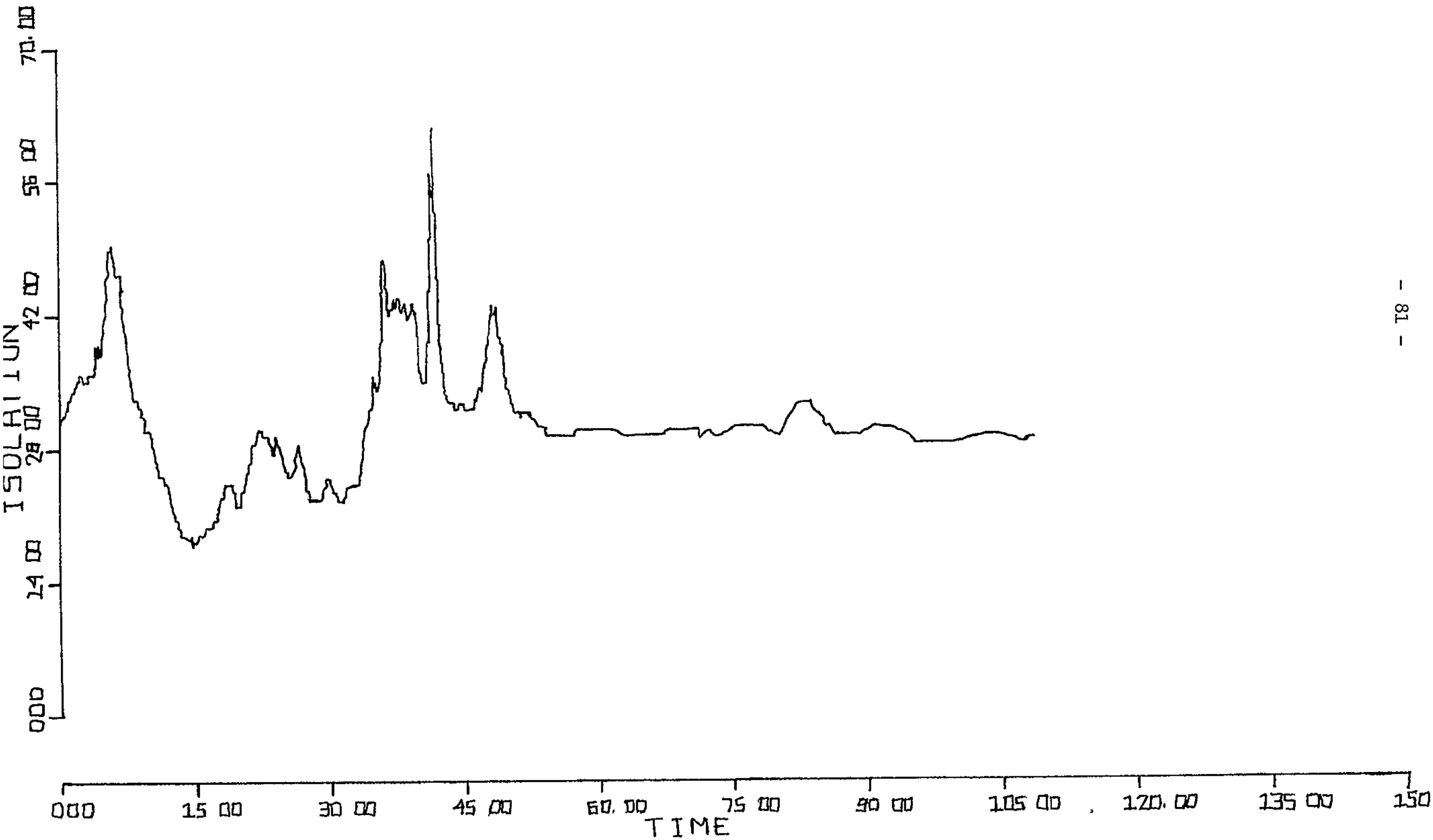

Isolation versus Attenuation
(10 second time constant)

June 26, 1976 (Day 178)
Start time: 23:04:51
End time· 00:53:19
vert. ISOLATION (dB)
hor. TIME (minutes)

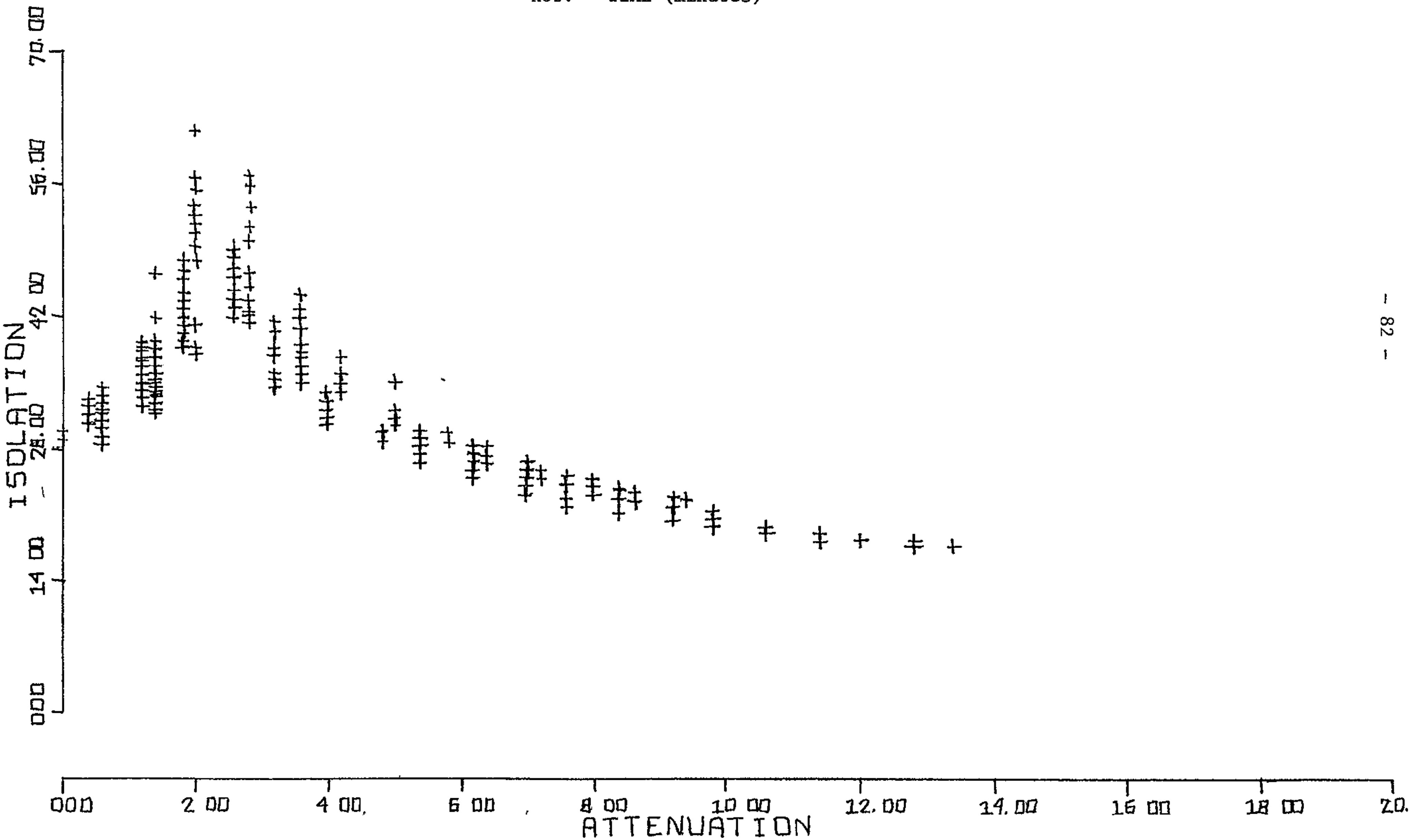

Rain Rate (RG #9 - Site Rain Gauge)

July 15, 1976 (Day 197)
Start time 19:26·16
End time: 23:12:51
vert. RAIN RATE (mm/hr)
hor. TIME (minutes)

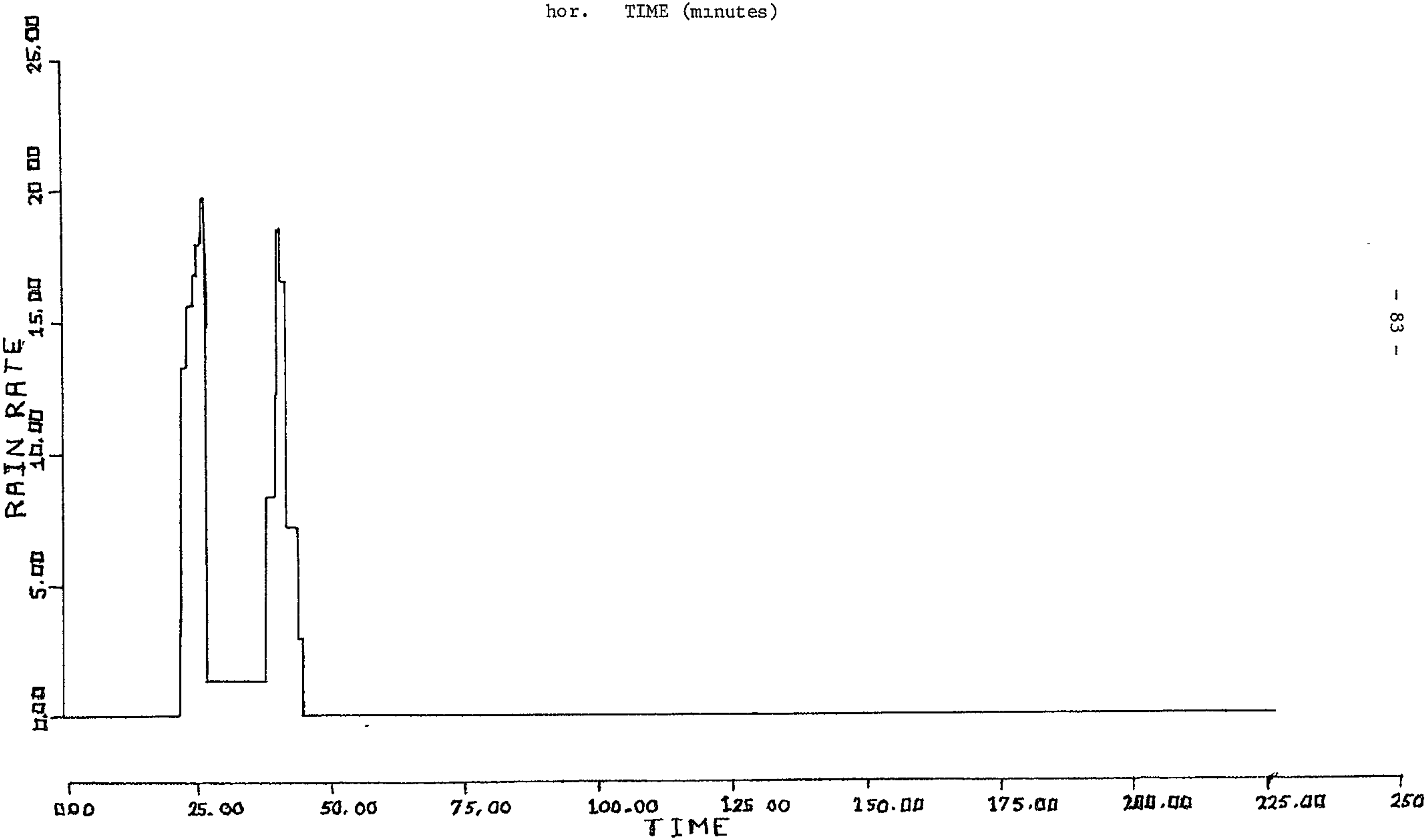

1510 183405 07 31 75 76 157

Rain Rate (RG #10 - 175 meters from

June 15, 1976 (Day 197)
Start time: 19:26:16
End time: 23:12·51
vert. RAIN RATE (mm/hr)
hor. TIME (minutes)

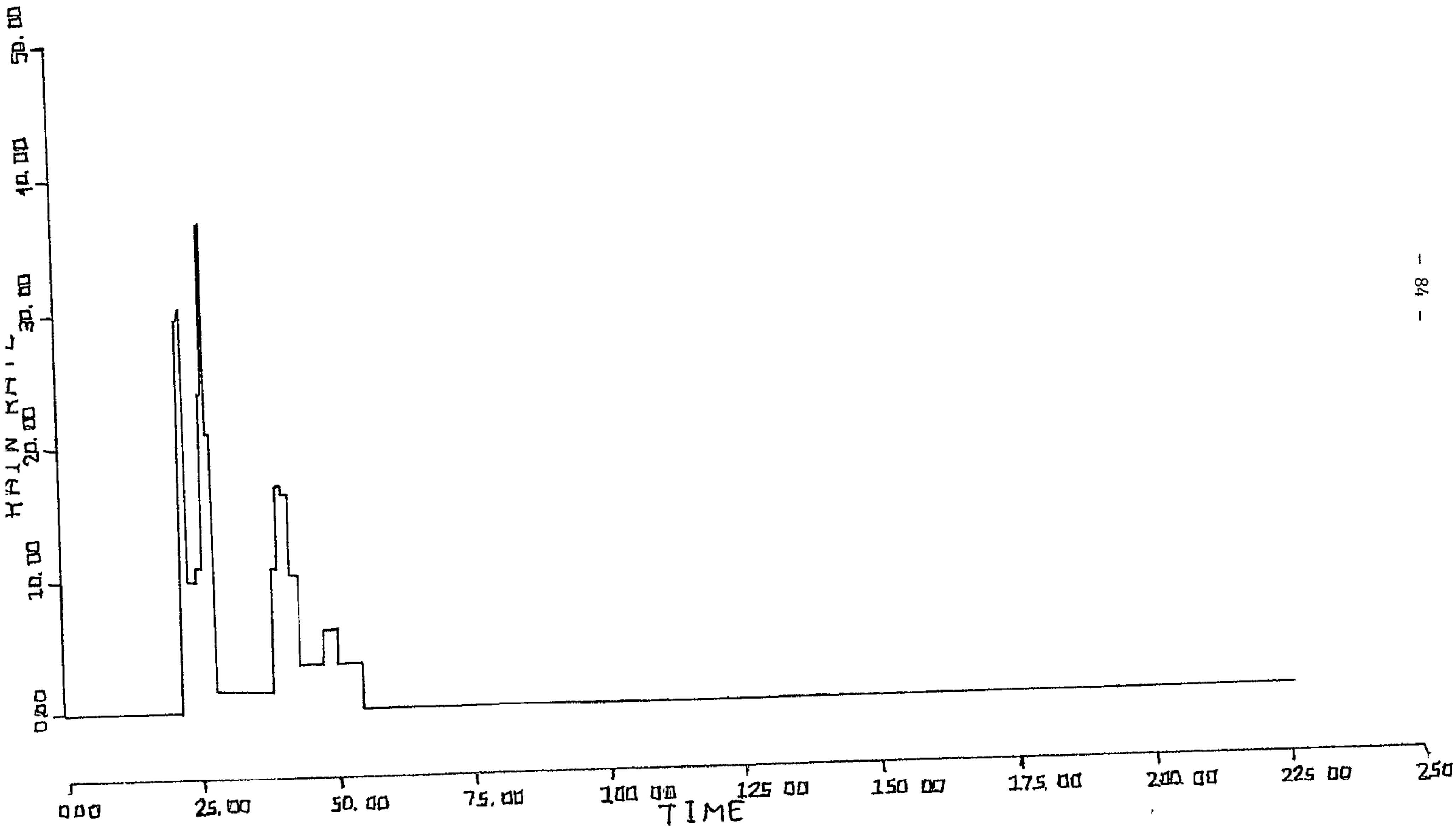

Rain Rate (RG #11 - 563 meters from

July 15, 1976 (Day 197)
Start time: 19:26:16
End time. 23·12:51
vert RAIN RATE (mm/hr)
hor. TIME (minutes)

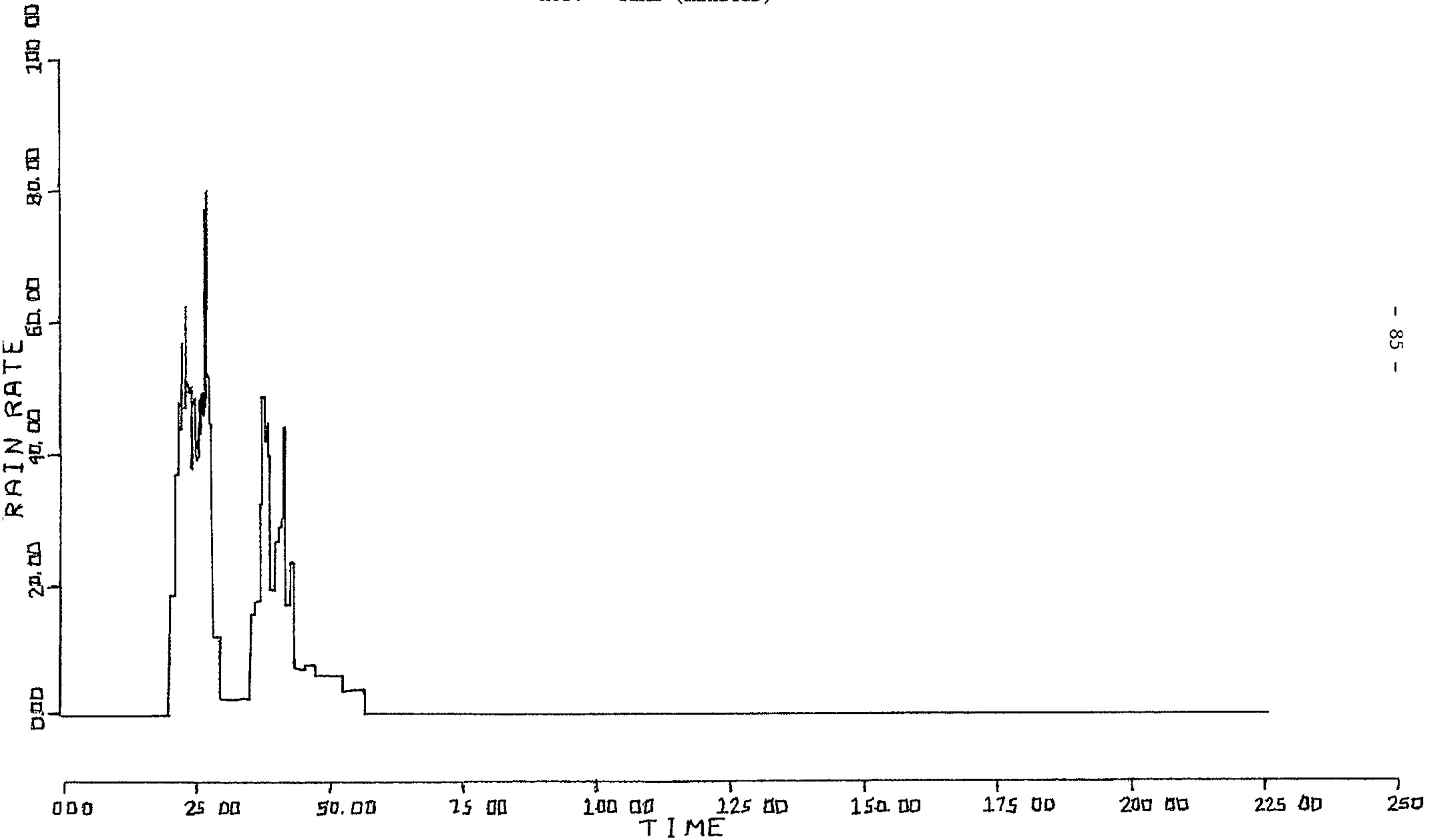

Co-Polarized Signal Level
(10 second time constant)

July 15, 1976 (Day 197)
Start time: 19:26:17
End time 23:12:51
vert. SIGNAL LEVEL (dBm)
hor. TIME (minutes)

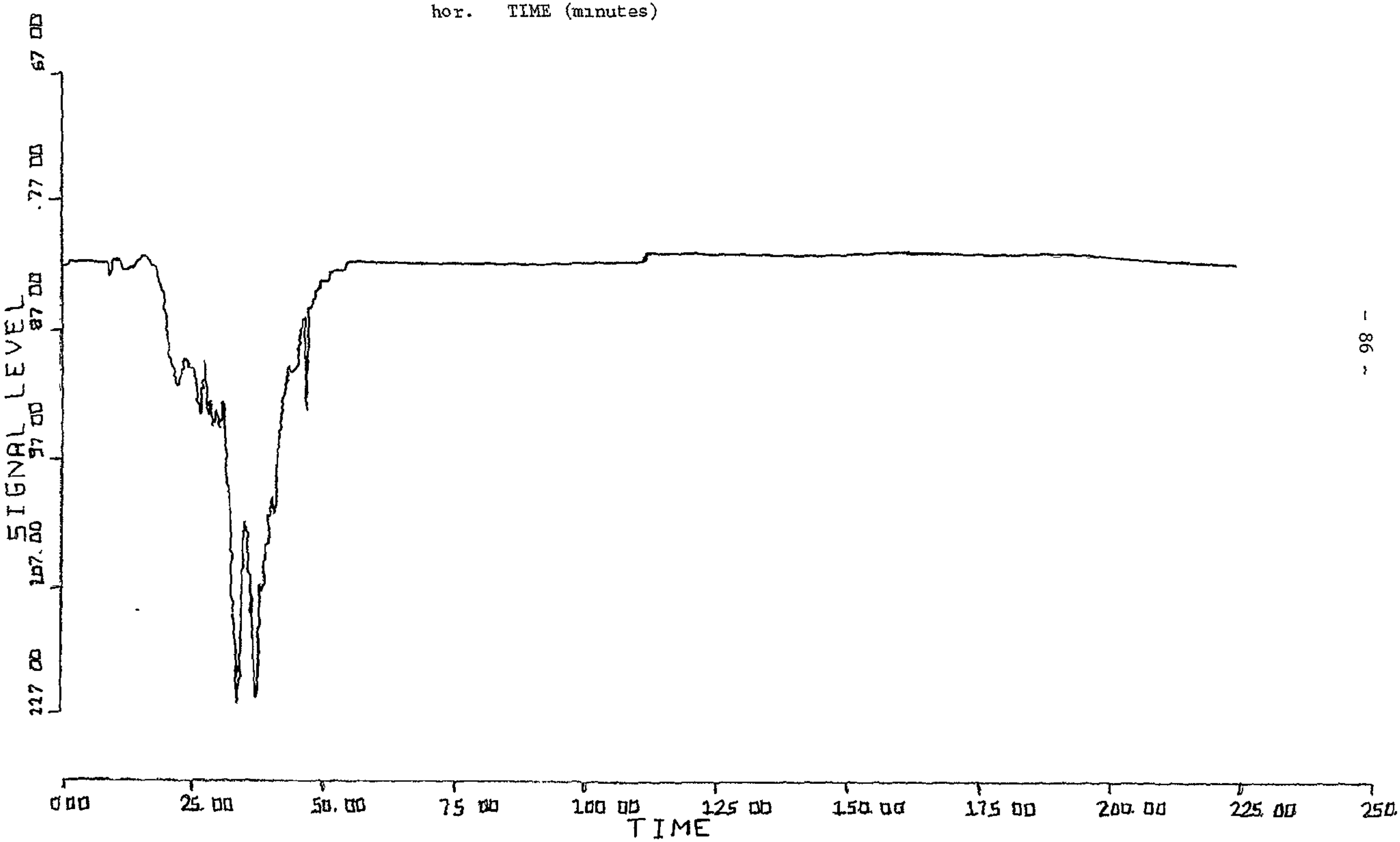

Cross-Polarized Signal Level
(10 second time constant)

July 15, 1976 (Day 197)
Start time: 19:26·17
End time: 23:12.51
vert. SIGNAL LEVEL (dBm)
hor. TIME (minutes)

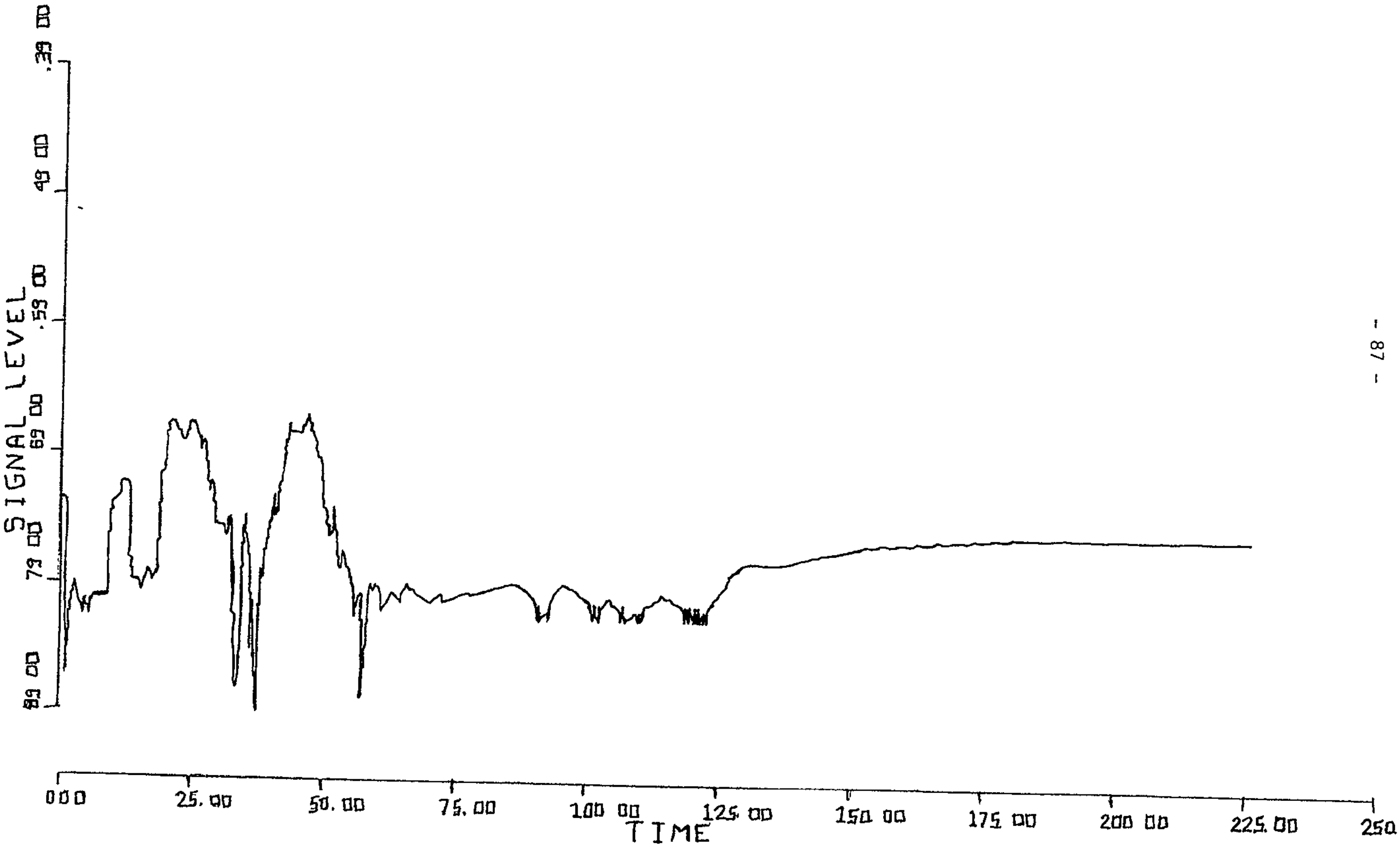

Attenuation (10 second time constant)

July 15, 1976 (Day 197)
Start time: 19:26:17
End time: 23:12·51
vert. ATTENUATION (dB)
hor. TIME (minutes)

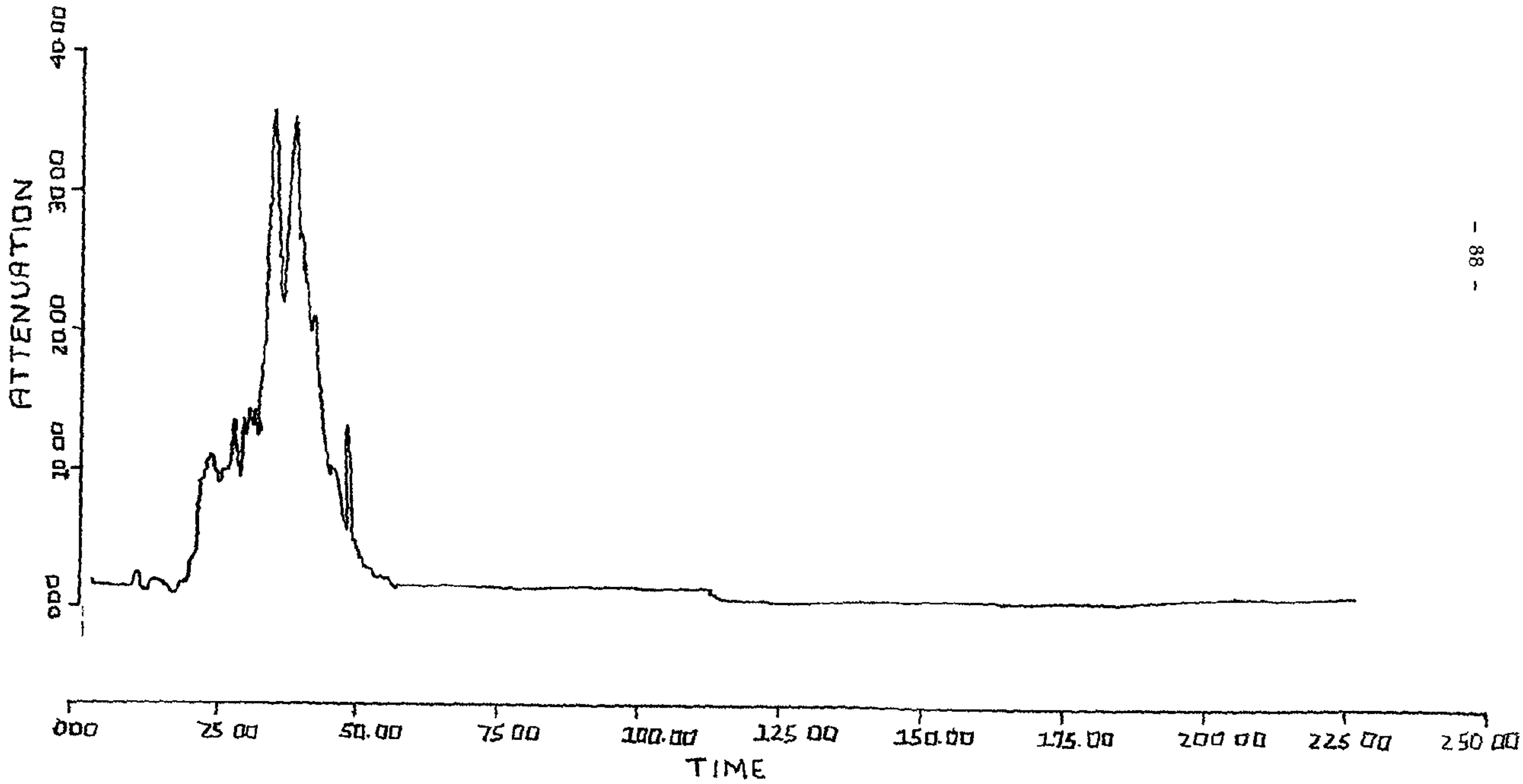

- 88 -

Isolation (10 second time constant)

July 15, 1976 (Day 197)
Start time· 19 26 17
End time· 23:12:51
vert. ISOALTION (dB)
hor. TIME (minutes)

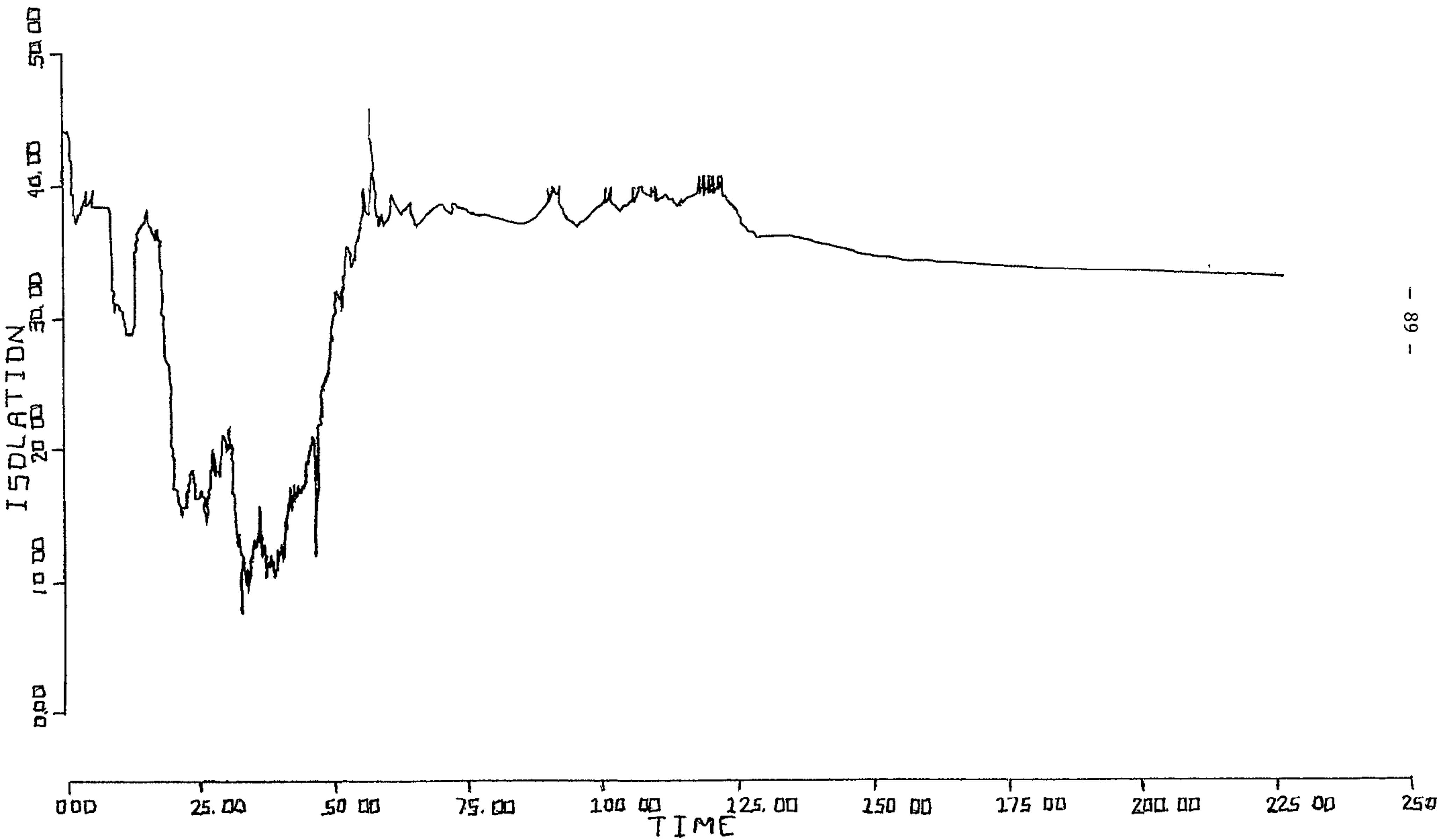

Isolation versus Attenuation
(10 second time constant)

July 15, 1976 (Day 197)
Start time: 19:26:16
End time: 23:12:51
vert. ISOLATION (dB)
hor. ATTENUATION (dB)

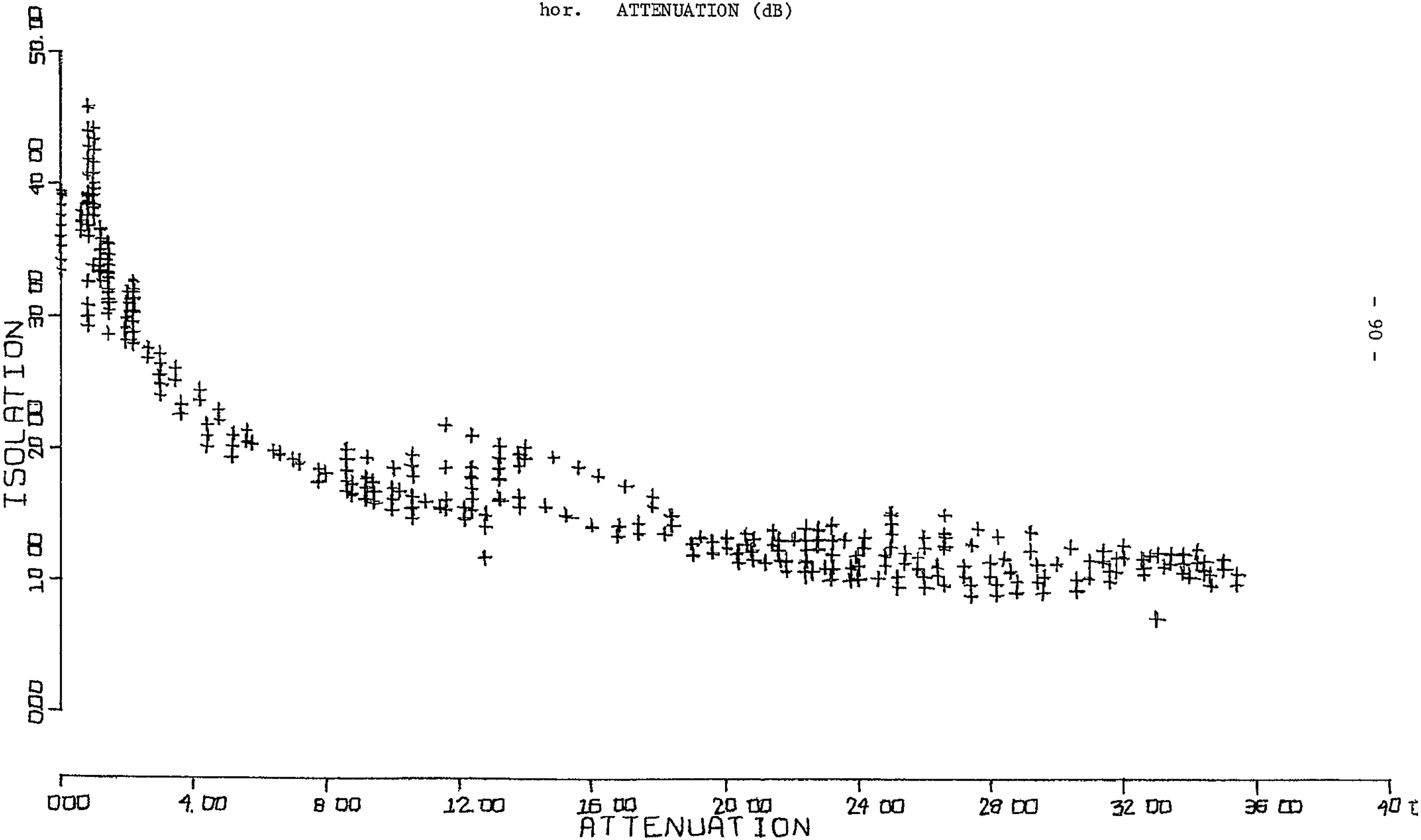

1503 149855 03 04 76 75 212 402.583 75 212 403.976

Rain Rate with Expanded Time Scale
(RG #9 - Site Rain Gauge)

July 30, 1976 (Day 212)
Start time: 18:37:08
End time. 18:49:59
vert. RAIN RATE (mm/hr)
hor. TIME (minutes)

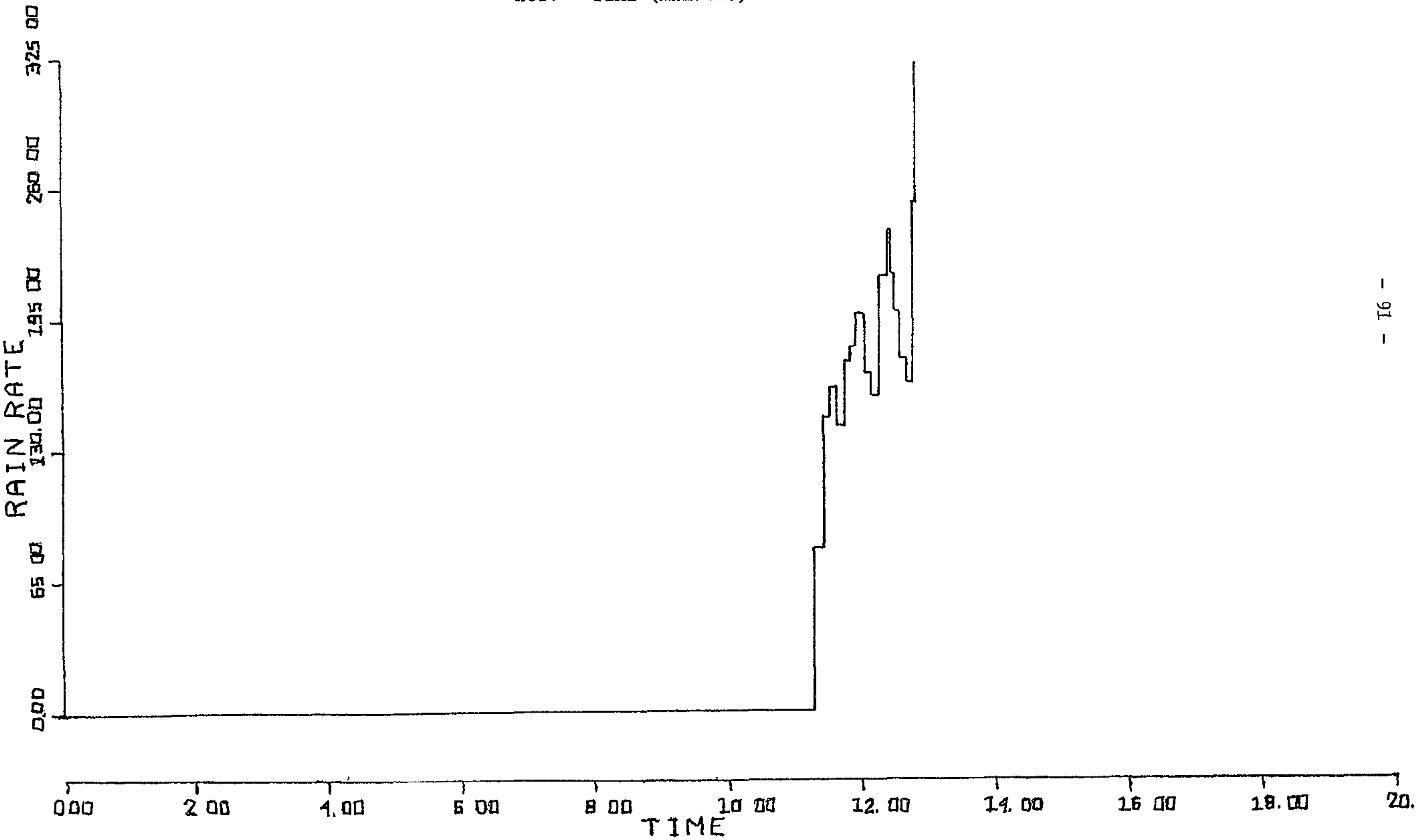

Rain Rate with Expanded Time Scale
(RG #10 - 175 meters from receiver along path)

July 30, 1976 (Day 212)
Start time: 18:37:08
End time. 18:49:59
vert. RAIN RATE (mm/hr)
hor. TIME (minutes)

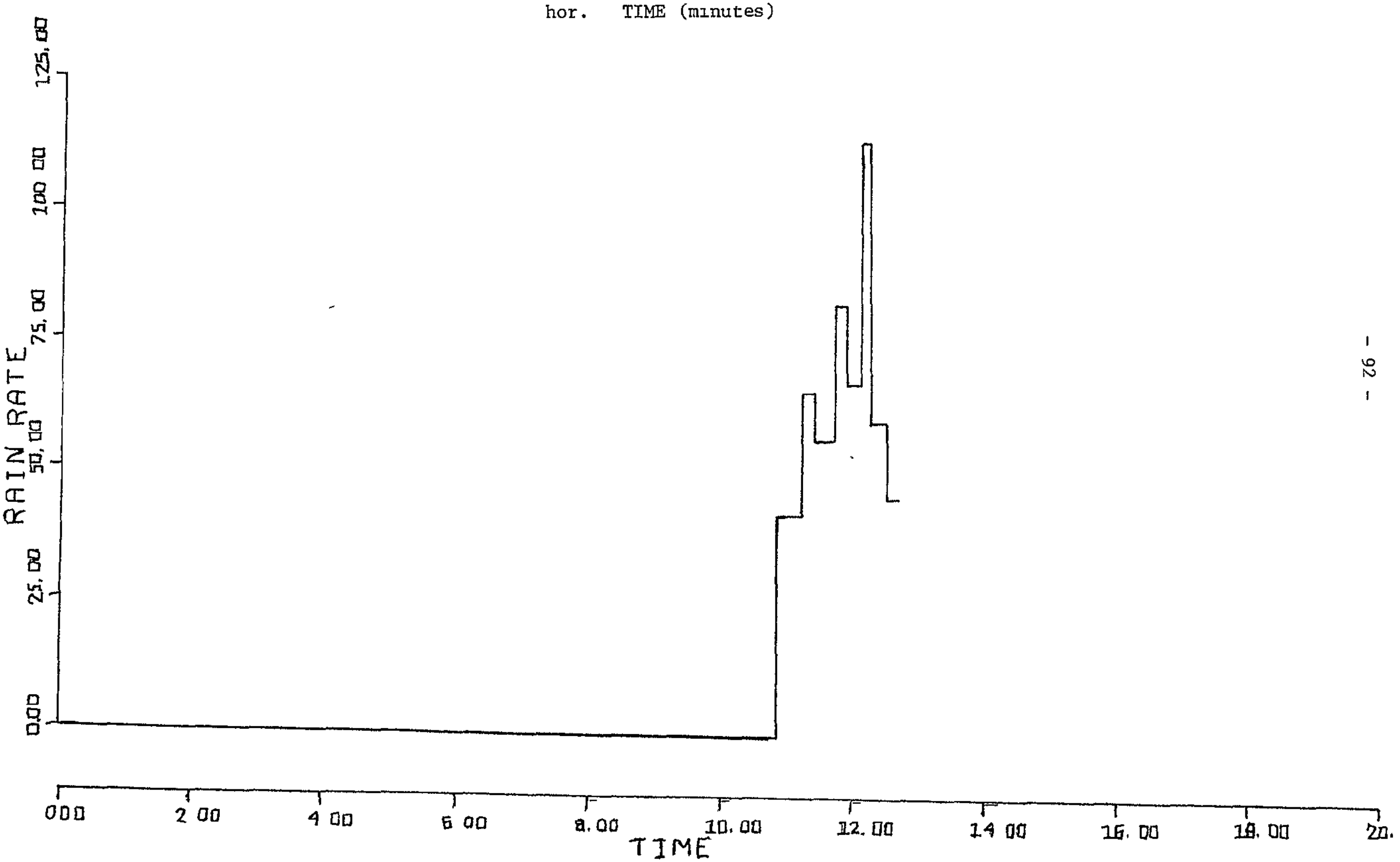

Rain Rate with Expanded Time Scale
(RG #11 - 563 meters from
receiver along path)

July 30, 1976 (Day 212)
Start time: 18:37:08
End time: 18:49:59
vert. RAIN RATE (mm/hr)
hor. TIME (minutes)

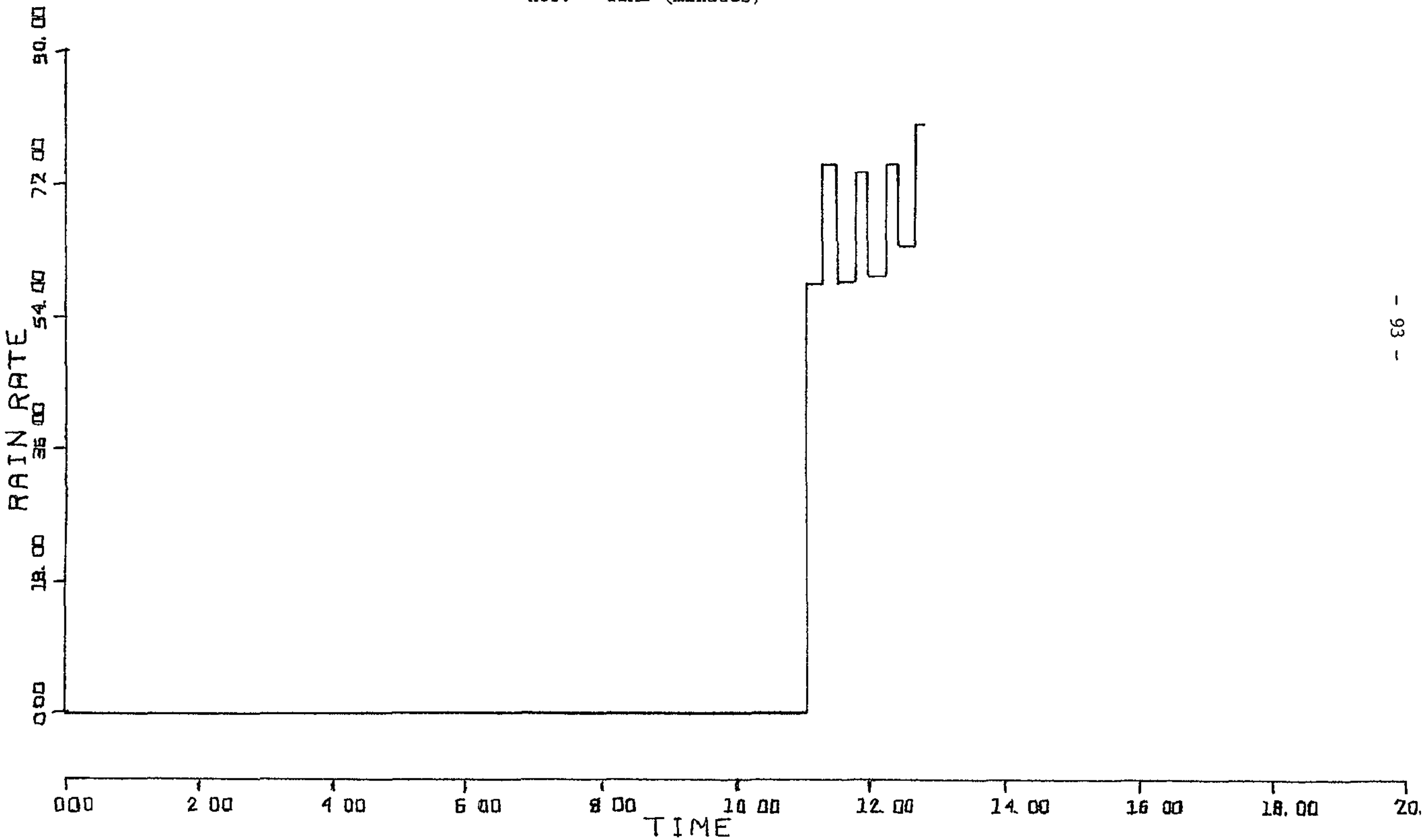

- 93 -

C-2

Co-polarized signal level at
IF receiver input, dBm

July 30, 1976 (Day 212)
Start time: 18:37·08
End time· 18:49:59
vert. SIGNAL LEVEL (dBm)
hor. TIME (minutes)

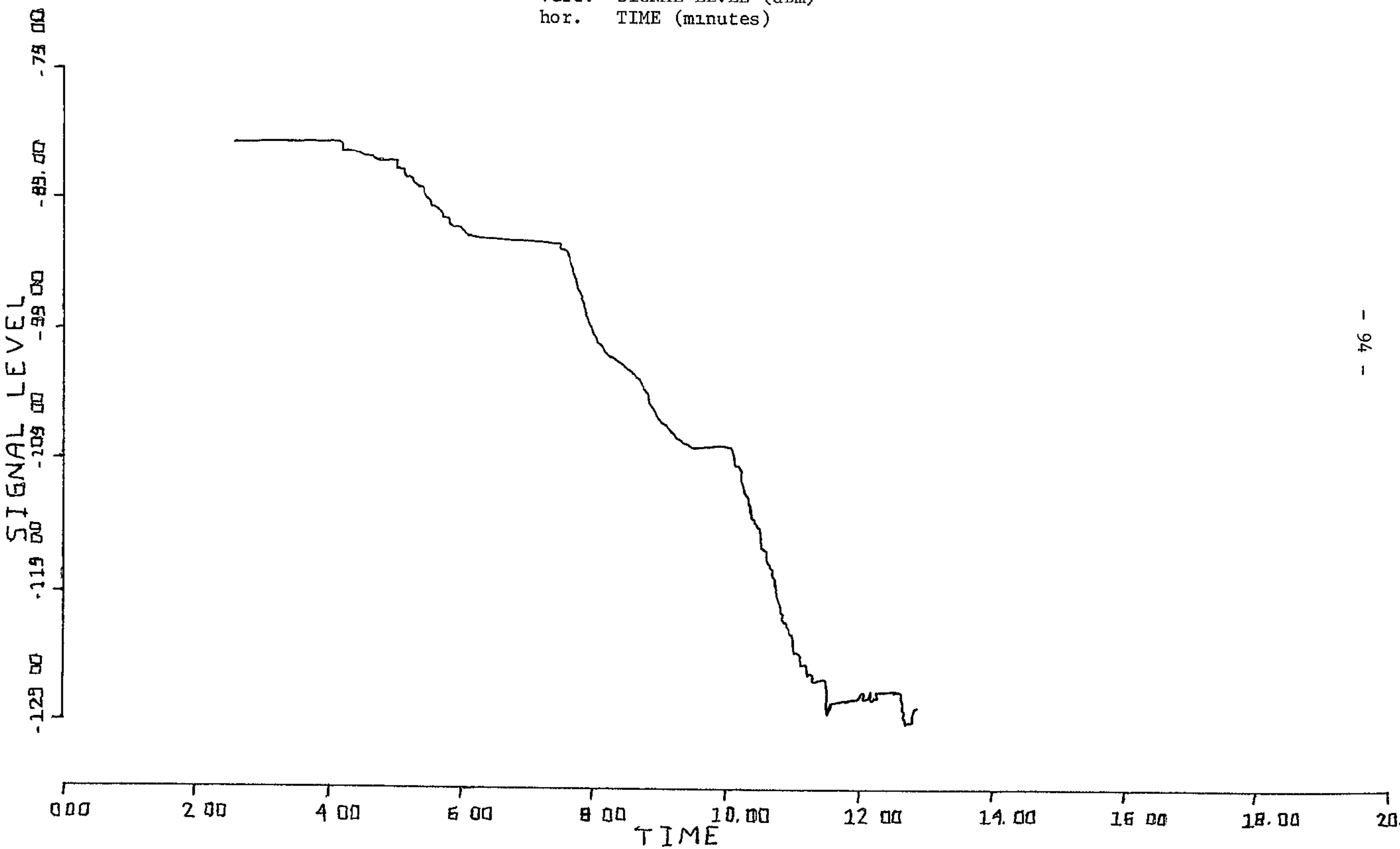

Cross-polarized signal level at
IF receiver input, dBm

July 30, 1976 (Day 212)
Start time: 18.37:08
End time. 18:49:59
vert. SIGNAL LEVEL (dBm)
hor. TIME (minutes)

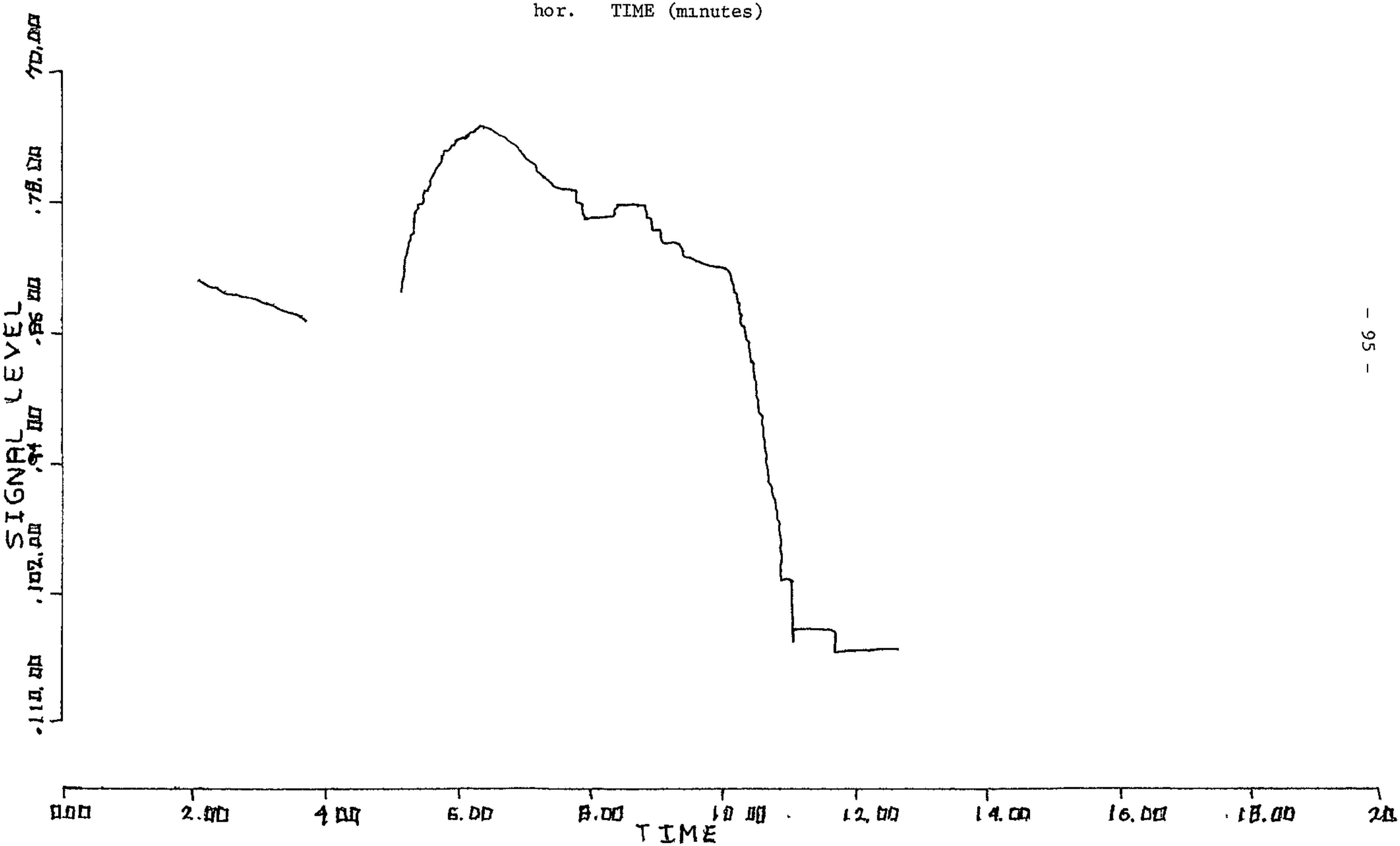

Attenuation (10 second time constant)

July 30, 1976 (Day 212)
Start time: 18:37:08
End time: 18:49:59
vert. ATTENUATION (dB)
hor. TIME (minutes)

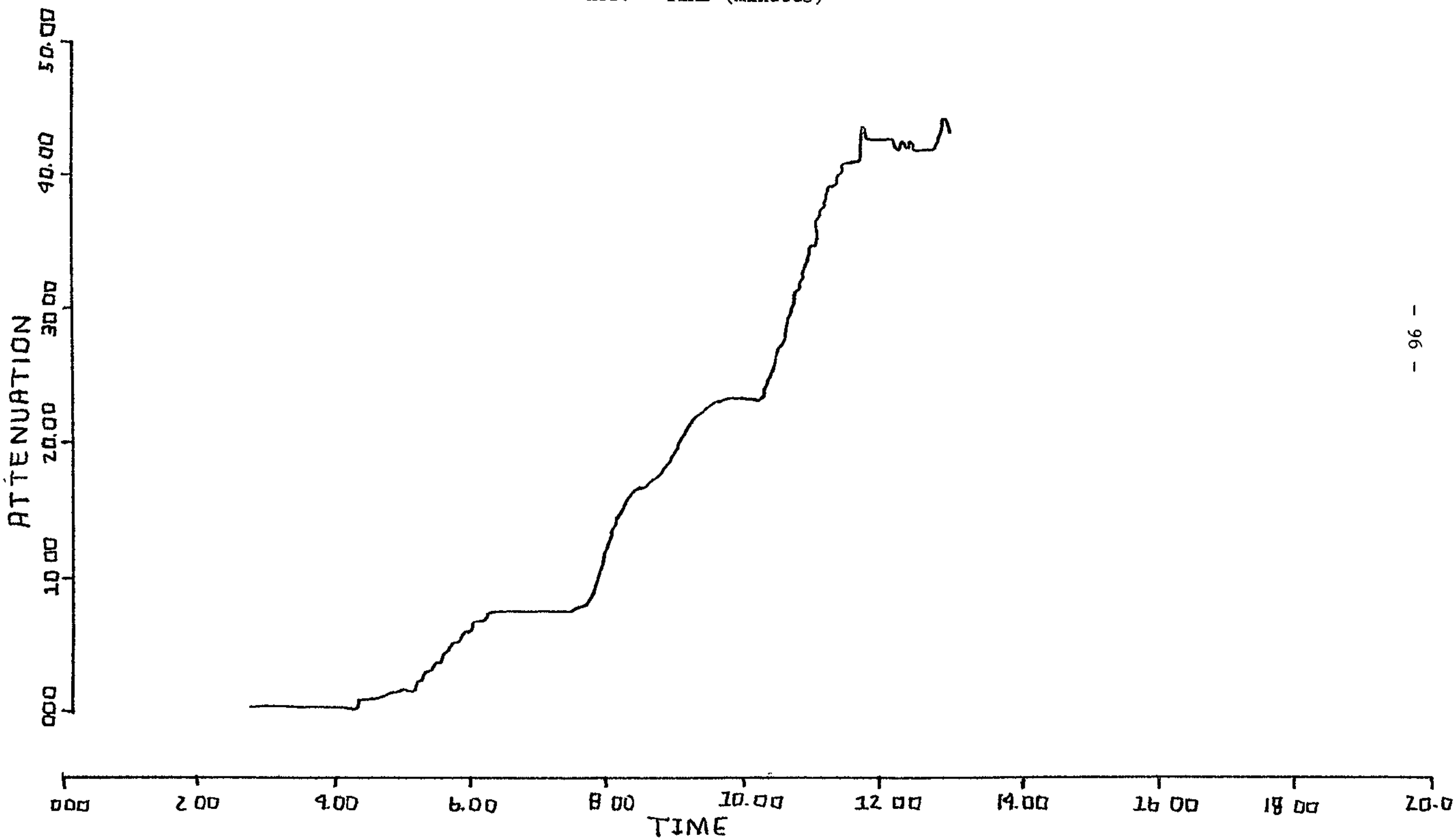

Polarization isolation in dB.

July 30, 1976 (Day 212)
Start time: 18:37:08
End time 18:49:59
vert. ISOLATION (dB)
hor. TIME (minutes)

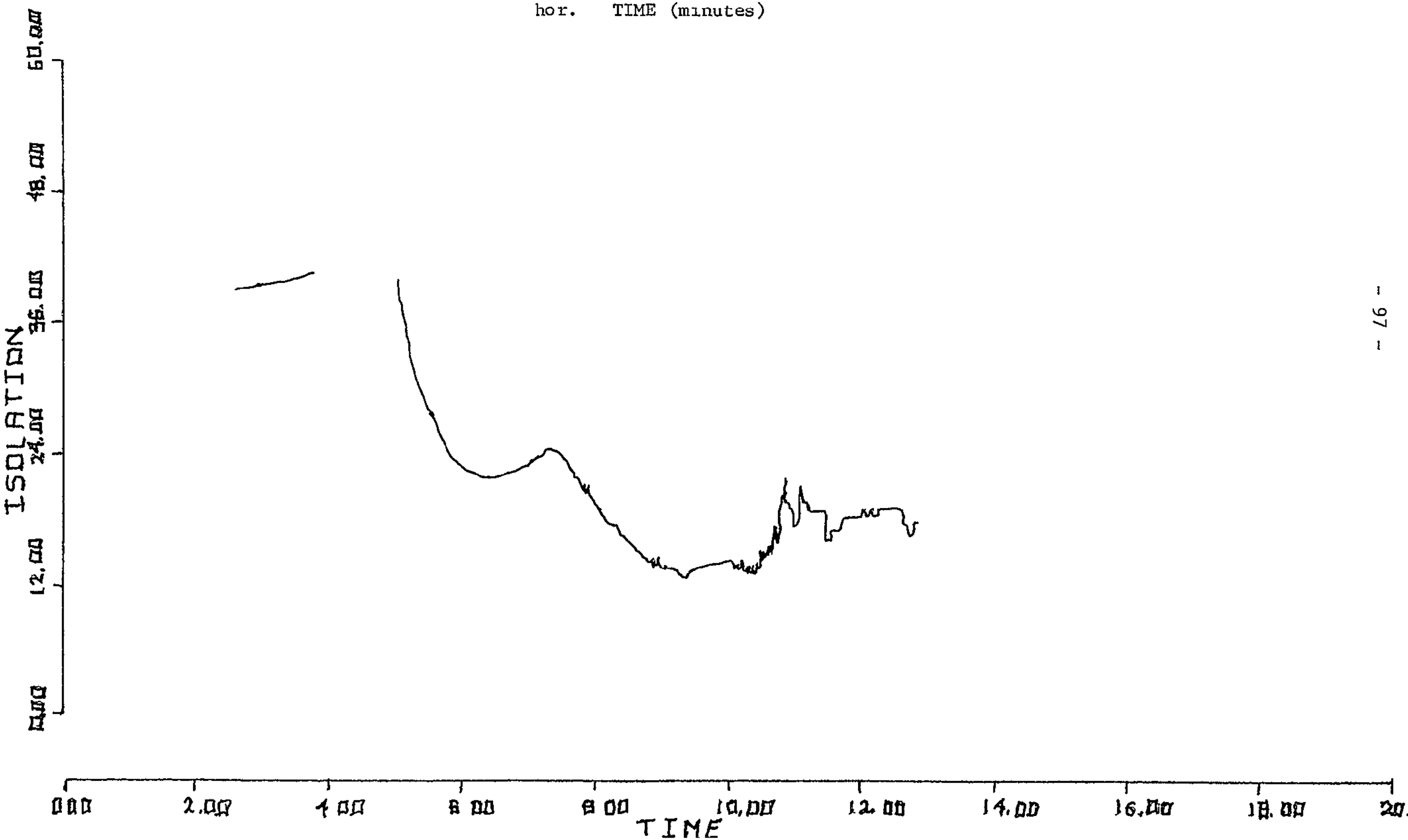

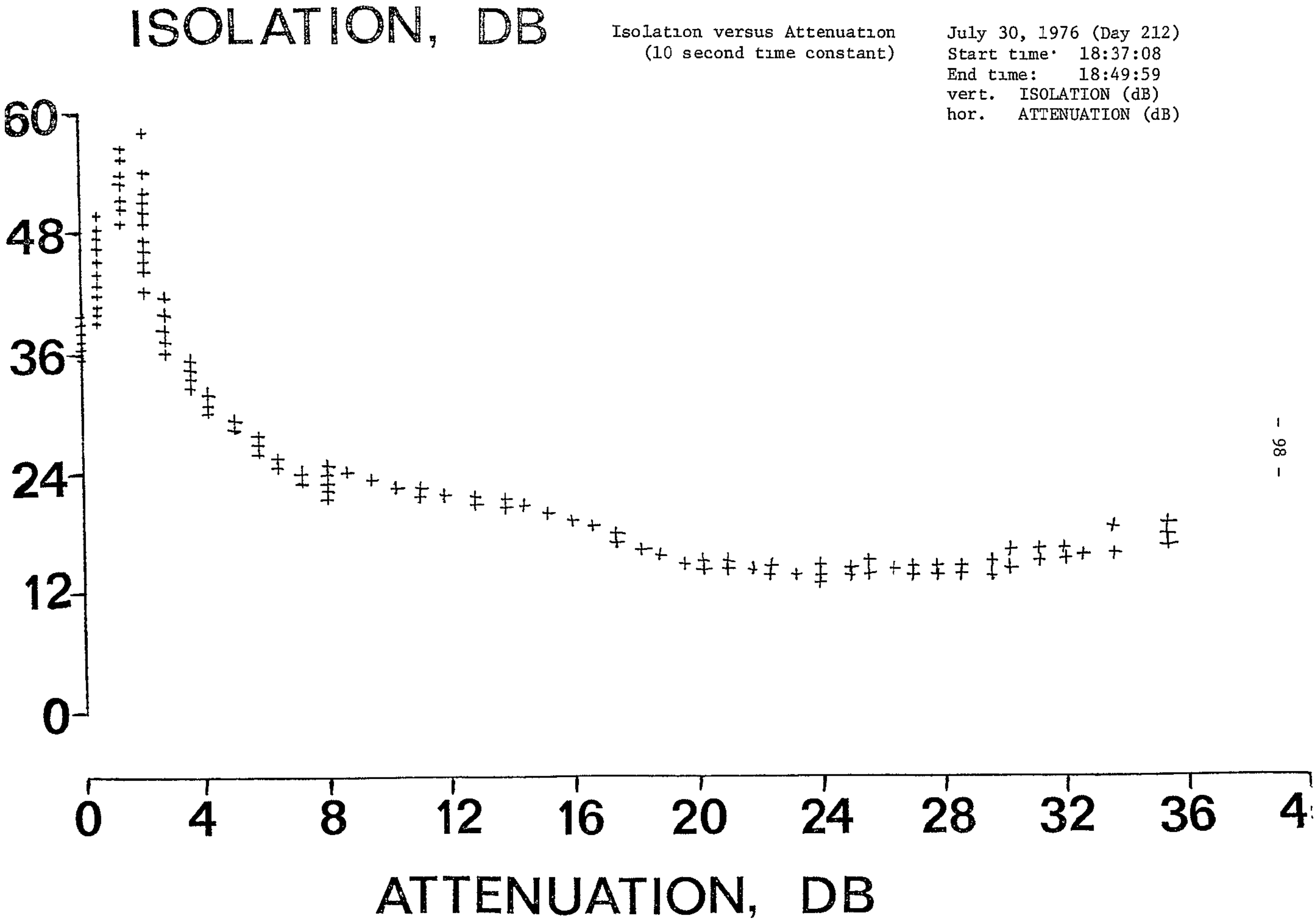
ISOLATION, DB
Isolation versus Attenuation
(10 second time constant)
July 30, 1976 (Day 212)
Start time: 18:37:08
End time: 18:49:59
vert. ISOLATION (dB)
hor. ATTENUATION (dB)
60
48
36
24
12
0
0
4
8
12
16
20
24
28
32
36
ATTENUATION, DB

References

1. T. Oguchi and Y. Hosoya, "Scattering Properties of Oblate Raindrops and Cross Polarization of Radio Waves Due to Rain (Part II): Calculations at Microwave and Millimeter Wave Regions," Journal of the Radio Research Laboratories, Vol. 21, No. 105, pp. 191-259, 1974.

2. J. A. Morrison and M. J. Cross, "Scattering of a Plane Electromagnetic Wave by Axisymmetric Raindrops," BSTJ, Vol. 53, pp. 955-1019, August, 1974.

3. D. J. Fang and J. M. Harris, "A New Method of Estimating Microwave Attenuation over a Slant Propagation Path Based on Rain Gauge Data," IEEE Transactions on Antennas and Propagation, Vol. AP-24, No. 3, pp. 381-384, May 1976.